Addressing Millimeter-Wave 5G Challenges Through Simulation Software p29

Meet the Challenge of Designing Electrically Small Antennas p46

Capitalize on EDA When Developing MIMO, Phased-Array Antenna Systems p98

Microwaves & RF®

YOUR TRUSTED ENGINEERING RESOURCE FOR OVER 50 YEARS

SEPTEMBER 2017 mwrf.com

SOFTWARE-CENTRICITY

Solving difficult challenges through software interoperability p90

$10.00


SKYWORKS

September 2017 VOLUME 56, ISSUE 9

IN THIS ISSUE

40

FEATURES

57

PRODUCT TECHNOLOGY

NEWS & COLUMNS

90

defense electronics

Starts on page **63**

94

JOIN US ONLINE

follow us @MicrowavesRF

become a fan at facebook.com/microwavesRF

MICROWAVE COMPONENTS

Broad Range of Products up to 40 GHz

Filters

Multiplexer Assemblies

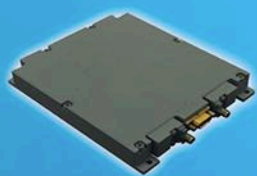

Switched Multiplexers

Switches

Limiters

Equalizers

MMICS

Up to 40 GHz

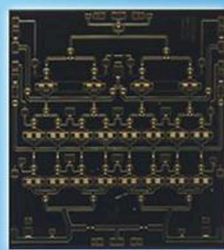

Power Amplifiers

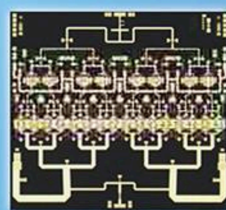

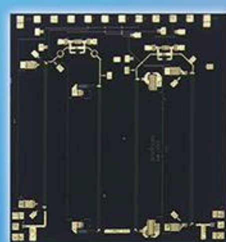

Phase Shifters

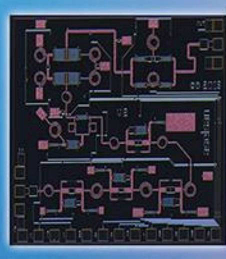

MICROWAVE MODULES

Reliable Products up to 40 GHz

SSPAs

T Modules

R Modules

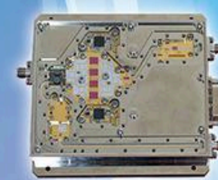

T/R Modules

Up/Down Converters

DFDs

DLVAs

MICROWAVE GROUP
Tel: 90-312-5926000 Fax: 90-312-5926006 rehismarketing@aselsan.com.tr
www.aselsan.com.tr

aselsan

ASELSAN is a Turkish Armed Forces Foundation company.

The Trusted Name in High

X-Band Satcom / Radar Chip-set Solution

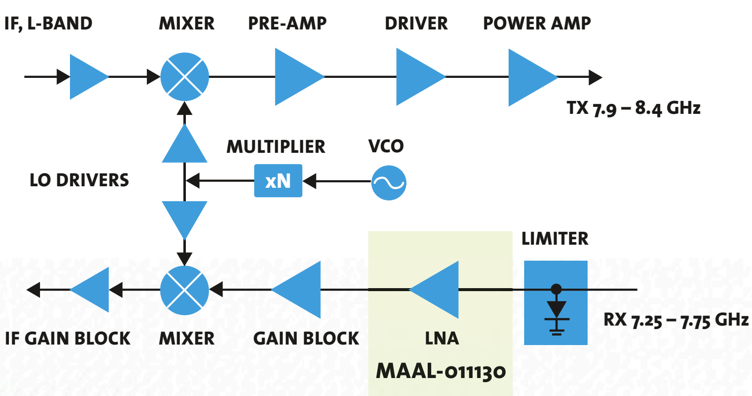

ON MICROWAVES&RF.COM

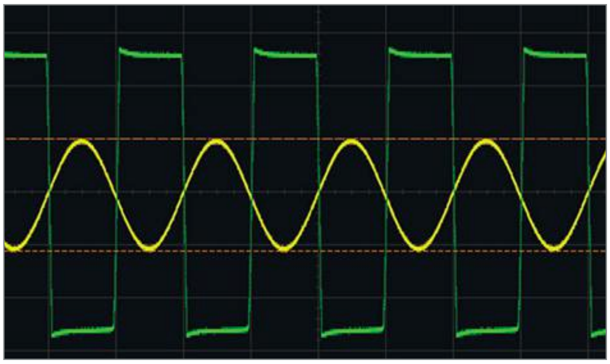

TCXO Performance Guide (And 4 Common Types)

This post, part of a series that discusses different oscillator types, covers temperature-compensated crystal oscillators (TCXOs). More specifically, you will learn some of the best qualities TCXOs typically offer for your applications.

http://www.mwrf.com/components/tcxo-performance-guide-and-4-common-types

Spectrum Apocalypse: The Coming Death of Wireless

Uh-oh! What happens to the future of wireless when we run out of spectrum space? That may seem impossible, but we are already well along that path. Practically speaking, all of the spectrum from DC to visible light has already been used, allocated, or assigned in some way.

http://www.mwrf.com/systems/spectrum-apocalypse-coming-death-wireless

What are the Top Challenges Facing Smartphone Manufacturers?

Rising mobile data demand continues to create complex RF challenges for smartphone manufacturers. Globally, mobile data consumption grew 63% in 2016, and is projected to increase sevenfold by 2021, according to the Cisco Visual Networking Index. Growth is largely being driven by video traffic, which already accounts for more than half of mobile data use.

http://www.mwrf.com/systems/what-are-top-challenges-facing-smartphone-manufacturers

Trying to Keep the Noise Down

Noise is a limiting factor is many receivers and other systems. Essentially, it is unwanted energy that sets the sensitivity of a receiver. While it cannot be eliminated, it can be controlled and managed, enabling receivers to operate effectively with low-level signals.

http://www.mwrf.com/test-measurement/trying-keep-noise-down

twitter.com/MicrowavesRF facebook.com/microwavesrf

CHRIS DeMARTINO | Technical Editor
chris.demartino@penton.com

Are Millimeter Waves the "Wave" of the Future?

The overcrowded spectrum has carriers looking to millimeter-wave frequencies as a solution in the next generation of wireless communications.

Without question, millimeter-wave frequencies are a focal point in the RF/microwave industry today. Millimeter-wave technology is certainly not new, as these higher frequencies have been utilized in select applications for a long time. However, millimeter-wave technology is now being counted on to play a significantly larger role than it did in the past.

Of course, 5G communications is the primary reason behind the interest in millimeter-wave technology. As you have probably heard, 5G networks are expected to utilize millimeter-wave frequencies. One main reason why concerns the already overcrowded spectrum—millimeter-wave bands offer a way around this congestion issue.

Among the carriers, Verizon is surely invested in millimeter-wave technology. Furthermore, in recent news, AT&T announced that it will expand its fixed wireless 5G trials to business and residential customers in Waco, Texas; Kalamazoo, Michigan; and South Bend, Indiana by the end of the year. In the same press release, AT&T says that "it has gained new insights into millimeter-wave performance and propagation."

With all of the activity surrounding 5G and millimeter-wave technology, it should come as no surprise that test-and-measurement equipment suppliers are focused on delivering higher-frequency test capabilities. Don't expect this trend to stop anytime soon.

Two articles in this issue both discuss millimeter-wave technology from different perspectives. "Simulate Your Way to Millimeter-Wave 5G Design Success" discusses how the latest software can be used to overcome challenges associated with 5G development at millimeter-wave frequencies. It can address a variety of aspects, such as hybrid beamforming.

The article "Innovation Leads to Results in Millimeter-Wave Network Analysis" talks about how the latest vector-network-analyzer (VNA) solutions are addressing millimeter-wave testing. These test solutions provide measurement capabilities at frequencies above 100 GHz. Moreover, another article published earlier this year, "VNAs Prove to be Essential Tools for 5G Communications" (go to mwrf.com), discussed the role of VNAs with respect to 5G communications.

To summarize, it is clear that millimeter-wave technology has become a key focus area for many companies throughout the industry. With 5G still under development, millimeter-wave frequencies may very well represent the "wave" of the future. mw


MCL B 744
ADP-2-10
MCL
QBA-12
071838
MCL
BPNC
MCL
BP2C
MCL B 538
SCA-4-15
-75

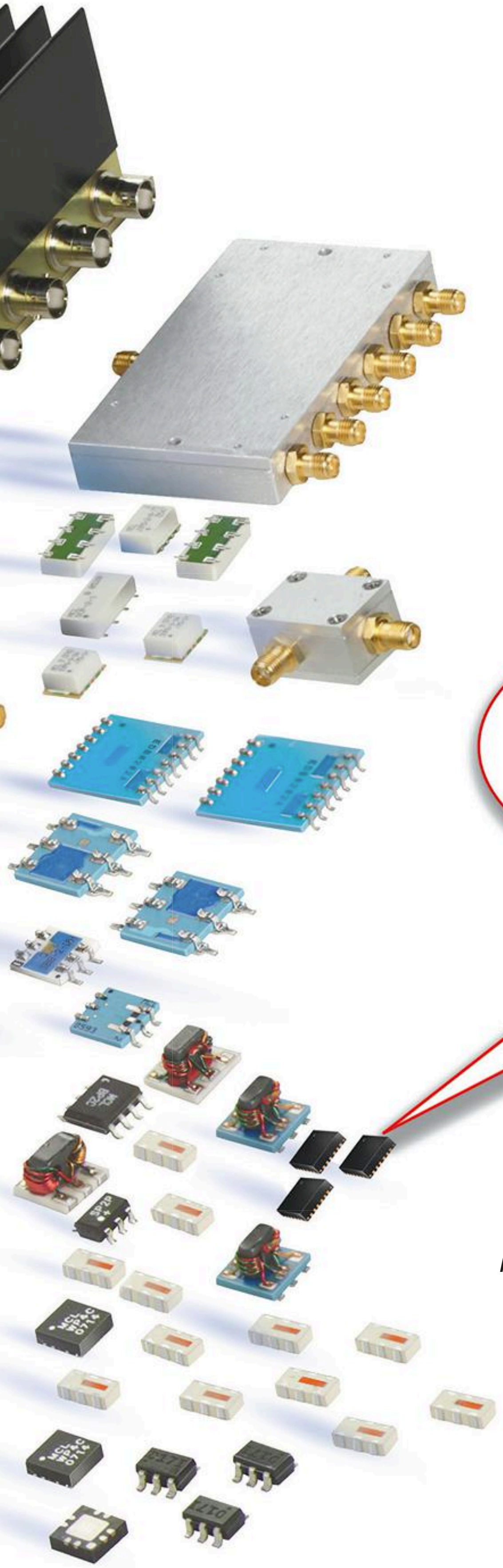

POWER SPLITTERS/ COMBINERS

from **2 kHz to 40 GHz** as low as 89¢ ea. (qty. 1000)

NEW!

THE WIDEST BANDWIDTH IN THE INDUSTRY IN A SINGLE MODEL!

EP2K1+ 2 to 26.5 GHz
EP2W1+ 0.5 to 9.5 GHz
EP2C+ 1.8 to 12.5 GHz

The industry's largest selection includes THOUSANDS of models from 2 kHz to 40 GHz, with up to 300 W power handling, in coaxial, flat-pack, surface mount and rack mount housings for 50 and 75Ω systems.

From 2-way through 48-way designs, with 0°, 90°, or 180° phase configurations, Mini-Circuits' power splitter/combiners offer a vast selection of features and capabilities to meet your needs from high power and low insertion loss to ultra-tiny LTCC units and much more.

Need to find the right models fast? Visit minicircuits.com and use Yoni2®! It's our patented search engine that searches actual test data for the models that meet your specific requirements! You'll find test data, S-parameters, PCB layouts, pricing, real-time availability, and everything you need to make a smart decision fast!

All Mini-Circuits' catalog models are available off the shelf for immediate shipment, so check out our website today for delivery as soon as tomorrow!

RoHS Compliant
Product availability is listed on our website.

Mini-Circuits®

www.minicircuits.com P.O. Box 350166, Brooklyn, NY 11235-0003 (718) 934-4500 sales@minicircuits.com 448 rev T

Microwaves&RF SEPTEMBER 2017

EDITORIAL

CONTENT DIRECTOR: **NANCY K. FRIEDRICH** nancy.friedrich@penton.com
TECHNICAL CONTRIBUTOR: **JACK BROWNE** jack.browne@penton.com
TECHNICAL ENGINEERING EDITOR: **CHRIS DeMARTINO** chris.demartino@penton.com
CONTENT PRODUCTION DIRECTOR: **MICHAEL BROWNE** michael.browne@penton.com
PRODUCTION EDITOR: **JEREMY COHEN** jeremy.cohen@penton.com
CONTENT PRODUCTION SPECIALIST: **ROGER ENGELKE** roger.engelke@penton.com
CONTENT OPTIMIZATION SPECIALIST: **WES SHOCKLEY** wes.shockley@penton.com
ASSOCIATE CONTENT PRODUCER: **LEAH SCULLY** leah.scully@penton.com
ASSOCIATE CONTENT PRODUCER: **JAMES MORRA** james.morra@penton.com

ART DEPARTMENT

GROUP DESIGN DIRECTOR: **ANTHONY VITOLO** tony.vitolo@penton.com
SENIOR ARTIST: **JIM MILLER** jim.miller@penton.com
CONTENT DESIGN SPECIALIST: **JOCELYN HARTZOG** jocelyn.hartzog@penton.com
CONTENT DESIGN SPECIALIST: **TIM DRIVER** tim.driver@penton.com
CONTENT & DESIGN PRODUCTION MANAGER: **JULIE JANTZER-WARD** julie.jantzer-ward@penton.com

PRODUCTION

GROUP PRODUCTION MANAGER: **CAREY SWEETEN** carey.sweeten@penton.com
PRODUCTION MANAGER: **VICKI MCCARTY** vicki.mccarty@penton.com
CLASSIFIED PRODUCTION COORDINATOR: **LINDA SARGENT** linda.sargent@penton.com

AUDIENCE MARKETING

USER MARKETING DIRECTOR: **BRENDA ROODE** brenda.roode@penton.com
USER MARKETING MANAGER: **DEBBIE BRADY** debbie.brady@penton.com
FREE SUBSCRIPTION/STATUS OF SUBSCRIPTION/ADDRESS CHANGE/MISSING BACK ISSUES
OMEDA **T** | 847.513.6022 **TOLL FREE** | 866.505.7173

SALES & MARKETING

MANAGING DIRECTOR: **TRACY SMITH** **T** | 913.967.1324 **F** | 913.514.6881 tracy.smith@penton.com

REGIONAL SALES REPRESENTATIVES
AZ, NM, TX: **GREGORY MONTGOMERY** **T** | 480.254.5540 gregory.montgomery@penton.com

AK, NORTHERN CA, OR, WA, WESTERN CANADA: **STUART BOWEN** **T** | 425.681.4395 stuart.bowen@penton.com

AL, AR, SOUTHERN CA, CO, FL, GA, HI, IA, ID, IL, IN, KS, KY, LA, MI, MN, MO, MS, MT, NC, ND, NE, NV, OH, OK, SC, SD, TN, UT, VA, WI, WV, WY, CENTRAL CANADA: **JAMIE ALLEN** **T** | 415.608.1959 **F** | 913.514.3667 jamie.allen@penton.com

CT, DE, MA, MD, ME, NH, NJ, NY, PA, RI, VT, EASTERN CANADA:
SHANNON ALO-MENDOSA **T** | 978.501.9116 shannon.alo-mendosa@penton.com

INTERNATIONAL SALES
GERMANY, AUSTRIA, SWITZERLAND: **CHRISTIAN HOELSCHER** **T** | 011.49.89.95002778
christian.hoelscher@husonmedia.com

BELGIUM, NETHERLANDS, LUXEMBURG, UNITED KINGDOM, SCANDINAVIA, FRANCE, SPAIN, PORTUGAL:
JAMES RHOADES-BROWN **T** | +011 44 1932 564999 **M** | +011 44 1932 564998 james.rhoadesbrown@husonmedia.com

ITALY: **DIEGO CASIRAGHI** **T** | +011 390 31 261407 diego@casiraghi-adv.com
PAN-ASIA: **HELEN LAI** **T** | 886 2 2727 7799 helen@twoway-com.com
PAN-ASIA: **CHARLES LIU** **T** | 886 2 2727 7799 liu@twoway-com.com

PLEASE SEND INSERTION ORDERS TO: orders@penton.com
PENTON REPRINTS: **WRIGHT'S MEDIA** **T** | 877.652.5295 penton@wrightsmedia.com
LIST RENTALS:
SMARTREACH CLIENT SERVICES MANAGER: **JAMES ADDISON** **T** | 212.204.4318 james.addison@penton.com

ONLINE

PRODUCT DEVELOPMENT DIRECTOR: **RYAN MALEC** ryan.malec@penton.com

DESIGN ENGINEERING & SOURCING GROUP

EXECUTIVE DIRECTOR OF CONTENT AND USER ENGAGEMENT: **NANCY K. FRIEDRICH**
GROUP DIRECTOR OF OPERATIONS: **CHRISTINA CAVANO**
GROUP DIRECTOR OF MARKETING: **JANE COOPER**

PENTON

1166 AVENUE OF THE AMERICAS, 10TH FLOOR, NEW YORK, NY 10036 **T** | 212.204.4200

Electronic Design | Machine Design | Microwaves & RF | Source ESB | Hydraulics & Pneumatics |
Global Purchasing | Distribution Resource | Power Electronics | Defense Electronics

Book Review

JACK BROWNE | Technical Contributor

Learn How to Get Started on a Vector Network Analyzer

PERHAPS NO INSTRUMENT is more synonymous with microwave engineering than the vector network analyzer (VNA). Even the name is offbeat, referring to the analysis of vectors rather than signals, frequency, or noise. But this instrument in an invaluable means of visualizing the flow of microwave signals back and forth through a circuit, whether forward or reflected, and its amplitude and phase characteristics.

For younger engineers, that first opportunity to connect a device under test (DUT) to a microwave VNA may be a bit intimidating, with so many scattering parameters (S-parameters) to check on a screen, and the potential to measure signals well into the microwave and millimeter-wave regions. Fortunately, Rohde & Schwarz *(www.rohde-schwarz.us)* has made the job of learning how to get started on a VNA much easier with all the guidance provided in its 46-page white paper, "Fundamentals of Vector Network Analysis: Primer," available at *www.mwrf.com*.

The white paper provides a clear explanation of why S-parameters are needed when analyzing the flow of signals through a two-port network or component. It uses measurements on a frequency converter as examples of how to use a microwave VNA, including analysis of single-function components within the frequency converters, such as a bandpass filter. The white paper simplifies the interpretation of the Smith chart and how it is used to graphically plot data from the different S-parameters.

The white paper steps through detailed explanations of all the key performance parameters of a VNA—such as directivity, to assist those who may need to specify a VNA, and may be overwhelmed by the number of commercial instruments on the market and the total number of performance parameters that must be compared to select the best analyzer for a particular set of applications. It also reviews the importance of calibration and methods for reducing measurement errors, with numerous measurement tips sprinkled throughout the text. This is a useful piece of literature for anyone with limited experience using a VNA, or even for those who know how to use a VNA but need a handy reference guide. mw

News

At TowerJazz, New Options for MANUFACTURING AUTOMOTIVE CHIPS

For years, automotive chipmakers have followed a formula. Larger suppliers like Infineon and Renesas have not only devised chips but also manufactured them personally. But foundries are trying to flip the script.

TowerJazz announced new manufacturing options for customers eyeing SiGe, RF CMOS, and RF SOI technology for cars, which have strict reliability and quality needs. The specialty purveyor is aiming to tap into the growing market for radar sensors that cover blind spots and wireless chips that chat with nearby cars about their location.

The "specific version of these technologies used for automotive have been optimized both in performance and to meet the high reliability and quality requirements of the automotive market," said Marco Racanelli, senior vice president of the RF and high performance analog business at TowerJazz, which already mints power management chips for electric cars.

That strategy has a strong economic basis. IHS Markit predicts that sales of advanced driver-assistance systems for safety applications will rise to 302 million in 2022, up from 115 million in 2016. These units require cameras, lidar, radar, and other chips that wirelessly share vehicle position and speed.

What TowerJazz changed is evident in its SiGe platform, which has been customized to handle more transistor options, metallization schemes, and passives like capacitors and inductors. That lets customers adjust for speed and noise to optimize radar transmit and receive functions. The firm also plans to make switches and other chips for wireless front ends that help with vehicle-to-everything communications – also known as V2X.

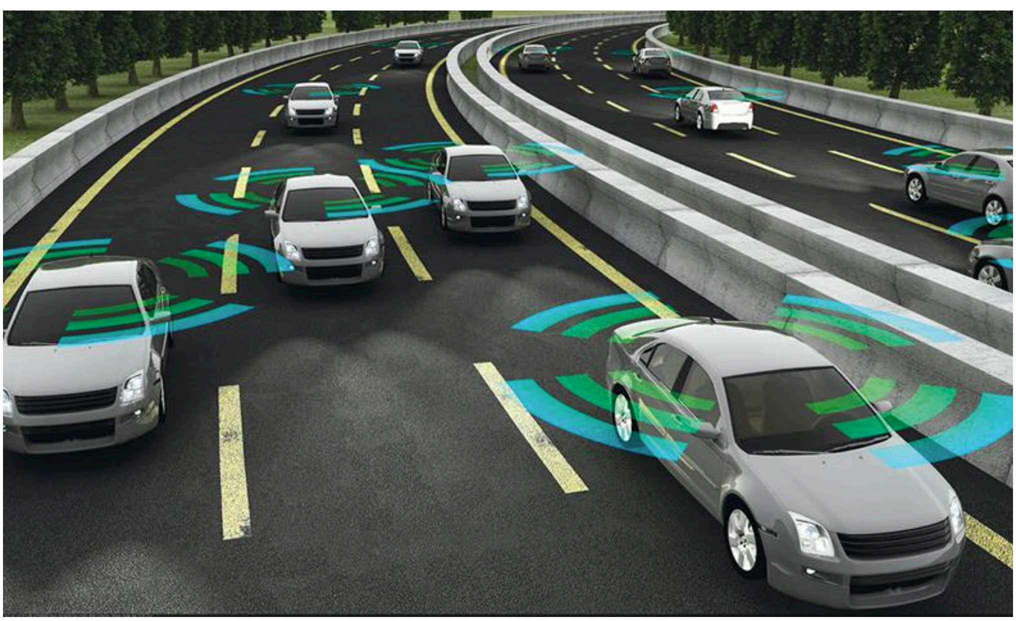

The foundry said that the Japanese parts supplier Denso had signed onto its SiGe process. With it, Denso devised a 24-GHz radar chip that aids collision warning systems while drivers change lanes or reverse. Another TowerJazz process can produce longer-range radar chips that operate from 76 to 81 GHz.

Denso said that it chose TowerJazz because its process could squeeze more functions on a single chip. The final product combined SiGe transistors, which transmit and receive radar signals, with CMOS circuits that control the chip's digital functions. The rear-and-side radar sensor is built into the bumper of the 2018 Toyota Camry.

"The foundry model in automotive is becoming more accepted," said Amol Kalburge, senior director of strategic marketing, in an email. "Our foundry platform solution levels the playing field and enables fabless and fab-light companies to bring multiple innovative products to market rapidly."

For TowerJazz, the circumstances could rally business through the end of its first decade. Founded in 2008, the Migdal Haemek, Israel-based firm recently reported second quarter sales of $345 million, up from $305 million in same span last year. Profit was $50 million, up 30% from last year's second quarter.

TowerJazz was formed following the merger of Tower Semiconductor, based in Israel, and Jazz Semiconductor, based in Newport Beach, Calif. The foundry, which runs two factories in Israel and two in the United States, partnered with Panasonic in 2014 to give customers access to three additional fabs in Japan. ■

TRACKING SLEEPERS BY Analyzing Radio Waves Around Them

AN ALGORITHM DEVISED by researchers at the Massachusetts Institute of Technology can closely monitor sleeping patterns by analyzing radio waves reflected off the human body.

The software, described in a paper presented at the International Conference of Machine Learning, measures frequency changes that occur when radio waves emitted from specialized sensors reflect off a person's body. That could let anyone analyze their sleep patterns at home without wearing smart wristbands and rings to bed.

"Our vision is developing health sensors that will disappear into the background and capture physiological signals and important health metrics," said Dina Katabi, a professor of electrical engineering and computer science, who led the development of the home-router-sized sensors.

Katabi, who co-founded home monitoring start-up Emerald, and her colleagues have been coming up with new applications for the radio sensors, which can analyze pulse and breathing rate and detect emotion. The sensors can measure walking speed, which experts say could help predict cardiac and pulmonary diseases.

The new algorithm calculate body movements, pulse, and breathing patterns to determine if someone is lightly sleeping or showing symptoms of rapid eye movement, which indicates dreaming. The software filters out irrelevant information depending on the layout of your bedroom and how furniture is arranged.

These variables can change how radio waves scatter around a sleeping person, confusing traditional algorithms. But the researchers used machine learning to train their software to only take relevant information into account.

"Imagine if your Wi-Fi router knows when you are dreaming, and can monitor whether you are having enough deep sleep, which is necessary for memory consolidation," Katabi said in a statement, referring to a process by which short-term memories are routed into the region of the brain that handle long-term storage.

These types of wireless sleep trackers are not exactly new, though. ResMed, which sells devices that help manage sleep apnea and other respiratory conditions, released a bedside device in 2014 that monitors sleepers by emitting radio waves to measure breathing and body movements.

The research team—which included Matt Bianchi, chief of the sleep medicine division at Massachusetts General Hospital in Boston—says that their system is 80% accurate, similar to electroencephalography (EEG) machines in hospitals, which connect to patients via electrodes.

In addition to monitoring and tracking treatments for disorders like sleep apnea and insomnia, Katabi and her colleagues suggested that the technology could be used to study Parkinson's, which is associated with complex sleep deficiencies, as well as other diseases like Alzheimer's. ■

ANSYS TRACES SIGNALS Emitted from Cars and Airplanes

ANSYS ADDED ALGORITHMS to its core software that faithfully will simulate how wireless signals react to colliding with trees and buildings as well as hitting patches of electromagnetic interference and rainfall.

The tweaks to the company's software come as engineers face challenges to understanding the nature of millimeter waves. These high-frequency bands are incapable of passing through walls and grapple with other shortcomings. But they are considered vital for 5G communications. Automotive radar systems also harness them to sweep roads for potential dangers.

The updates are not limited to Ansys' electromagnetic software. Mark Hindsbo, vice president of the firm's design and platform business, said in a statement that the software provides "enhanced speed and accuracy—enabling more users, no matter their level of experience, to reduce development time and increase product quality."

Ansys added shooting-and-bouncing-ray algorithms to its electromagnetic tool HFSS, which uses sophisticated solvers to flag emissions and coupling issues. The latest solver visualizes the performance of antennas mounted onto airplanes and cars, which are difficult to simulate without lots of processing power.

Ansys also now includes better visualization and modeling of antennas, which helps engineers find the ideal location for them inside gadgets or large structures like ships. The firm also rolled out an RF link analysis tool that shows how interference hampers radio waves. It can assess the effects of rain, buildings, atmospheric absorption, and statistical signal fading.

The software is another tool with which engineers can chart the behavior of millimeter waves, which are particularly susceptible to signal fading over long distances. Ansys is not alone in trying to make that evaluation process easier: In June, Remcom added diffuse scattering prediction to its radio propagation software.

Other changes also shave down the complexity of meshing, which entails laying triangular cells on models to prep them for simulation. Ansys added what it calls broadband adaptive meshing, which automates the ability of HFSS to refine and optimize the mesh using information taken from a device's frequency spectrum.

Also new are enhanced circuit simulation capabilities. Ansys allows engineers to assemble an electronic system with packaging, sockets, printed circuit boards, and connectors in three dimensions. Then, the entire system can be subjected automatically to electromagnetic and transient circuit analysis. ■

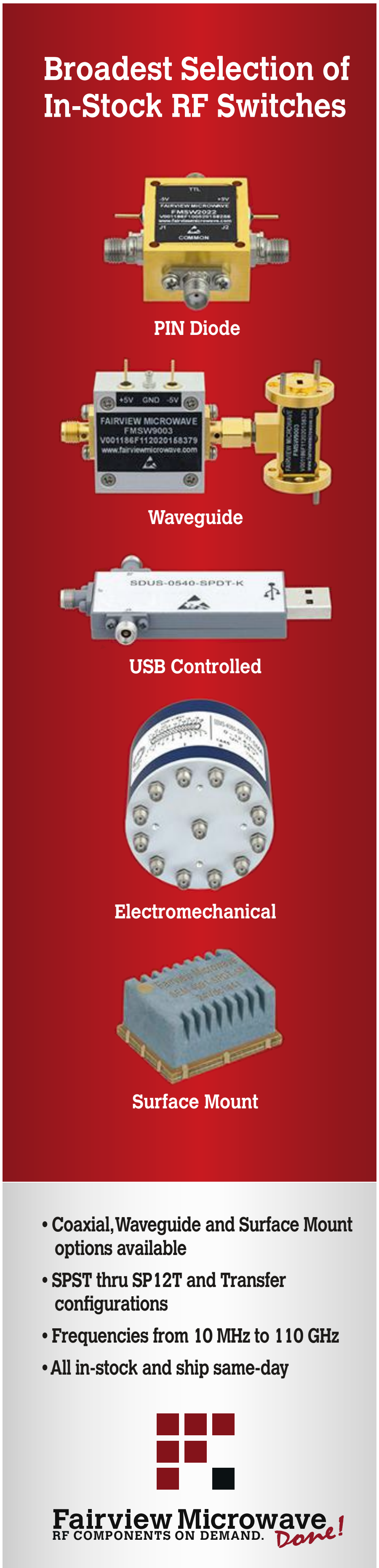

BROADCOM PILES INTO New Generation of Wi-Fi

BROADCOM ANNOUNCED ITS first series of chips for a new type of Wi-Fi, which uses multiple antennas to make more space in spectrum for wireless gadgets. The three products it launched last month are for routers, enterprise access points, and smartphones.

The new standard, more commonly called 802.11ax, will not be agreed upon until around 2019. But chipmakers like Broadcom and Qualcomm have run with early drafts of the standard, which in some ways reflects the fact that Wi-Fi remains the primary window to the internet for billions of people.

"Our reliance on Wi-Fi has increased tremendously as we stream live experiences over social media and upload pictures and files to the cloud while also connecting the many 'things' around our homes," said Greg Fischer, Broadcom's senior vice president of broadband carrier access, in a statement.

The new standard involves coordinating multiple antennas, which send multiple streams of data into devices. An individual stream is split again with orthogonal frequency division multiple access, or OFDMA, which is the same technology used in modern cellular networks. In contrast, earlier types of Wi-Fi created multiple streams but assigned only one to each device.

The standard, which is compatible with legacy protocols, creates a wider pipeline for information and eats through less power and spectrum. It aims to provide better coverage and faster loading times in apartment buildings, offices, stadiums, and other locations crowded with smartphones and other gadgets.

Broadcom, which has started sampling the chips to companies like Netgear and Microsoft, was not first out of the gate. It fell behind Quantenna, a scrappy competitor that began sampling a pair of 802.11ax chips in the wake of an initial public offering that raised $107 million late last year.

Broadcom hopes that its three products will inspire customers to create new Wi-Fi routers, gateways, enterprise access points, and smartphones that fit the standard. Competitors could also contribute to the larger market: This past February, Qualcomm also announced its first range of 802.11ax chips. ■

QUALCOMM'S ABERLE TO Leave at Year's End

DEREK ABERLE, QUALCOMM'S president and second-in-command, will leave the beleaguered chipmaker as it tries to repel revolts from regulators and customers unhappy with its patent licensing business.

Aberle, who will leave at the end of the year, has been president since 2014. For six years before that, he led the company's patent licensing unit, which has been rocked in recent years by regulatory battles and a major patent lawsuit from Apple.

Aberle's exit comes as customers and regulators air grievances with how Qualcomm calculates fees on devices sold using its wireless patents. Apple and other smartphone makers pay a percentage of their sales to access these patents, which contain standard technology for tapping into 3G and 4G wireless networks.

A statement from Qualcomm did not say why Aberle decided to leave. It also did not say whether the recent legal scuffles had anything to do with the decision or not. Qualcomm has cut revenue forecasts in recent months amid battles over patent royalties it charges customers.

After paying a $975 million fine over its licensing practices in China, Qualcomm has faced scrutiny in South Korea for allegedly holding its chip supply hostage to sign better licensing deals and giving rebates to companies that agreed to buy its chips exclusively. It is also under antitrust investigation in the United States, Europe, and Taiwan for withholding patents from competitors, among other allegations.

After Aberle leaves, the president of Qualcomm's licensing business, Alex Rogers, will start reporting directly to chief executive Steve Mollenkopf. Rogers has been the head of patent licensing since March 2016. ■

PACKING MULTIPLE ANTENNAS into a Compact Footprint

ANTENNAS ARE THE BEGINNINGS and ends of most wireless communications systems, and are growing in numbers as wireless RF/microwave technologies are increasingly employed in applications ranging from automotive radars to Internet of Things (IoT) sensors. But antennas add size and weight to a system, depending upon the frequency and wavelength, requiring newer antenna designs to consider multiple resonator arrangements for multiple-band frequency coverage with the equivalent of a single antenna.

With that goal in mind, researchers from the Society for the Applied Microwave Electronic Engineering and Research Center for Electromagnetics in Chennai, India have created an antenna design based on a shared-aperture-antenna (SAA) concept, in which multiple planar antennas are embedded into a single antenna structure. The multiple-frequency-band antenna is a possible lightweight solution for airborne and unmanned-aerial-vehicle (UAV) applications requiring lightweight antennas capable of operating over several different frequency bands.

The number of antennas carried by an aircraft continues to increase, but that number is limited by the size and weight of each discrete antenna. The SAA concept allows all of the antennas to share a common compact space and operate simultaneously, without causing interference with the other antennas in the shared aperture space. For this particular SAA design, each antenna was designed independently and simulated with a three-dimensional (3D) electromagnetic (EM) simulation software program, ignoring mutual coupling effects between the different antennas. Following the design of each independent antenna, they are integrated into the SAA configuration and measurements are performed on the common structure.

The researchers found that the critical factor in the design of an SAA structure is the optimum placement of the individual antennas. The coupling between ports plays a key role in finding the optimum performance of the integrated antenna structure. Optimization can be performed with the aid of measurements of the reflection coefficients of the separate antennas in different placements. The L-band antenna was set in the middle of the antenna structure as a reference, and the other four antennas were moved one at a time within the SAA configuration to observe the effects on different antenna gain and reflection coefficient parameters.

Once optimum positions were found for each antenna, the placement of the SAA relative to the body of the aircraft upon which it was mounted was analyzed and optimized to better understand finite ground-plane effects on the SAA structure. Measurements of the prototype, five-antenna structure revealed that the design concept is a feasible solution for aircraft requiring multiple antennas for different applications.

See “Optimizing Phase-Noise Performance,” *IEEE Microwave Magazine*, Vol. 18, No. 4, June 2017, p. 108.

APPLYING ORTHOGONAL Beamforming for Multiple Wireless Users

FREQUENCY BANDWIDTH IS a limited resource, a fact made more apparent as the number of wireless communications users continues to grow. To explore the most efficient use of available bandwidth, Researchers from the Suranaree University of Technology in Nakhon Ratchasima, Thailand examined the use of orthogonal beamforming methods (OBFMs) for multiple wireless communications users operating at the same frequency.

Wireless technology has become more or less a technological fixture in the lives of many people, and that is expected to only grow with time; more and more people depend upon wireless devices for transferring and storing personal and business information on both fixed and mobile communications devices. The OBFM concept provides multiple-beam formation at the same time and at the same frequency for multiple-user communications. All of the signal beams operating at the same frequency are orthogonal to one another, ideally with maximum gain in the direction of desired users and beam nulls in the directions of other users.

The researchers developed an OBFM approach in which only signal direction-of-arrival (DOA) information on an incoming signal was needed for effective multiuser communications with conventional beamforming techniques. A multiple-user wireless system based on this approach consists of each user having a wireless design with a single antenna element and a base station with a sufficiently large array antenna to handle the multiple users and their individual antenna elements. The researchers developed straightforward formulations for calculating the signal vectors of the individual users' signals at the base station.

Users' signals consist of line-of-sight (LOS) and non-line-of-sight (NLOS) signals which are modeled with Rayleigh fading effects to account for accurate signal characteristics, as observed at the base station. Four omnidirectional antenna elements equally spaced by one-half wavelength ($\lambda/2$) at 2.4 GHz were arranged in a linear manner, thus achieving signals at directions of 30, 60, 90, and 120 deg.

Even though the beams exhibited relative high sidelobes, the researchers' OBFM approach resulted in main beams with strong attenuation of interference effects from neighboring beams at the same frequency. A number of simulations were run with random beams within a 120-deg. sector, and the gain was maximized in the desired beam direction by using the proposed OBFM approach. All of the beams operating at the same frequency are orthogonal to one another so that beam nulls are pointed in the direction of another beam's main energy for minimal interference.

See “Orthogonal Beamforming for Multiuser Wireless Communications,” *IEEE Antennas & Propagation Magazine*, Vol. 59, No. 4, August 2017, p. 38.

HOW-SIANG YAP | Keysight Technologies
www.keysight.com

Simulate Your Way to MILLIMETER-WAVE 5G DESIGN SUCCESS

Software tools specifically geared to 5G can help designers overcome the challenges associated with development at millimeter-wave frequencies.

Modern wireless networks have come to a crossroads as mobile users consume more data than ever before, with no signs of that trend abating anytime soon. Data consumption is crammed into an already overcrowded spectrum, which means less bandwidth for each user. The end result is slower service and increasingly dropped connections.

Enter the millimeter-wave (mmWave) spectrum. This underutilized frequency spectrum is now being eyed as the answer to the bandwidth shortage. However, the ability to transmit large amounts of data isn't the only trait that makes mmWaves so appealing. These waves are broadcast at extremely high frequencies, between 30 and 300 GHz, and those high frequencies can deliver faster wireless communication—exactly what 5G aims to deliver.

With its ability to handle much more data traffic at much higher speeds than today's cellular networks, mmWave is seen as a critical linchpin in making 5G a reality. But that vision is not without its engineering challenges.

PHASED ARRAYS AND BEAMFORMING: CHALLENGES AHEAD

Two crucial technologies in the delivery of 5G services are the phased-array antenna and hybrid beamforming. Phased-array antennas provide a way to leverage high-capacity—but high-loss—mmWave frequencies for 5G systems. Beamforming controls the direction of the reception or transmission of signals at the antenna array.

Together, these technologies improve signal quality, reduce interference, and boost cell coverage. This is especially vital at the cell edge, where performance demands are at their highest and user devices experience the most degraded signal-to-noise conditions and highest levels of inter-cell interference.

A key advantage of using beamforming with the phased-array antenna design is that it provides higher link-level gains to overcome direct path loss and undesirable interference sources in 5G systems. The downside is it can be costly to implement, often requiring a transmit/receive (T/R) module dedicated to each antenna-array element.

Hybrid beamforming offers designers a way to mitigate this cost by partitioning beamforming between the digital and RF domains. Hybrid-beamforming designs combine multiple array elements into subarray modules. Also, because a single T/R module can be dedicated to multiple elements in the array, the 5G system requires fewer T/R modules.

While it's clear that phased-array antennas and hybrid beamforming will be critical to supporting a 5G future, these technologies present two important challenges:

- *Accurate verification and visualization of hybrid-beamforming signal performance at the phased-array antenna:* Accurate verification is critical to ensuring the 5G system works optimally and that it complies with emerging 5G specifications. The issue is that there are many aspects of a 5G system. Without the right channel models and simulation functionality, accurately verifying that they all work together is next to impossible.
- *Addressing spurious harmonics and intermodulation interference (intermods):* An often overlooked, but extremely important aspect of phased-array antenna design, is simulation of the spurious harmonics and intermods generated by amplifiers and mixers radiating through the phased array. Spectrally, when these beams are at spurious frequencies, they may violate FCC emission rules on allowable effective isotropic radiated power (EIRP). Spatially, the spurious beams may also interfere with nearby antennas or multi-beam operation of the active electronically steered array (AESA). These factors can result in phased-array deployment failures in the field, both in 5G and aerospace/defense applications, which are typically costly and difficult to fix.

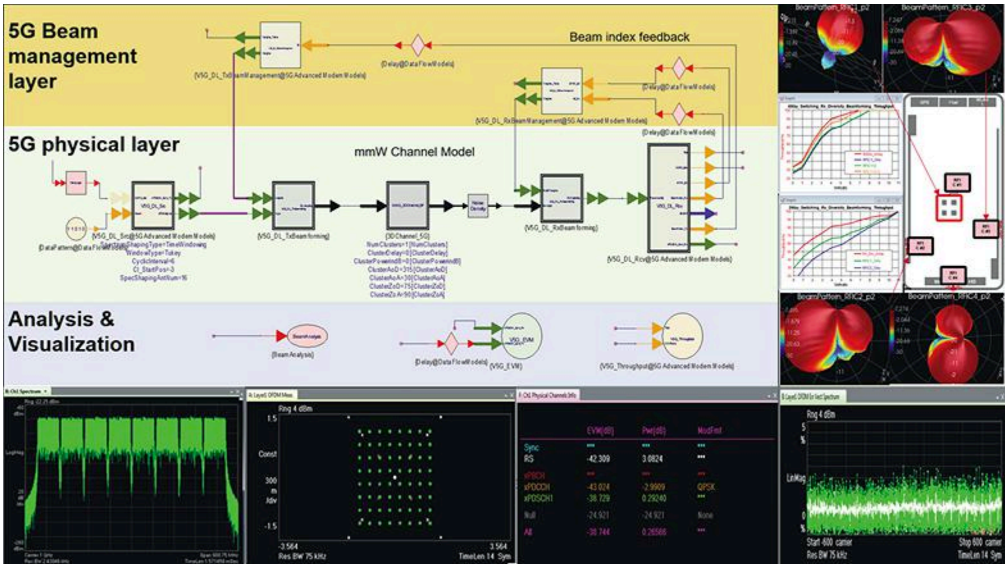

1. Keysight's SystemVue 2017 supports 5G link-level validation with phased-array antennas and hybrid beamforming in a 100-GHz mmWave channel (based on 3GPP). It is the only simulation tool to implement this advanced channel model.

TURNING TO SIMULATION

These issues can be addressed through simulation, but not just with any commercially available simulation tool. On the contrary, the ideal solution must support emerging and future 5G standards and offer a range of 5G functionality, as well as support for mmWave channels. It should give designers the flexibility to create pre-5G-compliant reference designs. Furthermore, it must allow for verification of phased-array hybrid beamforming and antenna diversity between the base station and handset in 0.5- to 100-GHz mmWave channels with Verizon-KT 5G signals.

The ideal simulation solution should also be able to account for a range of RF effects (e.g., the ability to incorporate S-parameters of off-the-shelf phase shifters and attenuators, and X- or Sys-parameters of nonlinear amplifiers and mixers). As a result, designers could characterize the radiation of spurious intermodulation signals from the array in terms of direction and power, ensuring accurate phased-array antenna design. Additionally, it should offer a 5G standards verification library that cellular systems and component designers can use to start pre-5G now, and continue using when the final 5G New Radio (NR) standards become available.

How would such a simulation tool address the two previously identified challenges? Consider the first challenge: verification. 5G hybrid beamforming requires the design of phased-array antennas that are fed with phase and amplitude excitations. These excitations are generated through the combination of analog-RF phase shifters and attenuators, together with baseband complex precoding signals.

Baseband precoding is a computationally intensive process. It is performed in the base station by estimating the mmWave-channel state information from received user signals, and then selecting the optimal precoding complex modulation from a code book to be applied to the signal streams for each user.

Each user signal stream is further refined through additional complex baseband precoding. This added step ensures optimal transmission from the base-station phased array to the user handset. As shown in *Figure 1*, the handset may also include multiple antennas. In this figure, the actual electromagnetic (EM) antenna pattern is used to realistically model the signal gain from different orientations of the handset with respect to the base station. A commercially available simulation tool with 5G verification functionality is used for this exercise. Handset diversity simulation is enabled by adaptively switching between antennas with the highest received signal strength for the best data throughput.

Using this process, the complete 5G end-to-end data throughput rate can be simulated realistically to verify that all aspects of the systems are optimally designed to work together, including:

- Hybrid RF-digital beamforming and pre-coding DSP algorithms
- RF phased-array MIMO system architecture at base station
- Handset multiple-antenna placement and radiation patterns
- 5G signals and modulation formats for optimizing time, frequency, and spatial resources
- RF linear and nonlinear components characterized by S-, X-, or Sys-parameters

Much like the solution to the verification challenge, the solution to addressing spurious harmonics and intermods is simulation. By employing a simulation tool with 5G functionality, designers can accurately predict the frequency, direction, and root cause of spatially radiated spurious harmonics and intermods.

By analyzing the root cause of spurious intermods, designers can easily identify how they are generated, the components that generate them, and through what signal paths in the RF chain. With this information, it then becomes possible to fix any flaws before hardware implementation and before they turn into costly, difficult-to-fix problems *(Fig. 2)*.

AN EASIER PATH TO 5G

While 5G standards are still evolving, it's clear the quest for higher data rates will not dissipate any time soon. Higher-frequency mmWave spectrum is one way to accommodate increases in data consumption, but its use further complicates the design and verification process. Fortunately for designers, these challenges can be mitigated through the appropriate simulation.

Granted, finding a simulation tool specifically equipped to handle emerging 5G standards like Verizon-KT 5G, as well as work with mmWave channels, is paramount. A simulation solution can also be used for pre-5G development right now. Once the 5G NR standard is finalized, the tool is even better. It not only gives RF and baseband designers the earliest possible head start in entering the high-margin 5G system and component market, but also puts them on the right path to 5G success. mw

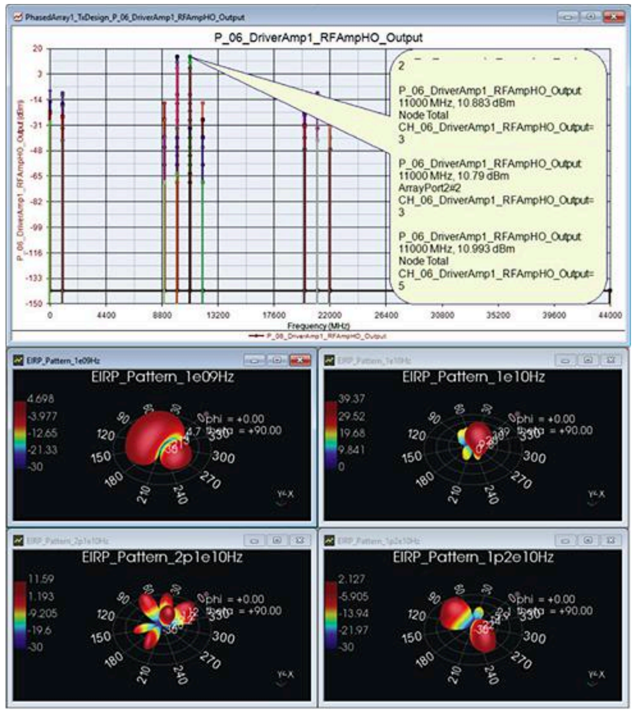

2. Using SystemVue 2017 can help identify the root cause of spurious intermod beams from a phased array.

JACK BROWNE | Technical Contributor

Metamaterials Provide Novel EM Capabilities

Metamaterials have been under study for several decades due to their novel electrical characteristics and becoming more practical with the growing use of 3D metal printing.

METAMATERIALS ARE ENGINEERED materials that are capable of characteristics not found in naturally occurring materials. They can be fabricated with negative refractivity, which causes an electromagnetic (EM) wave to reflect in a direction opposite of what might be expected. Since metamaterials can be structured to affect sound and light waves as well, a great deal of experimentation has been performed with these materials to control audio sound levels and even to control the amount of light reflecting from an object, possibly to the point of invisibility—having all light reflecting away from a viewer. One of the attractions for performing research on metamaterials, which can be produced by three-dimensional (3D) metal printers, is that they can render an object invisible to sound, light, and EM waves, enabling them to be used as a "cloaking" device against radar detection.

Metamaterials are composites formed with an artificial periodic structure (*Fig. 1*). It is the configurations of these periodic structures that result in "unnatural" material characteristics, including the modification of a material's electrical permittivity (ε) and magnetic permeability (μ). By designing the configuration of the periodic structures, the dispersion, refraction, and reflection of an EM wave can be controlled.

In terms of practical RF/microwave engineering, the use of metamaterials with certain transmission-line structures has enabled the miniaturization of microwave filters in ways that defy the normal impedance/transmission-line/wavelength relationships (*see "Metamaterials Form Miniature Bandstop Filters" on mwrf.com) http://www.mwrf.com/passive-components/metamaterials-form-miniature-bandstop-filters*). The effect of metamaterials on EM waves extends from radio waves to well into the optical region. In the microwave frequency range, the use of metamaterials as the basic for transmission-line structures such as split-ring resonators (SRRs) and complementary split-ring resonators (CSRRs) has led to the development of much-needed components that can be significantly miniaturized by fabricating them on these materials, including antennas, filters, phase shifters, and resonators. Such structures can be combined with conventional microwave transmission-line technologies, such as microstrip, to create circuits that operate at "subwavelengths" of a design frequency, resulting in component sizes a fraction that of conventional circuit designs.

1. Compact radar systems have been built around metamaterial electronically scanned array (MESA) antennas and other metamaterial-based components. *(Photo courtesy of Echodyne)*

Finite-element three-dimensional (3D) EM simulation software has proven to be an invaluable tool in the design of these "mixed-technology" circuits, since material parameters can be entered and stored to create working models of the metamaterials. When it is time to manufacture a metamaterial microwave circuit, additive manufacturing techniques, in which different materials are layered on top of each other to create a composite, have proven to be an effective method for producing metamaterial components. Additive manufacturing is becoming more practical with the increasing availability of 3D direct metal printers that can transform the powdered forms of the metals required into the film layers needed for a metamaterial circuit.

CREATING AN ILLUSION

Through manipulation of the period structures of these materials, it is possible to achieve simultaneous negative permittivity and permeability, resulting in what is known as left-handed materials (for having refraction and reflection characteristics that behave in the reverse manner as standard, right-handed materials). The phenomenon of producing materials with negative permittivity and permeability has led to a great deal of the "sensationalism" attached to metamaterials in recent years, including the possibility that metamaterials could be used to achieve optical invisibility by altering the way that light waves reflect and refract from the surface of a metamaterial, essentially by steering the light waves away from the path of a view so that the object covered with the metamaterial is rendered invisible.

These same material capabilities at lower EM frequencies have captured the attention of military systems designers and

2. Ground-based radar systems used metamaterial-based flat-panel antennas can provide surveillance of the ground and UAVs simultaneously. (*Photo courtesy of Echodyne*)

defense research organizations such as the Defense Advanced Research Projects Agency (DARPA, *www.darpa.mil*), which see many possibilities for the application of metamaterials beyond just the miniaturization of high-frequency components, including for terahertz (THz) frequency applications and as "cloaking" devices. By using the negative permittivity and permeability characteristics of metamaterials, for example, an aircraft or a ground vehicle covered in the metamaterials could be rendered invisible to an adversary's radar beams and detection.

DARPA recently awarded nearly $8 million (USD) to Penn State University, specifically to Doug Werner, John McCain, and Genevieve McCain, to continue their research into metamaterials. This is actually a combined award from DARPA, the U.S. Navy, and Lockheed Martin (*www.lockheedmartin.com*), with DARPA 'chipping in" more than $5 million. Werner is the director of the Computational Electromagnetics and Antennas Research Lab (CEARL) at the university, and the funding is intended to develop EM cloaking technology, as might be used as a defense against detection by enemy radars. The funding is also expected to deliver advanced software simulation tools for the modeling and design of metamaterials and metamaterial-based components. Penn State will take the lead on the project, and will collaborate with researchers from Purdue University, Rensselaer Polytechnic Institute, and ExH Inc.

INTEREST IS SPREADING

A number of leading universities are involved in metamaterial research, including Duke University and its Center for Metamaterials and Integrated Plasmonics (CMIP, *www.metamaterials.duke.edu*), the University of Notre Dame, Oregon State University, and Boston University. In addition, a number of new companies are forming to pursue the promise of metamaterials throughout the EM spectrum. At "lower" microwave wavelengths, for example, Echodyne (*www.echodyne.com*) has developed a series of metamaterial electronically scanned array (MESA) antennas and other metamaterial-based products that are providing unique capabilities to military, industrial, and commercial customers. The patented MESA products are enabling the development of compact, lightweight radar transceivers with electronically scanned radar capabilities for small aircraft and unammed aerial vehicles (UAVs). These metamaterial antennas (*Fig. 1*) and systems show negligible radar cross-sections (RCSs) to an enemy radar and are well suited for integration in UAVs intended for surveillance applications. The company also offers a ground version (MESA-SSR) of the metamaterial-based radar system which can be integrated into any site for surveillance and security applications. This ground-based system operates like a phased-array radar with true beam scanning in both azimuth and elevation. It can track airborne and ground-based targets at the same time (*Fig. 2*), as well as walkers from a distance of about 1.4 km.

Kymeta Corp. (*www.kymetacorp.com*) has also commercialized metamaterials, into several lines of innovative antennas and antenna modules. The mTenna antenna subsystem modules (ASMs) are compact, lightweight flat-panel antenna assemblies with no moving parts that can be used for transmit and receive functions with a single aperture. The metamaterial-based antenna designs realize the capability of these materials to perform amplitude and phase control of separate antenna elements, to achieve the performance of a phased-array antenna in a fraction of the size. Electronic beam steering is performed by means of software control.

At optical wavelengths, Metamaterial Technologies Inc. (MTI, *www.metamaterial.com*) has developed metamaterial product lines based on altering the flow of light waves. The company's product lines include Lamda Guard optical filters, to block light and protect vision;

Lamda Lux films, to enhance the efficiency and output of light-emitting-diode (LED) lighting; and Lamda Solar films, to absorb light and increase the efficiency of solar cells. The Lamda Guard filters, for example, can be engineered to block specific wavelengths of light to protect vision, such as for pilots. The materials and light in weight and adhesive, and can be attached to any surface. Since 2014, the company has worked in partnership with Airbus to develop optical filters to protect pilots' vision from laser strikes. MTI recently signed a $5.6 million agreement with Lockheed Martin to develop MTI's metaSOLAR product line. The materials will be used for solar energy harvesting.

Research on metamaterials is ongoing and is sure to lead to wide acceptance of these novel materials in applications throughout the EM spectrum. While efforts are being made to better understand the materials and how to efficiently manufacture them, much research is also focused on the modeling and simulation of the materials, with broad opportunities ahead for suppliers of software simulation tools ready and willing to integrate accurate metamaterial models within their simulation programs. mw

HIGH POWER

5 - 500 WATTS PRODUCTS

POWER DIVIDERS RoHS

Model #	Frequency (MHz)	Insertion Loss (dB) [Typ./Max.] ◊	Amplitude Unbalance (dB) [Typ./Max.]	Phase Unbalance (Deg.) [Typ./Max.]	Isolation (dB) [Typ./Min.]	VSWR (Typ.)	Input Power (Watts) [Max.] ◦	Package
2-WAY								
CSBK260S	20 - 600	0.28 / 0.4	0.05 / 0.4	0.8 / 3.0	25 / 20	1.15:1	50	377
DSK-729S	800 - 2200	0.5 / 0.8	0.05 / 0.4	1 / 2	25 / 20	1.3:1	10	215
DSK-H3N	800 - 2400	0.5 / 0.8	0.25 / 0.5	1 / 4	23 / 18	1.5:1	30	220
P2D100800	1000 - 8000	0.6 / 1.1	0.05 / 0.2	1 / 2	28 / 22	1.2:1	2	329
DSK100800	1000 - 8000	0.6 / 1.1	0.05 / 0.2	1 / 2	28 / 22	1.2:1	20	330
DHK-H1N	1700 - 2200	0.3 / 0.4	0.1 / 0.3	1 / 3	20 / 18	1.3:1	100	220
P2D180900L	1800 - 9000	0.4 / 0.8	0.05 / 0.2	1 / 2	27 / 23	1.2:1	2	331
DSK180900	1800 - 9000	0.4 / 0.8	0.05 / 0.2	1 / 2	27 / 23	1.2:1	20	330
3-WAY								
S3D1723	1700 - 2300	0.2 / 0.35	0.3 / 0.6	2 / 3	22 / 16	1.3:1	5	316
4-WAY								
CSDK3100S	30 - 1000	0.7 / 1.1	0.05 / 0.2	0.3 / 2.0	28 / 20	1.15:1	5	169S

◦ With matched operating conditions

HYBRIDS RoHS

Model #	Frequency (MHz)	Insertion Loss (dB) [Typ./Max.] ◊	Amplitude Unbalance (dB) [Typ./Max.]	Phase Unbalance (Deg.) [Typ./Max.]	Isolation (dB) [Typ./Min.]	VSWR (Typ.)	Input Power (Watts) [Max.]	Package
90°								
DQS-30-90	30 - 90	0.3 / 0.6	0.8 / 1.2	1 / 3	23 / 18	1.35:1	25	102SLF
DQS-3-11-10	30 - 110	0.5 / 0.8	0.6 / 0.9	1 / 3	30 / 20	1.30:1	10	102SLF
DQS-30-450	30 - 450	1.2 / 1.7	1 / 1.5	4 / 6	23 / 18	1.40:1	5	102SLF
DQS-118-174	118 - 174	0.3 / 0.6	0.4 / 1	1 / 3	23 / 18	1.35:1	25	102SLF
DQK80300	800 - 3000	0.2 / 0.4	0.5 / 0.8	2 / 5	20 / 18	1.30:1	40	113LF
MSQ80300	800 - 3000	0.2 / 0.4	0.5 / 0.8	2 / 5	20 / 18	1.30:1	40	325
DQK100800	1000 - 8000	0.8 / 1.6	1 / 1.6	1 / 4	22 / 20	1.20:1	40	326
MSQ100800	1000 - 8000	0.8 / 1.6	1 / 1.6	1 / 4	22 / 20	1.20:1	40	346
MSQ-8012	800 - 1200	0.2 / 0.3	0.2 / 0.4	2 / 3	22 / 18	1.20:1	50	226
180° (4-PORTS)								
DJS-345	30 - 450	0.75 / 1.2	0.3 / 0.8	2.5 / 4	23 / 18	1.25:1	5	301LF-1

◊ In excess of theoretical coupling loss of 3.0 dB

COUPLERS RoHS

Model #	Frequency (MHz)	Coupling (dB) [Nom]	Coupling Flatness (dB)	Mainline Loss (dB) [Typ./Max.]	Directivity (dB) [Typ./Min.]	Input Power (Watts) [Max.] ◦	Package
KFK-10-1200	10 - 1200	40 ±1.0	±1.5	0.4 / 0.5	22 / 14	150	376
KDS-30-30	30 - 512	27.5 ±0.8	±0.75	0.2 / 0.28	23 / 15	50	255 *
KBS-10-225	225 - 400	10.5 ±1.0	±0.5	0.6 / 0.7	25 / 18	50	255 *
KDS-20-225	225 - 400	20 ±1.0	±0.5	0.2 / 0.4	25 / 18	50	255 *
KBK-10-225N	225 - 400	10.5 ±1.0	±0.5	0.6 / 0.7	25 / 18	50	110N *
KDK-20-225N	225 - 400	20 ±1.0	±0.5	0.2 / 0.4	25 / 18	50	110N *
KEK-704H	850 - 960	30 ±0.75	±0.25	0.08 / 0.2	38 / 30	500	207
SCS100800-10	1000 - 8000	10.5 ±1.5	±2.0	1.2 / 1.8	8 / 5	25	361
KBK100800-10	1000 - 8000	10.5 ±1.5	±2.0	1.2 / 1.8	8 / 5	25	322
SCS100800-16	1000 - 7800	16.8 ±1.5	±2.8	0.7 / 1.0	14 / 5	25	321
KDK100800-16	1000 - 7800	16.8 ±1.5	±2.8	0.7 / 1.0	14 / 5	25	322
SCS100800-20	1000 - 7800	20.5 ±2.0	±2.0	0.45 / 0.75	12 / 5	25	321
KDK100800-20	1000 - 7800	20.5 ±2.0	±2.0	0.45 / 0.75	14 / 5	25	322
KEK-1317	13000 - 17000	30 ±1.0	±0.5	0.4 / 0.6	30 / 15	30	387

* Add suffix - LF to the part number for RoHS compliant version.
◦ With matched operating conditions

Unless noted, products are RoHS compliant.

SYNERGY® MICROWAVE CORPORATION

Phone: (973) 881-8800 | Fax: (973) 881-8361
E-mail: sales@synergymwave.com
Web: WWW.SYNERGYMWAVE.COM
Mail: 201 McLean Boulevard, Paterson, NJ 07504

SUREN SINGH | Industry Application Specialist, Keysight Technologies
www.keysight.com

Innovation Leads to Results in Millimeter-Wave Network Analysis

These broadband network analyzer solutions have been unleashed to meet the growing need for millimeter-wave testing.

1. The broadband millimeter-wave network analyzer solution includes an advanced VNA, a test-set controller, and compact frequency extenders.

THE CHARACTERIZATION AND modeling of broadband devices presents many challenges, and these become more difficult as new-generation designs move up to millimeter-wave frequencies. When assessing a vector network analyzer (VNA), which is the most commonly used tool, the crucial attributes beyond single-sweep frequency range include stability and uncertainty across the entire measurement band.

A new solution is a broadband millimeter-wave network analyzer, which provides exceptional measurement performance with stability within 0.015 dB and 0.15° over a 24-hour period. Keysight Technologies' N5290A and N5291A broadband millimeter-wave network analyzers cover a frequency range of 900 Hz to 120 GHz *(Fig. 1)*. They leverage the company's capabilities in terms of metrology and calibration, providing traceable, metrology-grade results across the full frequency range.

INNOVATING IN TECHNOLOGY AND OPENING NEW DOORS

Millimeter-wave technology has been around for decades, primarily in aerospace/defense and backhaul applications where the benefits have justified the high costs of development, manufacturing, and support. More recently, advancements in fabrication have been driving down the cost of extremely high frequency (EHF) devices, making them more viable in commercial and consumer applications. For example, developers using complementary metal-oxide semiconductor (CMOS) technology have produced devices with f_T greater than 500 GHz, and some are aiming to extend this cost-effective technology into the terahertz (THz) range.

Keysight is among the firms developing EHF components. The company's in-house capabilities in microwave semiconductor technology have led to the creation of a next-generation indium-phosphide (InP) process that supports transistor switching frequencies above 300 GHz. This makes it possible to achieve wider bandwidth in the integrated circuits (ICs) used in test equipment and other devices.

OVERCOMING THE OBSTACLES TO BETTER MEASUREMENTS

Two key issues—guiding signals and generating power—are especially challenging in the creation of commercial, off-the-shelf test equipment that produces accurate, repeatable results at millimeter-wave frequencies. Waveguide is a crucial example, as it must be as close to perfect as possible to ensure proper internal operation of a millimeter-wave instrument.

Managing signals between 100 GHz and 1 THz requires use of different waveguide bands. At such short wavelengths, any skew in a flange connection can cause unwanted reflections that will degrade signal quality and reduce signal power.

Generating adequate power levels is challenging because it is difficult to maintain amplifier efficiency and linearity simultaneously at these frequencies. This tends to limit the maximum power level that a signal generator or network analyzer can produce.

Once these problems have been solved, the next big issues concern calibration of the instrument and its surrounding test setup. It is difficult to accurately calibrate power levels at extremely high frequencies. However, precise control of power is essential to ensure measurement accuracy and avoid damage to the device-under-test (DUT).

For novices, millimeter-wave measurements may seem to involve a combination of art, science, and luck. In reality, engineers will benefit from a fresh start: set aside old habits, take a deliberate approach, and adjust all expectations. For example, it's necessary to pay careful attention to every stage of a measurement setup: instruments, cables, and accessories. This means taking time to ensure pristine connections, clean upconversion of output signals, precise downconversion of incoming signals, low-level internal spurious signals, and well-managed internal harmonics. These factors are crucial to successful network analysis and the characterization of passive or active devices (S- or X-parameters, respectively).

UNITING THE ESSENTIAL MEASUREMENT CAPABILITIES

Keysight has addressed these details with its new broadband millimeter-wave solutions. The measurement platform is a PNA or PNA-X VNA operating at either 26.5 or 67 GHz. The other core elements are a two- or four-port millimeter-wave test-set controller and a set of compact frequency extenders ("smart modules"). The latter include ruggedized 1.0-mm connectors, convection cooling, and built-in characterization data to enable fully calibrated port power at turn-on. To simplify benchtop measurements, engineers can mount the frequency extenders on an optional desktop positioner.

The new solutions produce measurements that are traceable to national measurement institutes. The foundation is a 1.0-mm calibration kit, and the result is traceable measurement uncertainty for key performance parameters such as residual calibration errors, system dynamic accuracy, and stability. A companion USB thermocouple power sensor (U8489A) covers a frequency range of dc to 120 GHz and simplifies source-power calibration with a 1.0-mm connector and single-connection convenience *(Fig. 2)*. To further enhance measurement results, the user can choose to apply automatic fixture de-embedding to connectorized measurements or perform calibration at the probe tips to enhance the accuracy of on-wafer measurements.

2. Providing high accuracy and stability, the companion USB thermocouple power sensor enables users to quickly and confidently make average-power measurements.

ENHANCING STABILITY AND PRECISION WITH MECHANICAL INNOVATIONS

At millimeter-wave frequencies, the overall performance of a measurement system also depends on its physical and mechanical design. Inside the new smart modules, Keysight has applied advanced machining capabilities to fabricate wideband coupler technology that provides exceptional stability during measurement calibration.

In the test-set controllers and smart frequency-extender modules, ruggedized 1.0-mm test ports ensure repeatable connections from measurement to measurement, day after day. This reduces calibration uncertainty and further improves system-level measurement precision.

TESTING MULTIPLE COMPONENTS IN ONE SETUP

New-generation monolithic microwave integrated circuits (MMICs) incorporate components that operate in different frequency ranges: baseband, RF, microwave, and millimeter-wave. A VNA with single-sweep coverage from Hz to GHz enables developers to test all those components in one test setup.

Wider frequency coverage also reduces the cost of the test solution. For example, a 900-Hz start frequency in a millimeter-wave network analyzer may eliminate the need to purchase a dedicated low-frequency VNA. An added benefit is this: The ability to use one analyzer saves time and reduces complexity by streamlining the development of test system software.

Greater integration inside MMICs and other wideband designs often means testing more functions per device through fewer access points. The need to connect, disconnect, and reconnect the DUT to a VNA or spectrum analyzer is inconvenient and time-consuming, whether done manually or automatically through a switch matrix.

The most convenient solution is a VNA with a single-connection/multiple-measurement (SCMM) architecture. As implemented in the PNA-X network analyzers, engineers can measure key characteristics of passive or active devices with one set of connections: S-parameters, noise figure, gain compression, total harmonic distortion, intermodulation distortion, and more. For additional versatility, the SCMM capability supports the PNA family's spectrum analysis measurement application.

SIMPLIFYING COMPLEX TASKS WITH MEASUREMENT APPLICATIONS

To help users save time and easily configure complex tasks, measurement applications address specific tests and enable deeper insights into device performance. The capabilities include:

- Scalar mixer/converter measurements: Support scalar characterization of mixers and frequency converters
- Gain-compression application: Provides complete characterization of amplifiers and frequency converters
- Noise-figure measurements: Enable further characterization of frequency-converter performance
- Differential and I/Q devices application: Simplifies testing of amplifiers and mixers
- Spectrum analyzer application: Provides calibrated multi-channel spectrum analysis up to 120 GHz, or into the THz range with compatible frequency extenders

These measurement applications are also touch-enabled, further simplifying complex operations and providing an intuitive approach to investigating, characterizing, and troubleshooting broadband millimeter-wave devices *(Fig. 3)*.

LEVERAGING A COMMON PLATFORM

Good usability is beneficial when performing basic measurements such as S-parameters, and it becomes essential when delving into complex tasks such as the characterization of mixers and other frequency-conversion devices. To help ensure meaningful results in less time, many customers asked Keysight to build measurement guides into its instruments and to present those tools on the screen of the analyzer. This is an important concept, given the time pressures and design requirements most engineers face. It's also a logical and feasible idea that utilizes the processor, memory, and display resources in the latest VNAs.

To address these needs, the Keysight design team pursued parallel development along two tracks: measurement performance and front-panel usability. To provide a foundation for next-generation Keysight VNAs, the development team created a common platform that leverages the best attributes of the established ENA and PNA network analyzer families.

Two guiding principles were paramount: Be inviting and intuitive for new users, but remain familiar and comfortable for existing users. The result is a graphical user interface (GUI) that is helpful to engineers who, from time to time, need to make a variety of measurements—simple or complex—while characterizing or troubleshooting a variety of RF components or subsystems. It is also useful to experienced users who occasionally need to make highly complex measurements and will benefit from reminders about the crucial steps and settings *(Fig. 4)*.

All users will appreciate the familiarity of touch-enabled GUI technology akin to that used in smartphones, tablets, and laptops. The updates include the following attributes:

- 12.1-in. widescreen display with multi-touch GUI
- Easy access to frequently used functions
- Quick setups using touch-activated tabbed softkeys and dialog menus
- Intuitive single- and multi-touch gestures to drag-and-drop or magnify traces
- Versatile, touch-driven marker capabilities

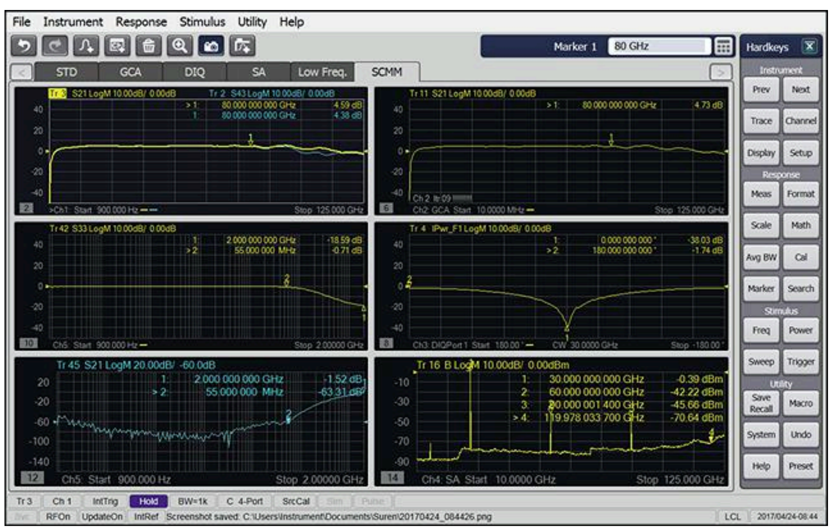

3. The combination of SCMM capability and touch-enabled measurement applications accelerates and simplifies the characterization of gain compression (top right), differential devices (middle right), and harmonic content (lower right).

At millimeter-wave frequencies, the overall performance of a measurement system also depends on its physical and mechanical design.

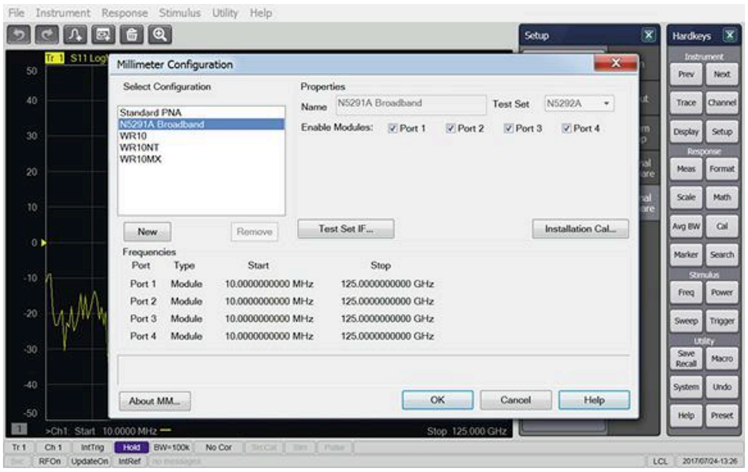

4. The interface includes tasks-specific guides such as this "Millimeter Configuration" screen that helps new or infrequent users achieve better results.

For added flexibility, the user can also customize the placement of traces and windows on the analyzer screen. Example capabilities include optimal arrangement of traces from multiple measurement channels and multipage measurement displays through a "tabbed sheet" function.

TAKING THE MYSTIQUE OUT OF MILLIMETER-WAVE

The N5290A and N5291A broadband millimeter-wave solutions embody Keysight's ongoing mission to provide easier access to accurate, repeatable measurements at ever-higher frequencies and wider bandwidths. Built on a foundation of electronic and mechanical innovations, the N5290A and N5291A deliver metrology-grade precision that ensures exceptional system-level performance. With these tools, today's developers can take the mystique out of millimeter-wave technology and confidently characterize and optimize their devices from 900 Hz to 120 GHz. mw

HUBER+SUHNER
Excellence in Connectivity Solutions

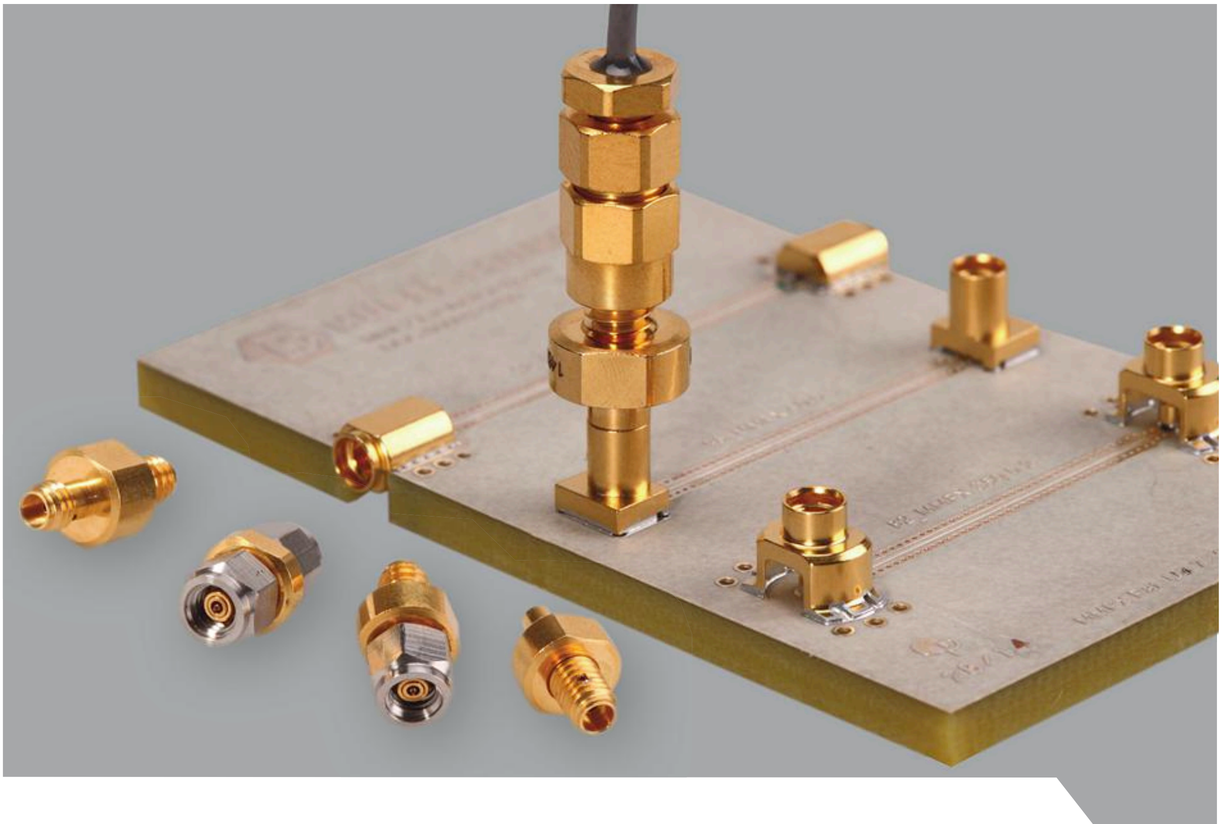

80 GHz coaxial-to-PCB all-in-one solution

The unique HUBER+SUHNER MMPX 80 GHz solution features a true 80 GHz coaxial-to-PCB transition with outstanding electrical performance combined with an easy snap connection mechanism to the PCB.
The broadband characteristics, excellent electrical performance and easy handling facilitate high-end measurement setups for high-speed digital testing and RF testing.

Key characteristics

- Broadband characteristics from DC to 80 GHz
- Excellent return loss
- Easy handling
- Reliable snap interface
- PC 1.0 to MMPX (80 GHz) and PC 1.0 to PC 1.0 (110 GHz) adaptors available

For more facts: › testandmeasurement.hubersuhner.com

HUBER+SUHNER AG 9100 Herisau/Switzerland
HUBER+SUHNER INC. Charlotte NC 28273/USA

Design Feature

SAMEER KUMAR SHARMA | Researcher
Department of Electrical Engineering, Indian Institute of Technology Kanpur, Kanpur, India 208016; e-mail: sharma.sameer16@gmail.com

DEEPAK SINGH NAGARKOTI | Researcher
Isotropic Systems Ltd., London, United Kingdom; e-mail: deepak@isotropicsystems.com

Meet the Challenge of Designing Electrically Small Antennas

Antenna Q diminishes with shrinking antenna size, although it is still possible to achieve acceptable Q performance even as antenna designs become electrically small.

Antennas are vital for communications devices, although the continuing miniaturization of communications products has forced antenna designers to follow suit. However, due to the fundamental limitations in size and performance (Chu's limit), achieving miniaturization with good antenna performance is challenging. Electrically small antennas (ESAs) are limited in bandwidth and radiating efficiency.

By understanding the effects of antenna size reduction on quality factor (Q), bandwidth, efficiency, and gain, it is possible to design a miniature antenna without drastically compromising performance. To demonstrate the effectiveness of this approach, an ESA was designed and developed for GPS (1.575 GHz) at one-tenth the operating wavelength. As will be shown, the Q of this proposed antenna design is closer to Chu's limit than an equivalent-sized dipole or loop antenna.

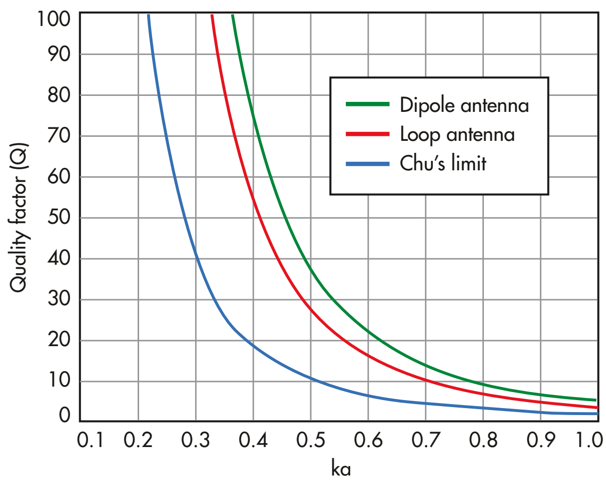

1. These plots of Q vs. electrical size (wavelength) compare dipole and loop antennas with Chu's limit.

Antenna sizes for many communications applications are mainly driven by customer requirements, and are generally much smaller than simple quarter-wavelength monopoles. Due to fundamental limitations, however, antennas can only be made so small without sacrificing tradeoffs in performance. Similarly, very compact antennas with ground planes too close to the radiating element suffer from certain performance issues.[1] The tangential components of alternating current (AC) flowing on the antenna's radiating surface tend to be nullified by the induced surface current on the ground plane.

Attempting to miniaturize an antenna by having radiating element(s) very close to the ground plane results in low radiation resistance, high reactance, narrow bandwidth, and poor radiation efficiency. The bandwidth capacity of a small antenna is approximately inversely related to the radiation Q. Hence, antenna miniaturization is quite challenging. Metamaterials have been quite popular as far as antenna miniaturization is concerned.

These artificial structures can be engineered to support negative and zeroth-order modes, which were not available in traditional microstrip antennas.[2] In general, the frequencies of these resonances are lower than resonances obtained at positive modes and, thus, miniaturization is possible without sacrificing performance. However, metamaterial-based structures inherently have high Q and narrow bandwidth.[3]

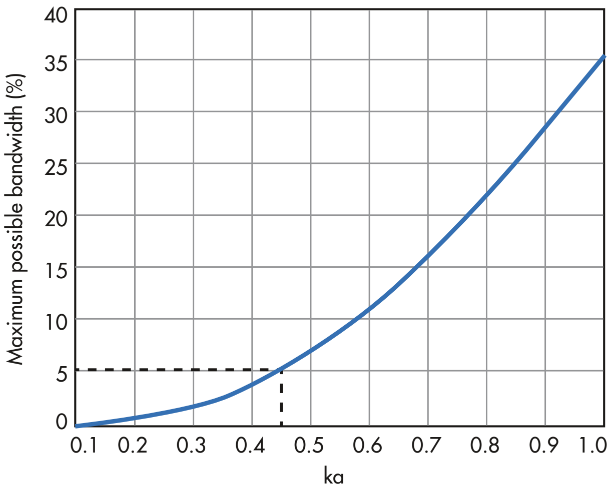

2. The normalized bandwidth bound is plotted as a function of antenna electrical size.

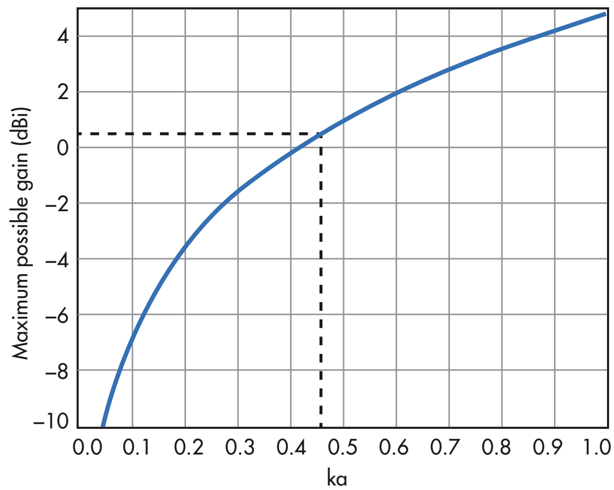

3. The variation in gain bound is shown in relation to antenna electrical size.

Due to the small radiator size of miniaturized antennas, the available gain is usually quite low. Various antenna designs are available in the technical literature, but most suffer from negative gain (loss) and narrow bandwidths.[4,5] Recently, a non-Foster circuit-based matching technique was introduced to overcome the fundamental limits in antenna miniaturization previously reported.[6-8]

To evaluate the challenges of designing ESAs, their performance parameters were studied and applied to the design of an ESA at the GPS frequency (1.575 GHz) using a split-ring resonator (SRR) which exhibits negative permeability. The methodology and layout of the antenna will be presented—and the performance of the antenna evaluated—to better understand the fundamental limits of an ESA.

The fundamental limit for ESAs was addressed by Wheeler in 1947.[9] It defined the maximum dimension of an ESA as being less than $\lambda/2\pi$. In 1948, Chu[10] proposed that these small antennas have an inherent minimum value of Q. Since the lower limit of Q is inversely proportional to the electrical size of an antenna, it restricts the attainable impedance bandwidth for a given antenna size. McLean[11] modified this earlier work on minimum antenna Q for a perfect lossless matching network, and proposed a new Q limit for a small linear antenna (Q_L) as:

$$Q_L = 1/ka + 1/(ka)^3 \quad (1)$$

The results were in agreement with Chu.[10] Also, the minimum Q for a circularly polarized ESA is given by Eq. 2:

$$Q_L = 0.5[(2/ka) + 1/(ka)^3] \quad (2)$$

where $k = \lambda/2\pi$ and a = the radius of the sphere enclosing the antenna. *Figure 1* depicts the relationship between Q and the electrical size of the antenna. The estimations of Q values for loop and dipole antennas are also plotted and are above the fundamental Chu's limits for those antennas.

For the ESA, the antenna radiation Q is represented by Q_a and the matching network Q is represented by Q_m. Given certain assumptions, the efficiency of an antenna, η_a , can be expressed in terms of the efficiency of the matching network, η_m, as:

$$\eta_a = \eta_m(1 + Q_a/Q_m) \quad (3)$$

The efficiency of an antenna can be measured using the "Wheeler Cap" method in which a metallic "Wheeler Cap" with $\lambda/2\pi$ radius covers the ESA, and the near-field reactive and radiated power is trapped within this cap.

In a different measurement case, the radiated power propagating in free space is obtained without the cap. The efficiency is subsequently estimated, since the loss resistance can be separated from the radiation resistance in the post-processing of both test cases. The approximate normalized bandwidth (BW) for the maximum VSWR in terms of Q can be found by Eq. 4:

$$BW = (VSWR – 1)/[Q(VSWR)0.5] \quad (4)$$

Figure 2 shows the maximum possible bandwidth that can be achieved by an ESA with respect to any change in electrical size. Since the radiating element is close to the ground plane, the radiation efficiency of an ESA is low, the energy stored in the near field increases, and the Q is high, resulting in a small impedance bandwidth. Also, the gain of an ESA is restricted according to the Harrington bound[12] as:

$$G(dBi) = 10\log[(ka)^2 + 2(ka)] \quad (5)$$

Figure 3 shows the variation in the gain bound with antenna size. For an ESA, ka < 1 and the maximum achievable gain is 3 dBi.

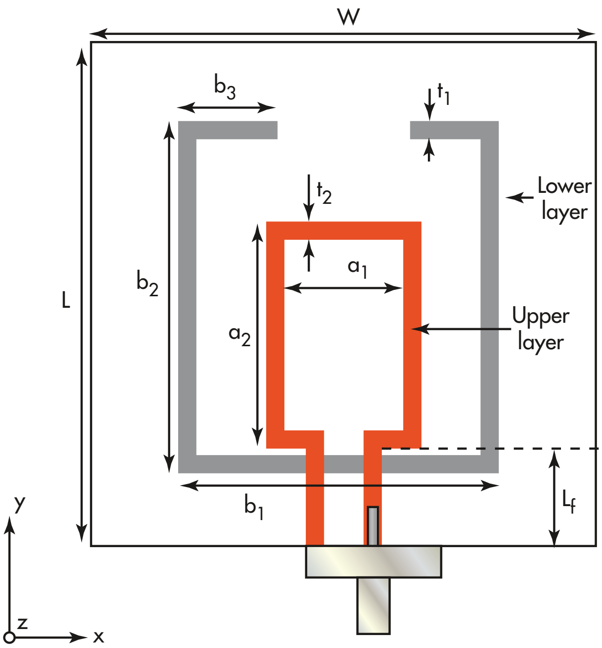

4. This is the layout of the proposed ESA. All dimensions are in mm: L = 30, W = 30, Lf = 5, a1 = 8, a2 = 14, b1 = 18.4, b2 = 21, b3 = 5.2, t1 = 0.8, and t2 = 1.

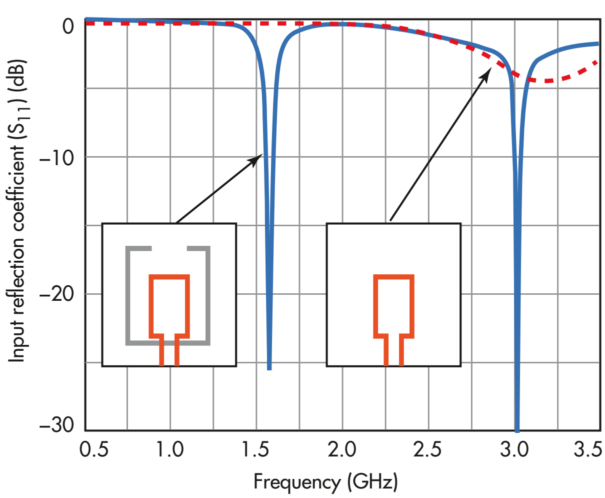

5. The plot of input reflection shows the effect of including the SRR on the loop antenna.

ESA DESIGN EXAMPLE

Figure 4 shows the circuit geometry of the proposed ESA. It consists of a square loop on the top circuit layer, which is capacitively coupled to a rectangular split-ring resonator (SRR) on the bottom circuit layer. The antenna was designed on 1.6-mm-thick FR-4 circuit material with a permittivity of 4.4 and loss tangent of 0.02. *Figure 5* shows the impact of coupling the SRR and the loop antenna. The square loop structure attempts to resonate at 3.02 GHz but suffers from poor impedance matching. However, by including the SRR in the bottom circuit layer, not only are these reflections improved, but an additional resonance is achieved at 1.575 GHz (as shown in Fig. 5).

Figure 6 shows the surface current density of the proposed ESA. As can be seen, the current at 1.575 GHz is largely concentrated in the bottom layer due to the presence of the SRR. At the higher frequency (3.02 GHz), the current is mainly present in the square loop. The radius of the sphere that encloses the antenna is a = 13.9 mm.

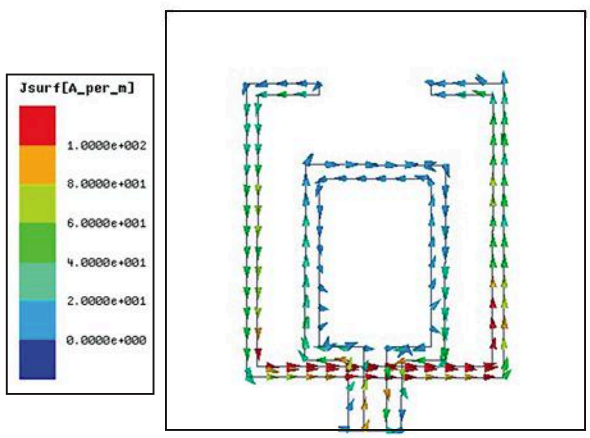

(a) at 1.58 GHz

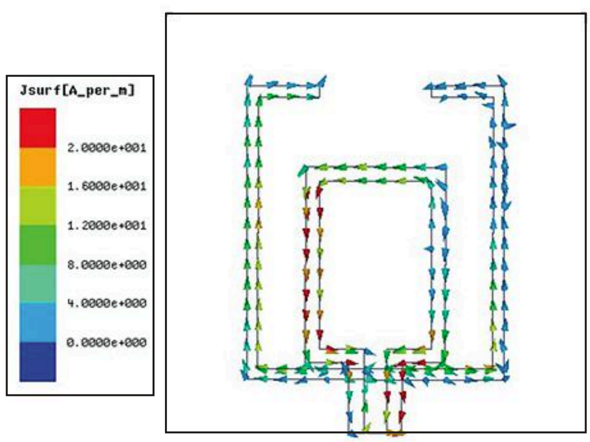

(b) at 3.02 GHz

6. These EM plots show the surface current distributions at (a) 1.58 GHz and at (b) 3.02 GHz.

Since the antenna is resonating at 1.575 GHz, the corresponding free-space wavelength, λ_0, is 189.9 mm and the wavenumber, k, is 0.033 radians/mm. The value of ka is 0.457. Since the antenna is linearly polarized, using the McLean fundamental limit for calculating the minimum Q is:

$$Q_L = (1/0.457) + 1/(0.457)^3 = 12.25 \quad (6)$$

The normalized bandwidth for a 2.0:1 VSWR can be estimated by the use of Eq. 7:

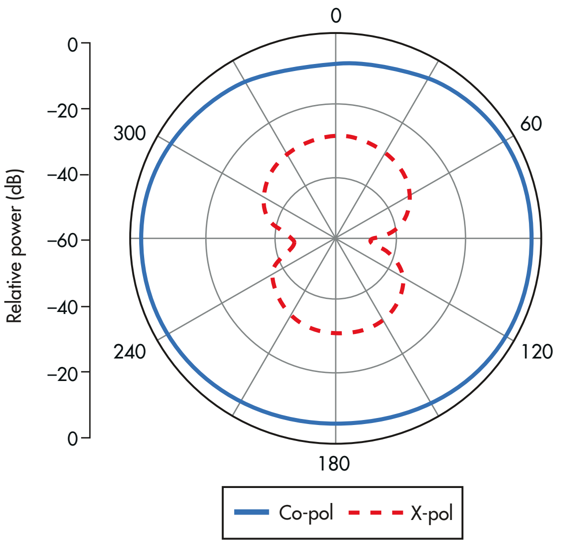

7. This is an E-plane radiation pattern of the proposed 1.575-GHz ESA.

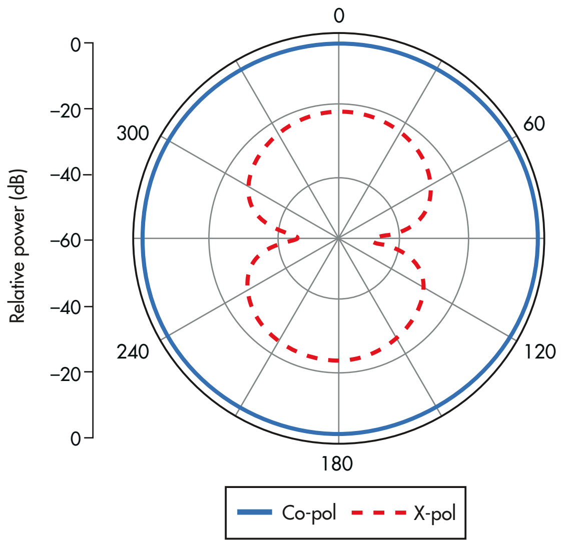

8. This is an H-plane radiation pattern of the proposed 1.575-GHz ESA.

$BW = 1/Q(2)^{0.5} = 5.77\%$ (7)

The maximum possible gain of the proposed antenna is calculated as 0.5 dBi. This is less than the directivity of a short dipole (e.g., 1.76 dBi). *Figures 7 and 8* show the E- and H-plane radiation patterns, respectively, for the proposed antenna at 1.575 GHz. The radiation patterns are nearly omnidirectional, with low cross-polarization levels in both of the planes.

The designed metamaterial antenna exhibits a percentage impedance bandwidth of 2.35% at f_0 = 1.58 GHz. This corresponds to a Q of 30, which is close to the minimum Q obtained from Chu's limit, as shown in Fig. 2. Thus, the realized gain of the designed antenna is higher than the maximum gain bound (e.g., 0.5 dBi, by 0.22 dB), with a simulated radiation efficiency of 53.5%.

Figure 9 compares the Q of the proposed antenna with the fundamental limits for an ESA, loop antenna, and dipole antenna. For the same size, it can be seen that lower Q has been achieved for the ESA compared to the loop and dipole antennas. Also, for the same bandwidth, the electrical size of the proposed antenna is much smaller than the other antenna structures. This is worth noting because the design of small antennas for ka < 0.4 results in negative gain.

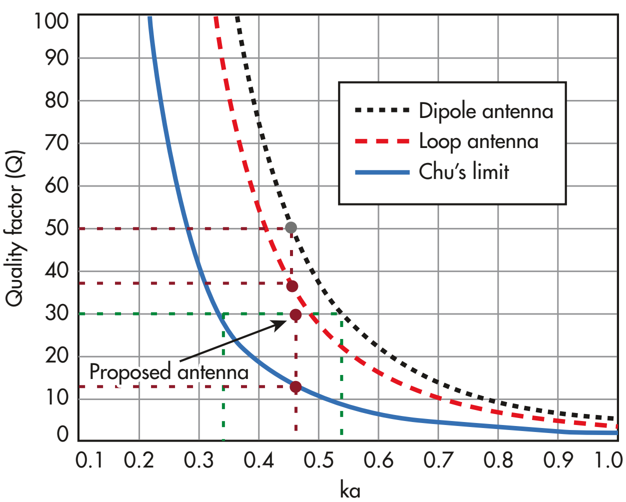

9. The plot shows the estimated Q of the proposed ESA next to values for a loop antenna, dipole antenna, and Chu's limit.

In summary, attempts to reduce the size of any antenna will yield certain performance tradeoffs because of fundamental design limits. However, it has been possible to develop a novel ESA with better Q and bandwidth compared to equivalent-sized standard dipole or loop antennas. The proposed ESA has ka = 0.457, 2.35% bandwidth, and Q = 30, which is still higher than the fundamental limit for an antenna of this small size.

Attempts to reduce the size of any antenna will yield certain performance tradeoffs because of fundamental design limits. However, it has been possible to develop a novel ESA with better Q and bandwidth compared to equivalent-sized standard dipole or loop antennas.

REFERENCES

1. J. Sten, A. Hujanen, and P.K. Koivisto, "Quality factor of an electrically small antenna radiating close to a conducting plane," *IEEE Transactions on Antennas and Propagation*, Vol. 45, No. 5, 2001, pp. 829-837.

2. S.K. Sharma, A. Gupta, and R.K. Chaudhary, "Epsilon negative CPW-fed zeroth-order resonating antenna with backed ground plane for extended bandwidth and miniaturization," *IEEE Transactions on Antennas and Propagation*, Vol. 63, No. 11, 2015, pp. 5,197-5,203.

3. A. Li, K.M. K.. Leong, and T. Itoh, "Infinite wavelength resonant antennas with monopolar radiation pattern based on periodic structures," *IEEE Transactions on Antennas and Propagation*, Vol. 55, No. 3, 2007, pp.868-876.

4. S.K. Sharma and R.K. Chaudhary, "A compact zeroth-order resonating wide-band antenna with dual-band characteristics," *IEEE Antennas andWireless Propagation Letters*, Vol. 14, 2015, pp. 1,670-1,672.

5. M.A. Abdalla, S. Karimian, and Z. Hu, "Dual band spurious-free sir metamaterial antenna," 2014 IEEE Antennas and Propagation Society International Symposium (APSURSI), Memphis, TN, 2014 conference proceedings, pp. 1,005-1,006.

6. S. Sussman-Fort and R.M. Rudish, "Non-Foster impedance matching of electrically small antennas," *IEEE Transactions on Antennas and Propagation*, Vol. 57, No. 8, 2009, pp. 2,230-2,241.

7. D.S. Nagarkoti, Y. Hao, D.P. Steenson, L. Li, E.H. Linfield, and K.Z. Rajab, "Design of broadband non-Foster circuits based on resonant tunneling diodes," *IEEE Antennas and Wireless Propagation Letters*, Vol. 15, 2016, pp. 1,398-1,401.

8. J. Tian, D.S. Nagarkoti, K.Z. Rajab, and Y. Hao, "Graphene-based tunable non-Foster circuit for VHF applications," AIP Advances, Vol. 6, No. 6, 2016, 065202.

9. H.A. Wheeler, "Fundamental limitations of small antennas," Proceedings of IRE, Vol. 35, No. 12, 1947, pp. 1,479-1,484.

10. L.J. Chu, "Physical limitations of omni-directional antennas," *Journal of Applied Physics*, Vol. 19, No. 12, 1948, pp. 1,163-1,175.

11. J.S. McLean, "A re-examination of the fundamental limits on the radiation Q of electrically small antennas," *IEEE Transactions on Antennas and Propagation*, Vol. 44, No. 5, 1996, pp. 672-676.

12. R.F. Harrington, "Effect of antenna size on gain, bandwidth, and efficiency," *Journal of Research of the National Bureau of Standards-D. Radio Propagation*, Vol. 64D, No. 1, 1960, pp. 1-12.

MAHMOUD A. ABDALLA | Ph.D. Candidate
Military Technical College, Cairo, Egypt; e-mail: maaabdalla@ieee.org

ZIHRUN HU | Senior Lecturer
School of Electronics and Electrical Engineering, University of Manchester, P.O. Box 88, Manchester M60 1QD, UK; e-mail: Z.Hu@manchester.ac.uk

Metamaterial Loads Provide Compact Matches

The unique magnetic properties of ferrite substrate material can be harnessed for a wideband coplanar-waveguide impedance transformer capable of matching a 200-Ω load to a 50-Ω line.

A high-impedance tunable composite right/left-handed (CRLH) coplanar-waveguide (CPW) transformer provides an effective means of matching a 200-Ω load to a 50-Ω line. By applying DC magnetic bias, it is possible to tune the bandwidth of the transformer, with the center frequency changing from 2.8 to 3.4 GHz.

With a length of 2.4 mm, this transformer represents about a 78% reduction compared to a conventional transformer in the same frequency band. The CRLH transformer's CPW configuration employs a horizontally magnetized ferrite substrate with small demagnetization field so that very little DC magnetic bias is needed for tuning compared to microstrip configurations.

Composite right/left-handed (CRLH) transmission lines (TLs) have been proposed as a form of transmission line with novel properties.[1-4] These TLs have been shown to have effective negative dielectric permittivity and magnetic permeability. The CRLH TLs have been incorporated in many compact, multiband microwave components (phase shifters, power dividers, filters, oscillators, and antennas).[16-21] From these components, microwave impedance transformers based on CRLH TLs have been developed, characterized by small size and wide bandwidth.[5,6]

A need for tunable and nonreciprocal microwave devices and antennas has encouraged researchers to create tunable and nonreciprocal CRLH TLs using ferrite substrates.[22-26] A ferrite medium has nonreciprocal dispersive properties due to its dispersive permeability tensor.[27] The tuning characteristics are achieved by varying the applied DC magnetic bias.

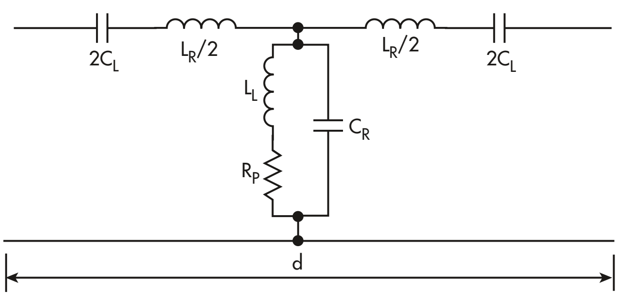

1. Shown is the equivalent circuit model of a ferrite CRLH TL unit cell (for transformer case: C_L = 0.54 pF, L_L = 0.715 nH, L_R = 0.2645 nH, C_R = 2.028 pF, and R_P = 0.05Ω).

Over the ferrite CRLH TLs, it has proven that CPW-based devices require less DC magnetic bias compared to microstrip configuration.[22] Examples of these devices include tunable/nonreciprocal couplers, resonators, circulators, phase shifters,[28-41] and antennas.[42,43]

Ferrite CRLH TLs can be designed by periodically loading a hosting planar ferrite TL by a shunt inductive load, L_L, and a series capacitive load, C_L. The shunt inductive load yields negative effective permittivity, while series capacitive load results in negative effective permeability. Analysis of a ferrite CRLH TL can be performed in a manner similar to that for a CRLH TL based on dielectric substrate, using either periodic circuit analysis or CRLH analysis.

For simplicity in both analysis methods, the ferrite TL will be expressed in terms of its medium parameters. The propagation constant along the hosting ferrite TL and its characteristic impedance can be expressed in terms of the permittivity and permeability of its medium as[44]:

$$k = \omega(\mu_0\mu_f\varepsilon_0\varepsilon_f)^{0.5} \quad (1)$$

$$Z_0 = (\mu_0\mu_f/\varepsilon_0\varepsilon_f)^{0.5} \quad (2)$$

where μ_0 and ε_0 are the free space permeability and permittivity, respectively, while ε_f is the relative ferrite permittivity and μ_f is the equivalent relative ferrite permeability of the hosting TL, which changes according to the direction of the applied DC magnetic field. The equivalent circuit of a lossless ferrite CRLH TL unit cell of length (d) can be expressed using a standard lossless CRLH unit cell *(Fig. 1)*.

In the equivalent-circuit model, the parasitic inductance (L_R) and capacitance (C_R) of the hosting ferrite TL substrate are calculated in terms of the ferrite medium permittivity and the equivalent relative ferrite permeability, which depends of the direction of the applied DC magnetic bias. For periodic analysis of a ferrite CRLH TL with (a) properly defined equivalent relative permeability of the hosting ferrite TL according to the direction of the DC magnetic bias, and (b) the periodic length of the unit cells (d) being very small compared to the propagating wavelength hence, the dispersion equation can be written as:[44]

$$\cos(\beta d) = 1 - 0.5\omega^2 d^2(\mu_0\mu_f - 1/\omega^2 C_L d)(\varepsilon_0\varepsilon_f - 1/\omega^2 L_L d) \quad (3)$$

where β denotes the complex propagation constant of the travelling wave along the periodic structure.

Figure 2 shows a front view of the three-dimensional (3D) geometry of the proposed CPW ferrite CRLH transformer, with a layout of the transformer in *Fig. 3a*. The CRLH LH unit cell consists of a CPW section loaded by two series air gap capacitor and a meandered line inductor *(Fig. 3b)* and fed by CPW TLs at the ends.

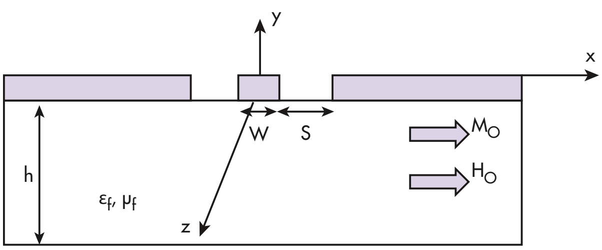

2. This front view shows the different ferrite CRLH CPW transformers. The ferrite substrate was G-113 material from Trans Tech (www.transtechinc.com), with h = 1 mm, ε_f = 15, saturation magnetization $4\pi M_S$ = 1780 G, and magnetic linewidth ΔH_0 = 25 Oe.

An internal DC magnetic field (H_0) is applied to the ferrite substrate, producing the saturation magnetization in the direction shown. The progressive phase shift and the characteristic impedance of a CRLH TL unit cell, of length d, implemented on a ferrite substrate, can be redefined approximately in terms of its medium parameters, the ferrite relative permittivity ε_f, and the relative permeability μ_f (as illustrated in ref. 44):

$$\phi_{CRLH} = \omega d\,[(\mu_0\mu_f - 1/\omega^2 C_L d)\,)(\varepsilon_0\varepsilon_f - 1/\omega^2 L_L d)]^{0.5} \quad (4)$$

$$Z_{CLRH} = Z_L[(1 - \omega^2\,\mu_0\mu_f C_L d)/(1 - \omega^2\varepsilon_0\varepsilon_f L_L d)]^{0.5} \quad (5)$$

Because of the dispersive nature of the ferrite substrate, the ferrite TL has a dispersive permeability such that the progressive phase shift and the CRLH characteristic impedance are dispersive.

The ferrite CRLH transformer makes use of these dispersive, progressive phase shifts and characteristic impedance so that their combination always meets the impedance-matching condition. The transformer does not behave like a typical quarter-wave transformer. The electrical length, ϕ_{CRLH}, will no longer be 90 deg. as the DC bias varies, and the characteristic impedance, Z_{CRLH}, will also change. But, the overall effect of these changes is that the input impedance, Z_{in}, will be almost constant for its desired value, forming a tunable transformer.

The initial design of the CRLH transformer was based on considering the ferrite substrate as an isotropic material. This can be done by assuming a very high DC magnetic bias applied to the ferrite substrate (H_0 = 50,000 Oe). At this bias, the onset frequency of the negative permeability is shifted to greater than 60 GHz, which is much higher than the target design frequency band.[44] Therefore, the ferrite substrate for the frequency bands of interest can be characterized as an isotropic material.

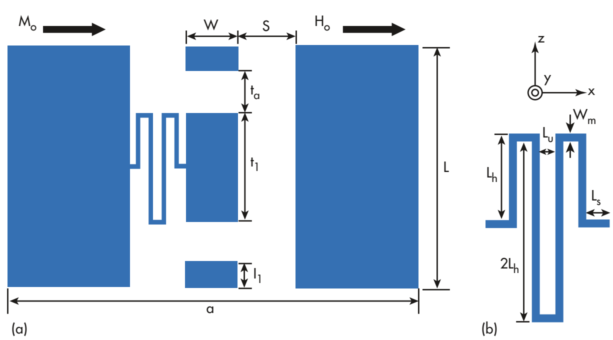

3. The layout geometry of the ferrite LH CPW high impedance ferrite transformer is a = 32.75 mm, L = 2.4 mm, W = 1.8 mm, t_1 = 0.4 mm, t_a = 0.5 mm, l_1 = 0.5 mm (a). The detailed geometry of meander line inductor is W_m = 0.05 mm, L_s = 0.357 mm, L_h = 0.6 mm, L_v = 0.475 mm (b).

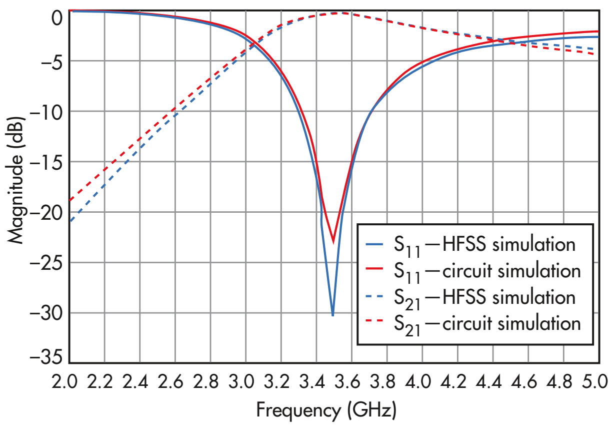

4. Shown are the simulated scattering parameter magnitudes of the high impedance ferrite transformer, full wave simulation (HFSS) for H_0 = 50,000 Oe, and equivalent-circuit model.

Hence, the ferrite substrate can be characterized only with its electric properties within the transformer operating frequency. Under this condition, the ferrite CRLH transformer was designed to match a 200-Ω load (Z_{load}) to a 50-Ω TL (Z_{ol}) at 3.45 GHz. Accordingly, the CRLH transformer should have 100-Ω characteristic impedance (Z_{LH}), [$Z_{LH} = (Z_{ol}\ Z_{load})^{0.5}$], and +90-deg. phase shift at its output terminal.

These two conditions were fulfilled by the proper selection of both loading and hosting CPW TL elements. Comparison of the two simulation results is shown in *Fig. 4*, where good agreement of both simulations is apparent.

The phase shift of the ferrite CRLH transformer, achieved by applying a high DC magnetic bias of H_0 = 50,000 Oe, is shown in *Fig. 5*. The transformer exhibits almost 90-deg. phase shift in the LH passband at 3.5 GHz. Figure 5 also shows the return and transmission losses of the transformer terminated with a 200-Ω load. It is evident that the transformer has minimum return loss better than 25 dB and close to 0-dB insertion loss at 3.5 GHz. Also, it has a 3-dB bandwidth from 3.05 to 4.4 GHz (36%).

The CRLH transformer is tuned by varying the applied DC magnetic bias. Because of the magnetization of the ferrite material, the internal magnetic field (H0) is different than the external magnetic field (Hex). The relationship between the two magnetic fields can be expressed as[44]:

$$H_{ex} = H_0 + 4\pi M_S N \qquad (6)$$

where N is the demagnetization factor for the applied DC magnetic bias direction. The demagnetization factor depends on the geometry of the ferrite material. As explained in ref. 44, the demagnetization factor is almost 1 if the DC bias direction is perpendicular to the plane of a rectangular ferrite specimen, while it is almost zero if the DC magnetic bias is in plane. Therefore, for a CPW structure, the in-plane demagnetization field for the shown applied field direction in Fig. 1 has little effect.

However, for improved accuracy, the current study compensates for the external applied DC magnetic bias. Accordingly, a uniform demagnetization filed was calculated to be equal to 70 Oe, which represents the difference between the external and internal DC magnetic fields.

To illustrate the CRLH transformer's tuning capability, two more lower DC magnetic bias cases of 1,000 Oe and 3,000 Oe were numerically studied *(Fig. 6)*. It is clear that the operating frequency of the CRLH transformer can be tuned from 2.8 GHz in the first case to 3.35 GHz in the second case with better than 15-dB return loss and about 0.5-dB insertion loss in both cases. The operating bandwidth is tuned from 2.55 to 3.1 GHz (20%) in the first case and 2.95 to 4.2 GHz (35%) in the second case.

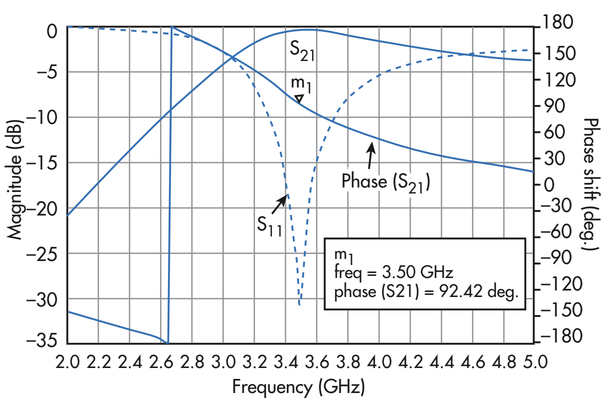

5. Shown is the full-wave simulated scattering parameter (magnitudes and phase) of the high impedance ferrite transformer, H_0 = 50,000 Oe.

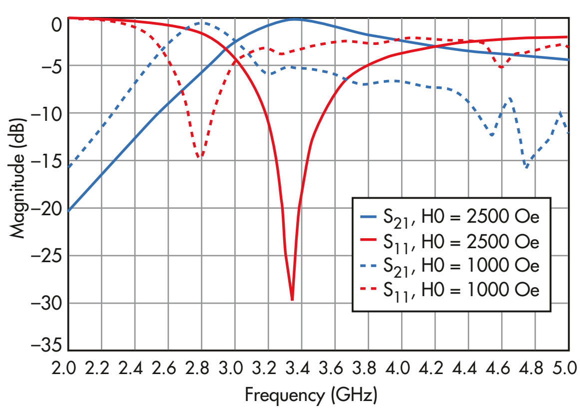

6. Depicted are the full-wave simulated scattering parameters of the high impedance ferrite transformer for H0 = 1,000 Oe (dotted lines) and H_0 = 3,000 Oe (solid lines).

By increasing the DC bias further, the transformer tenability becomes even more apparent. *Figure 7* shows change of center frequency versus DC bias. The transformer center frequency exhibits nonlinear variation with the applied DC magnetic bias. It increases from 2.8 GHz at H_0 = 1,000 Oe to 4 GHz at H_0 = 1,500 Oe and decreasing to 3.05 GHz at 2,000 Oe. This increase/decrease process then repeats two times with small frequency variations steps. Finally, the matching frequency reaches 3.4 GHz at 4,500 Oe and remains constant to 5,000 Oe.

The nonlinear variation of the center frequency, and specifically its drop at H_0 = 2000 Oe, can be explained as due to the nonlinear variation of the hosting ferrite TL permeability versus frequency. By emphasizing its change in value versus frequency, it can be seen that its value increases from 1 and then decreases to negative values within the frequency band of negative ferrite permeability, before finally returning to unity

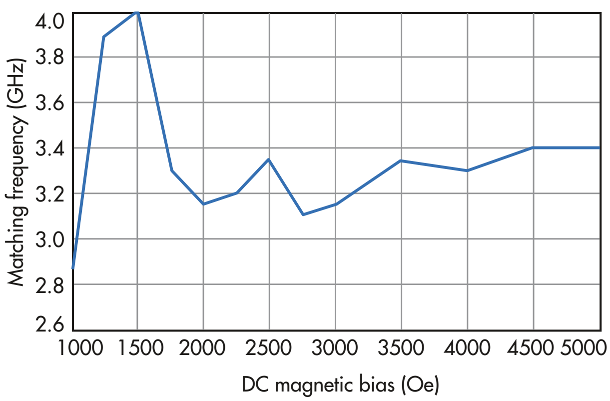

7. This is the variation of the high impedance ferrite transformer center frequency against the DC magnetic bias.

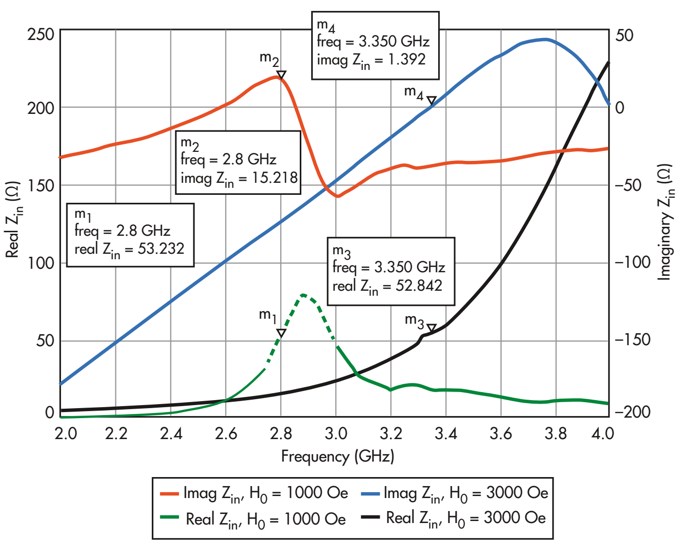

8. Shown is the full wave simulated input impedance of the high impedance ferrite transformer for H_0 = 1,000 Oe (dotted lines) and H_0 = 3,000 Oe (solid lines).

beyond this frequency band. As a consequence, this nonlinear variation is expected to affect both the progressive phase shift and the characteristic impedance of a CRLH TL unit cell (defined in eqs. 4 and 5, respectively).

Verification of the theoretical concept of an CRLH transformer can be done by studying the input impedance for different DC magnetic bias values. For these two studied cases of H0, the input impedance of the CRLH transformer was calculated numerically *(Fig. 8)*. These calculations show that the input impedance is Z_{in}= 53.232 + j15.218 Ω at 2.8 GHz for H_0 = 1,000 Oe. This changes to Z_{in}= 52.842 + j1.392 Ω at 3.55 GHz for H_0 = 3000 Oe. It is clear that the CRLH transformer demonstrates close to 50-Ω input impedance at two different frequencies. mw

REFERENCES

1. C. Caloz and T. Itoh, *Electromagnetic Metamaterials Transmission Line Theory and Microwave Applications,* 1st ed., Wiley, New York, 2006.
2. H-X. Xu, G-M. Wang, C-X. Zhang, and X. Wang. "Characterization of composite right/left-handed transmission line," *Electronics Letters*, Vol. 47, No. 18, 2011, pp. 1,030-1,032.
3. Q. Yang, and Y. Zhang. "Non-radiative composite right/left-handed transmission line based on ridge substrate integrated waveguide," *Electronics Letters*, Vol. 49, No. 20, 2013, pp. 1,280-1,282.
4. Q. Shen, "Simple broadband via-free microstrip composite right and left hand transmission line," *Electronics Letters*, Vol. 52, No. 9, 2016, pp. 724-725.
5. C. Damm, J. Freese, M. Schubler, and R. Jakoby. "Electrically controllable artificial transmission line transformer for matching purposes," *IEEE Transactions on Microwave Theory & Techniques*, Vol. 55, No. 6, 2007, pp. 1,348-1,354.
6. A.F. Daw, M.A. Abdalla, and H.M. Elhennawy, "New Inductor Loaded Composite Right Left hand Impedance Transformer for UWB Wireless Applications," 2015 9th International Congress on Advanced Electromagnetic Material in Microwave and Optics, 2015, United Kingdom, pp. 231-233.
7. S.C. Wenjing Su, Manos, M. Tentzeris, and S. Lim. "A novel fluid-reconfigurable advanced and delayed phase line using inkjet-printed microfluidic composite right/left-handed transmission line," *IEEE Microwave and Wireless Components Letters*, Vol. 25, No. 2, 2015, pp. 142-144.
8. H-X. Xu, G-M. Wang, and X. Wang. "Compact Butler matrix using composite right/left handed transmission line," *Electronics Letters,* Vol. 47, No. 19, 2011, pp. 1,081-1,083.
9. M. Bemani, and S. Nikmehr, "Nonradiating arbitrary dual-band equal and unequal 1: 4 series power dividers based on CRLH-TL structures," *IEEE Transactions on Industrial Electronics,* Vol. 61, No. 3, 2014, pp. 1,223-1,234.
10. X. Ren, K. Song, M. Fan, Y. Zhu, and B. Hu. "Compact dual-band Gysel power divider based on composite right-and left-handed transmission lines," *IEEE Microwave and Wireless Components Letters*, Vol. 25, No. 2, 2015, pp. 82-84.
11. H-X. Xu, G.M. Wang, X. Chen, and T.P. Li. "Broadband balun using fully artificial fractal-shaped composite right/left handed transmission line," *IEEE Microwave and Wireless Components Letters,* Vol. 22, No. 1, 2012, pp. 16-18.
12. Y. Peng, X. Peng Yu, J.M. Gu, W.M. Lim, and W.Q. Sui, "An area-efficient CRLH (Composite Right/Left-Handed)-TL approach to the design of rotary traveling-wave oscillator," *IEEE Microwave and Wireless Components Letters,* Vol. 23, No. 10, 2013, pp. 560-562.
13. K. Song, Q. Duan, F. Chen, B. Hu, and Y. Fan, "Design of dual-bandpass filter using zeroth-order resonance and Bragg frequency," *IET Microwaves, Antennas & Propagation,* Vol. 9, No. 5, 2014, pp. 431-435.
14. M.A. Abdalla and K.S. Mahmoud, "A Compact SIW Metamaterial Coupled Gap Zeroth Order Bandpass Filter with Two Transmission Zeros," 2016 10th International Congress on Advanced Electromagnetic Material in Microwave and Optics, 2016, Greece, pp. 4-6.
15. M. Abdalla, A. Hassan, and A. Galal Eldin, "A Compact High Selective Coupled Gap CRLH TL Based Bandpass Filter," 2015 9th International Congress on Advanced Electromagnetic Material in Microwave and Optics, 2015, United Kingdom, pp. 237-239.
16. L. Li, Z. Jia, F. Huo, and W. Han, "A novel compact multiband antenna employing dual-band CRLH-TL for smart mobile phone application," *IEEE Antennas and Wireless Propagation Letters,* Vol. 12, 2013, pp. 1,688-1,691.
17. Y. Kushiyama, T. Arima, and T. Uno, "Differential-Type CRLH Leaky-Wave Antenna Using Stepped Impedance Resonators," *IEEE Antennas & Wireless Propagation Letters,* Vol. 15, 2016, pp. 321-324.
18. M.A. Abdalla, U. Abdelnaby, and A.A. Mitkees, "Compact and Triple Band Metamaterial Antenna for All WiMAX Applications," 2012 International Symposium on Antennas and Propagation, pp. 1,176-1179.
19. Mahmoud Abdalla, "A Dual Mode CRLH TL Metamaterial Antenna," 2014

IEEE AP-S International Antenna and Propagation Symposium Digest, 2014, pp. 793-794.
20. M. Abdalla, M. Abo El-Dahab, and M. Ghouz, “Dual/Triple Band Printed Dipole Antenna Loaded With CRLH Cells,” 2014 IEEE AP-S International Antennas & Propagation Symposium, pp. 1,007-1,008.
21. M.A. Abdalla, A.A. Awad, and K.M. Hassan, “Wide Band High Selective Compact Metamaterial Antenna for 2 GHz Wireless Applications,” 2014 Loughborough Antennas & Propagation Conference, 2014, United Kingdom, pp 350-354.
22. M. Tsutsumi and T. Ueda, “Nonreciprocal left-handed microstrip lines using ferrite substrate,” in Proceedings of the IEEE MTT-S International Symposium, 2004, pp. 249-253.
23. M. Tsutsumi and T. Ueda, “Left handed transmission characteristics of ferrite microstrip lines without series capacitive load,” *IEICE Transactions on Electronics*, Vol. E89, September 2006, pp. 1,318-1,323.
24. M. Abdalla and Z. Hu, “On the study of CWP dual band left handed propagation with reciprocal and nonreciprocal characteristics over ferrite substrates,” in IEEE AP-S International Symposium, 2007, pp. 2,578-2,581.
25. G. Sajin, I.A. Mocanu, F. Craciunoiu, and M. Carp, “MM-wave left-handed transmission line antenna on anisotropic substrate,” 43rd European Microwave Conference (EuMC), 2013, pp. 668-671.
26. Y.-J Huang, G. Wen, T. Q. Li, Li, and J. L. Kang Xie, “Design and Characterization of Tunable Terahertz Metamaterials With Broad Bandwidth and Low Loss,” *IEEE Antennas and Wireless Propagation Letters*, Vol. 11, 2012, pp. 264-267.
27. B. Lax and K.J. Button, *Microwave Ferrites and Ferrimagnetics*, McGraw-Hill, New York, 1962.
28. M.A. Abdalla and Z. Hu, “Multi-band functional tunable LH impedance transformer,” *Journal of Electromagnetic Wave and Applications*, Vol. 23, 2009, pp. 39-47.
29. M.A. Abdalla and Z. Hu, “Compact tunable left handed ferrite transformer,” *International Journal of Infrared and Millimeter Waves*, Vol. 30, No. 8, 2009, pp. 813-825.
30. M. Abdalla and Z. Hu, “Compact Novel CPW Ferrite Coupled Line Circulator with Left-handed Power Divider/Combiner,” 2011 European Microwave Week (EuMW) Digest, United Kingdom, pp. 794-797.
31. T. Kodera, and C. Caloz, “Integrated Leaky-Wave Antenna–Duplexer/Diplexer Using CRLH Uniform Ferrite-Loaded Open Waveguide,” *IEEE Transactions on Antennas and Propagation*, Vol. 58, No. 8, 2010, pp. 2,508-2,514.
32. T. Kodera, D.L. Sounas, and C. Caloz, “Tunable magnet-less non-reciprocal metamaterial (MNM) and its application to an isolator,” 2012 Asia-Pacific Microwave Conference (APMC) Proceedings, pp. 73-75.
33. M. Abdalla and Z. Hu, “Ferrite Tunable Metamaterial Phase Shifter,” 2010 IEEE AP-S International Antenna and Propagation Symposium Digest, July 11-17, 2010, Toronto, Canada, pp. 1-4.
34. M. Tsutsumi and K. Okubo, “Effect of stubs on ferrite microstrip line magnetized to wave propagation,” Asia Pacific Microwave Conference 2009 (APMC 2009), pp. 1,234-1,237
35. M.A. Abdalla and Z. Hu, “Compact tunable single and dual mode ferrite left-handed coplanar waveguide coupled line couplers,” *IET Microwaves, Antennas & Propagation*, Vol. 3, No. 4, June 2009, pp. 695-702.
36. M. Abdalla and Z. Hu, “Composite Right/Left-handed Coplanar Waveguide Ferrite Forward Coupled-Line Coupler,” *IET Microwaves, Antennas & Propagation*, Vol. 9, No. 10, 2015, pp. 1,104-1,111.
37. S. Karimian, M. Abdalla, and Z. Hu, “Tunable Metamaterial Ferrite Stepped Impedance Resonator (SIR),” 27th Progress in Electromagnetics Research Symposium, 2010, Xi’an, China, pp 165-168.
38. M.A. Abdalla and Z. Hu, “Compact Metamaterial Coplanar Waveguide Ferrite Tunable Resonator,” *IET Microwaves, Antennas & Propagation,* Vol. 10, No. 4, 2016, pp. 406-412.
39. M. Abdalla and Z. Hu, “Design and Analysis of Tunable Left Handed Zeroth Order Resonator on Ferrite Substrate,” *IEEE Transactions on Magnetics,* Vol. 44, November 2008, pp. 3,095-3,098.
40. J. Ghalibafan and Nader Komjani, “Tunable zeroth-order resonator based on a ferrite metamaterial structure,” *Chinese Physics B*, Vol. 22, No. 10, 2013, pp. 107805-1-107805-5.
41. A. Zermane, B. Sauviac, B. Bayard, B.P. Gervy, J.J. Rousseau, and A. Benghalia, “Experimental verification of tunable property of a zeroth-order resonator on ferrite substrate,” *Microwave and Optical Technology Letters,* Vol. 56, No. 12, 2014, pp. 2,805-2,809.
42. M. Abdalla and Z. Hu, “Compact and Tunable Metamaterial Antenna for Multiband Wireless Communication applications,” 2011 IEEE AP-S International Antennas & Propagation Symposium USA, pp. 2,951-2,953.
43. A. Porokhnyuk, T. Ueda, Y. Kado, and T. Itoh, “Design of nonreciprocal CRLH metamaterial for non-squinting leaky-wave antenna,” 2013 IEEE MTT-S Intenational Microwave Symposium (IMS), pp. 1-3.
44. Mahmoud Abdelrahman Abdalla, “Ferrite left-handed meta-materials for RF microwave applications,” Ph.D. dissertation, Manchester University, Manchester, UK, 2008.

JACK BROWNE | Technical Contributor

Opting for Single-Layer or Multilayer Capacitors

Miniature ceramic capacitors for surface-mount applications on PCBs are often available in single- and multiple-layer versions—but why use one type or the other?

Capacitors are one of the true "building-block" components of circuit design, along with resistors and inductors. They come in many shapes and sizes, in fixed and variable capacitance values, with tiny capacitors based on ceramic dielectric materials among the most popular for printed-circuit-board (PCB) applications.

Both single-layer and multilayer ceramic capacitors are commonly used in RF/microwave circuits, attractive for their small size for use in surface-mount electronic designs. The two types of ceramic capacitors are often available from the same manufacturer, which begs the question: Why use one type or the other? And what are the differences between them? Let's find out.

All capacitors are charge-storing components based on at least two electrical conductors or plates separated by some form of dielectric insulating material. For any capacitor, the amount of charge per amount of applied voltage is a function of the area of the plates, the characteristics of the dielectric material, and the distance between the plates. The capacitance for a capacitor formed with two conducting plates is simply:

$$C = \varepsilon A/d$$

where:
ε = the permittivity of the dielectric material,
A = the area of the plates, and
d = the separation distance of the plates.

The voltage potential between the plates is a function of the dielectric material and the distance between the plates, and is usually described by a parameter known as working DC voltage, or WVDC. The energy, E, that can be stored in a capacitor, is related to its capacitance value and the applied voltage:

$$E = (CV^2)/2$$

where:
E = the energy (in J or W/s),
C = the capacitance (in F), and
V = the applied voltage (in V).

An ideal capacitor would store all energy in the dielectric material; in real-world capacitors, however, some energy is lost due to some loss due to the equivalent series resistance (ESR) of the capacitor. Higher ESR values translate into higher amounts of loss for a capacitor. The ESR for a capacitor is usually listed in Ω with respect to a particular operating frequency.

1. Thin-film porcelain and ceramic dielectric materials provide the insulators in many different types of single-layer and multilayer capacitors. *(Courtesy of American Technical Ceramics)*

The amount of energy that a capacitor can store is indicated by its quality factor (Q). Capacitors with lower ESR values exhibit higher Q values, also specified at a particular operating frequency. The reciprocal of Q, 1/Q, is also known as the dissipation factor or loss tangent of a capacitor and its dielectric material. Usually given as a percentage, it indicates that portion of the total power in a capacitor that is dissipated or lost as heat.

The greatest number of capacitors that are used in modern electronic circuits are fabricated as passive components in integrated circuits (ICs), although discrete-component capacitors are still required in rather large numbers for PCB applications. Many of these are in surface-mount-technology (SMT) form when used for large-volume applications produced by automated manufacturing processes, such as tape-and-reel components being fed to robotic pick-and-place machines.

Ceramic materials are the most widely used dielectrics in modern discrete capacitors, with ceramic dielectric material providing insulation layers for a wide range of both single-layer ceramic capacitors (SLCCs) and multilayer ceramic capacitors (MLCCs). While the majority of ceramic capacitors for PCB mounting are in unpolarized leadless chip form for ease of surface mounting (*Fig. 1*), many different ceramic materials are also used in many sizes of ceramic disk capacitors, which are polarized with leads.

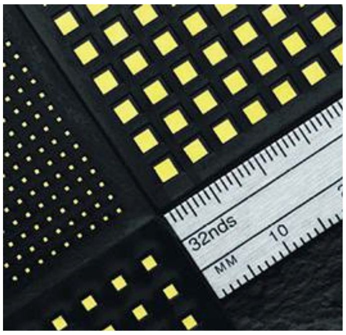

2. SLCCs are available in a wide range of sizes and capacitance values. *(Courtesy of Johanson Technology; www.johansontechnology.com)*

As the name suggests, SLCCs are typically formed monolithically, with a single thin ceramic layer plated with conductive electrode material on both sides and with plated connection points on top and bottom. These miniature, low-profile capacitors (*Fig. 1*) are available in a wide range of capacitance values, although voltage ratings are usually limited because of the small chip sizes.

An MLCC is formed with alternating layers of conductors and dielectric insulating layers, resulting in a structure that is the equivalent of a number of single-layer capacitors connected in parallel. This in turn results in an increased capacitance value for an increase in component height. Because of the construction and configuration, a MLCC is capable of higher capacitance with reduced loss and parasitic inductance compared to a SLCC, with the tradeoff being in slightly larger size and height than a SLCC. For high-frequency circuits that require relatively large current-carrying capacity, MLCCs provide excellent performance in small package sizes.

Ceramic capacitors are divided into two stability classes: Class 1, with high stability and compensation for the effects of temperature; and Class 2, with high value of capacitance per volume (high volumetric efficiency) as typically needed for higher-power applications, but with less stability with temperature and other factors than Class 1 capacitors.

COMPARING COMPONENTS

How do SLCCs and MLCCs compare in terms of basic characteristics and performance levels? A sampling of a leading supplier's SLCC and MLCC product lines may shed some light on the differences between the two types of ceramic capacitors. For example, American Technical Ceramics (*www.atceramics.com*) offers both SLCCs and MLCCs, available as negative-positive 0 ppm/°C (NPO) components with zero shift in capacitance as a function of temperature. This translates into very predictable temperature coefficients for these capacitors, with extremely flat capacitance across wide temperature ranges. Both types of capacitors are also available with high Q values and low dissipation losses.

The SLCCs are usable at frequencies to 100 GHz, covering a total capacitance range of 0.04 to 10,000 pF depending on package size and voltage ratings to 100 WVDC. The electrical performance of any series of SLCCs is dependent upon the type of ceramic insulator material and its dielectric constant (Dk), which includes insulator materials with extremely high Dk (to 25,000) to achieve the highest capacitance values.

For example, the company's ATC 116 series Microcap SLCCs offer typical capacitance values of 0.06 to 220 pF in square-sided chip capacitors measuring 0.015 × 0.015 in. (0.381 × 0.381 mm), and larger models [0.090 × 0.090 in. (2.29 × 2.29 mm)] available with capacitances as high as 6200 pF. The maximum dissipation factor at 1 kHz is 2.5%.

The same company's 700A and 700B Series of porcelain and ceramic multilayer capacitors also provide the temperature-stable characteristics of NPO dielectric materials in multilayer configurations. The smaller 700A Series capacitors measure 0.055 × 0.055 in. with capacitance values of 0.1 to 1000 pF; they are rated for WVDC to 250 V dc. The Q is greater than 10,000 for capacitance values to 110 pF and greater than 2000 for capacitance values above 110 pF. The twice-as-large 700B Series capacitors measure 0.110 × 0.110 in. with available capacitance values of 0.1 to 5100 pF and WVDC rating of 1,500 V dc. The Q is greater than 10,000 for capacitance values to 220 pF and greater than 2,000 for capacitance values above 220 pF.

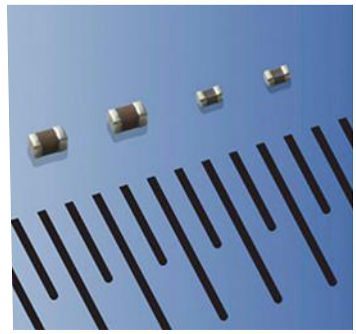

3. MLCCs are shown next to a scale with 0.5-mm increments. *(Courtesy of Tektronix Inc.)*

Several series of MLCCs from AVX (*www.avx.com*) are also based on NPO dielectric materials, featuring excellent capacitance stability as a function of temperature. All of the MLCCs are rated for WVDC of 200 V dc or more and temperature coefficient of capacitance (TCC) of ±30 ppm/°C or better. The Series 600L capacitors have capacitance values of 0.1 to 27.0 pF in a case size of 0.04 × 0.02 in. (1.02 × 0.51 mm), while the 600F MLCCs cover a capacitance range of 0.1 to 240 pF with WVDC rating of 250 V dc and somewhat larger case size of 0.079 × 0.049 in. (2.00 × 1.25 mm).

While there are no clear differences in SLCCs and MLCCs when based on similar materials—other than the height, higher capacitance values, and higher voltage ratings for MLCCs in similar-sized packages as SLCCs—SLCCs provide extreme compact and stable (with NPO materials) performance with temperature for lower values of capacitance at lower operating voltages. Ultimately, the choice of a capacitor for an application requires an assessment of the overall performance parameters of different capacitor models, whether SLCCs or MLCCs, to find the best component for that application. mw


... ALSO INTRODUCING THE NEW
SAGE STOCKROOM
IN STOCK
WG to Coax Adapters
Balanced Mixers
Orthomode Transducers
Bulkhead Adapters
Sector Antennas
Faraday Isolators
Harmonic Mixers
Power Dividers
Horn Antennas
Magic Tees
Omni Directional Antennas
Power Amplifiers
Directional Couplers
Level-Setting Attenuators
Taper Transitions
visit us online for more!
WWW.SAGEMILLIMETER.COM/STOCKROOM
Over 1,000 millimeterwave components off-the-shelf, in stock, and ready to ship guaranteed in only 1-3 days.
SAGE
STOCKROOM

defense electronics

A Special Section to PENTON'S DESIGN ENGINEERING & SOURCING GROUP SEPTEMBER 2017

JACK BROWNE | Technical Contributor

Army Gives Green Light to Manpack Radios

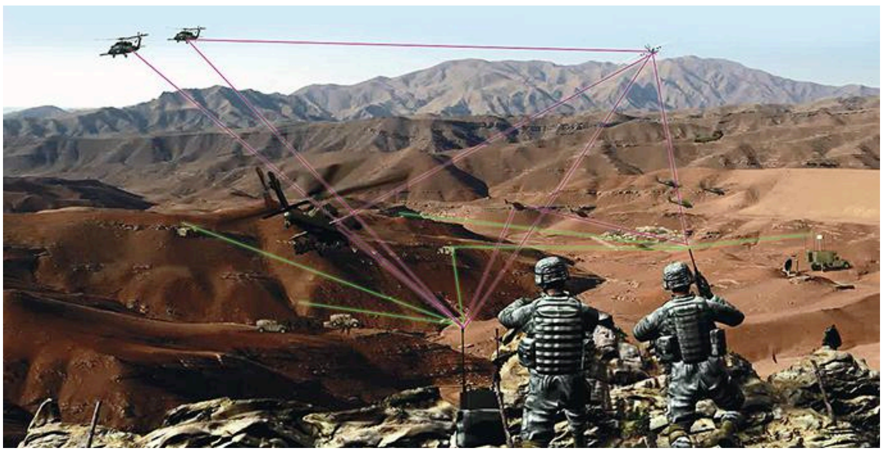

Network radio solutions such as the TruNet SDR-based systems provide secure, in-the-field military communications. *(Courtesy of Rockwell Collins)*

ROCKWELL COLLINS *(www.rockwellcollins.com)* has been selected by the U.S. Army Program Executive Office C3T to produce 101 Handheld, Manpack, and Small Form Factor (HMS) manpack radios and ancillaries beginning in August. This is a follow-on award to a contract signed with Rockwell Collins the previous year, qualifying the company to compete for the Army's HMS Manpack radio program, which has a potential 10-year value of $12.7 billion.

The follow-on award results after production and testing of 50 AN/PRC-162 two-channel, military communications radios incorporating flexible software-defined-radio (SDR) technology, which enables modification of basic radio operating parameters by means of software programming. The tactical radios are based on the company's TruNet networked communications family of products.

"For decades, Rockwell Collins has been the premier provider of VHF/UHF airborne radios for the Department of Defense. With our TruNet family of products, we are confident that our AN/PRC-162 will bring the same level of performance excellence to the ground domain," said Troy Brunk, vice president and general manager, Communication and Navigation Solutions. The next step in the radio evaluation (next year) will involve field-based risk reduction testing of the HMS Manpack radios. de

3D Printed Filter Flies in Space

SATELLITE COMMUNICATIONS (SATCOM) systems count on filters to keep signals in their proper channels. Because of the need for low passband insertion loss, the filters are typically metal waveguide types. For satcom applications, however, one challenge is designing and manufacturing waveguide filters that are light enough to launch on a satellite, especially within a high-density system that may require more than 600 filters.

As Airbus Defence and Space has discovered, 3D direct metal printing (DMP) of waveguide filters doesn't just produce components with high performance. By using special aluminum alloys and additive manufacturing methods with a 3D printer, can about 50% of filter weight can be

This waveguide filter was designed with 3D simulation software and fabricated with a 3D direct metal printer. It is the first RF waveguide filter manufactured by 3D printing that has been validated for use in a commercial telecommunications satellite.

(Continued on page 66)

Conquering the Complexity of Military Communications

TACTICAL COMMUNICATIONS have been wireless since messages were sent by smoke signals or banging on a drum. The signals are somewhat more sophisticated now and the equipment to send and receive them is quite complex. After all, it must provide reliable transmission and reception while also ensuring that the enemy doesn't get in the way of the communications.

Modern military communications no longer involves just the Army or Navy, but often multiple branches of the armed forces as part of a coordinated mission, in what has become known as multidomain communications—with systems based on the ground, at sea, in the air, and even in space involved in the process of creating a tactical communications network.

Modern military communications devices depend almost as much on software as on hardware. For the hardware part of communications systems design, an excellent reference source was published earlier this year by McGraw-Hill Education, the 4th edition of *Communications Receivers—Principles and Design* by Dr. Ulrich Rohde, chairman of Synergy Microwave Corp., and co-authors Jerry Whitaker and Hans Zahnd.

The book reviews the various receiver architectures used in commercial and military receiver systems, along with the essential analog and digital components, such as frequency mixers and local oscillators (LOs). The hardware design side of military radios is quickly becoming overshadowed by software, however, especially since many modern military communications systems are now based on software-defined-radio (SDR) technology.

The basic operating limits, such as frequency range, receive sensitivity, and transmit power, are still defined by the hardware, but the software programmability makes it possible to "fine-tune" modulation formats and signal encoding methods. And this latter feature is of growing importance as military users seek network-based interoperability among different branches of the armed forces and in different domains. de

Jack Browne, Technical Contributor

Rubidium Standard
Marks 20 Years on GPS Satellite

THE GLOBAL positioning system (GPS) provides navigational and directional guidance for civilians, as well as military forces. GPS satellites derive their accuracy from on-board frequency standards and one of these, a rubidium atomic frequency standard (RAFS) just celebrated 20 years of continuous, failure-free on-orbit operation aboard one of the U.S. Air Force's GPS IIR satellites. Manufactured by Excelitas Technologies, the rubidium frequency reference was placed in orbit as part of the U.S. Air Force's first GPS IIR satellite on July 23, 1997 and remotely activated on August 13, 1997.

The high reliability of a rubidium atomic frequency standard (RAFS) has contributed to the failure-free operation of one of the U.S. Air Force's GPS IIR satellites. *(Courtesy of Excelitas Technologies)*

The RAFS technology is a critical time- and frequency-keeping component of the navigation payloads designed by Harris Corp. for GPS IIR, GPS IIR-M, and next-generation GPS III satellite systems produced by Lockheed Martin. A total of 12 GPS IIR and 7 GPS IIR-M satellites are currently in orbit with the RAFS technology from Excelitas, with more than 250 total years of reliable operation. The 19 satellites represent more than 60% of the current GPS satellite constellation. The first GPS III satellite with an Excelitas RAF aboard is expected to launch in 2018.

"Achieving this 20-year IIR satellite milestone, and the GPS constellation's continued good health, emphasize Excelitas' continued long-term leadership in space-qualified and military tactical time frequency standards," said Doug Benner, executive vice president of Excelitas' Defense and Aerospace group. "We are proud of our contribution to these global positioning, navigation and timing systems and we look forward to continuing this legacy for many years to come," he added.

"Excelitas' high reliability RAFS technology was developed specifically for mission critical space applications," explained John Vaccaro, technical director of RAFS Systems for Excelitas Technologies. "We have built over 125 atomic standards with world class stability and low drift combined with the small size, low weight, and power advantages. The Excelitas RAFS is recognized as an enabling technology for global positioning systems." ■

3D Printed Filter Flies in Space

(Continued from page 63)

shaved off compared to traditional "subtractive" manufacturing methods.

Working with 3D Systems *(www.3dsystems.com)*, Airbus Defence and Space built upon research funded by the European Space Agency (A0/1-6776/11/NL/GLC: Modelling and Design of Optimised Waveguide Components Utilising 3D Manufacturing Techniques) to develop the first 3D printed RF filter that has been tested and validated for use in commercial telecommunications satellites. The filter is essential to a high-capacity satellite such as the Eutelstat KA-SAT manufactured by Airbus Defence and Space, which integrates more than 500 RF filters.

The waveguide filter was printed with a 3D Systems ProX DMP 320 printer, using aluminum alloy in powdered form to create the metal parts. The direct printing process made it possible to integrate two components into one and achieve a 50% weight reduction, with faster production time and lower costs than traditional manufacturing methods.

The waveguide filter was designed with the aid of a 3D electromagnetic simulation software program, CST Microwave Studio *(www.cst.com)*. The availability of a 3D printer made it possible to fabricate a uniquely shaped depressed super-ellipsoidal cavity filter with balanced tradeoffs between quality factor (Q) and out-of-band rejection. "The main benefits of a monolithic design enabled by 3D printing are mass, cost, and time," explained Paul Booth, an RF engineer for Airbus Defence and Space. "The mass is reduced because there is no longer the requirement to have fasteners.

"With direct metal printing there is also the no-cost bonus to have the outer profile more closely follow the inner profile, so only the really necessary metal needs to be used," he continued. "The cost/time benefit comes from the reduction in assembly and post-processing." ■

NuSil Recognized by Honeywell as 2016 Supplier of Year

NUSIL TECHNOLOGY was recently named a 2016 "Supplier of The Year by Honeywell Federal Manufacturing & Technologies (www.honeywell.com) for such factors as product quality, timely delivery, technical support, responsiveness, and cost control. This part of Honeywell manages the Kansas City National Security Campus of the U.S. Department of Energy (DoE). NuSil's medical and space-grade silicones are used in the most extreme environments, from deep inside the human body to the harsh conditions of outer space.

NuSil was recently recognized as a Honeywell 2016 "Supplier of the Year."

NuSil *(www.nusil.com)* is part of the Avantor company *(www.AvantorInc.com)*, with NuSil brand materials used in many different market areas. For example, Honeywell has been using NuSil products such as raw silicone components in mission critical components for more than 30 years. Corey Walker, executive vice-president, Biomaterials and Advanced Technologies at Avantor, said, "As an industrial partner, NuSil works to serve as an integral part of our customers' product development activities, providing the necessary transparency and technical information to meet their supply chain needs," said Corey Walker, executive vice president, Biomaterials and Advanced Technologies at Avantor. "We are honored NuSil was recognized with this award from Honeywell. It acknowledges the dedication of our employees and spirit of collaboration in meeting the unique needs of our customers and helping them succeed in their goals." ■

Self-Diagnosing Sensors Improve Aircraft Performance

HONEYWELL (WWW.HONEYWELL.COM) has introduced a series of self-diagnosing sensors designed to improve the performance of aircraft systems and reduce maintenance costs associated with false readings. The Integral Health Monitoring (IHM) proximity sensors can detect when a sensor has been damaged and/or is not functioning properly. The patented proximity sensors can be designed into a range of aircraft systems, including thrust reverser actuation systems, flight controls, aircraft doors, cargo loading systems, evacuation slide locks, and landing gear.

"Aircraft operators who receive a sensor reading often cannot be sure if they have a system issue that needs to be addressed or if the sensor itself is malfunctioning," said Graham Robinson, president of Honeywell's Sensing and Internet of Things (IoT) business. "Leveraging Honeywell's technical expertise in the aerospace industry, we innovated a circuit that can detect whether a sensor reading is correct or the result of damage or some other problem with the sensor itself."

The configurable, non-contact sensors are designed to sense the presence or absence of a target in harsh-duty aircraft applications such as determining when a thrust reverser is not fully closed. The sensors can detect most internal failures and display a fault output to a pilot or maintenance worker in order to help reduce aircraft downtime and maintenance costs. As Robinson noted: "The sensor fault-detection provides mechanics on the ground with the information they need to perform inspections and repairs without a long and costly troubleshooting process." ■

TOMMY NEU | Product Manager, Texas Instruments, P.O. Box 655303, Dallas, TX 75265
www.ti.com

High-Speed Converters Provide Direct Conversion at C-Band

A family of high-speed ADCs allows direct digitization of input signals across a 3-dB bandwidth of 8 GHz and usable bandwidth of 10 GHz.

HIGH-SPEED DIGITIZERS have enabled significant improvements in military electronic systems by converting analog input signals to the digital realm, where advanced digital-signal-processing (DSP) techniques can be applied. In a receiver, analog-to-digital converters (ADCs) are positioned at the output of an intermediate-frequency (IF) amplifier, and have enabled direct sampling of those signals at L-band frequencies from 1 to 2 GHz. These high-speed data converters show little compromise in AC performance compared to traditional IF sampling architectures.

But now, with the availability of such higher-speed converters as the ADC12DJ3200 family from Texas Instruments *(www.ti.com)*, direct conversion of RF input signals is possible at frequencies to 8 GHz and beyond. A 12-b ADC12DJ3200 digitizer can be used in single- or dual-channel modes, with single-channel sampling rates to 6.4 GSamples/s and dual-channel sampling rates to 3.2 GSamples/s. It represents the next step in the evolution of high-speed data converters and can benefit a wide range of applications, including communications, radar, electronic counter measures (ECM), electronic intelligence (ELINT), and signal intelligence (SIGINT) systems.

The ADC12DJ3200 ADC *(http://www.ti.com/product/ADC12DJ3200)* has a full-power 3-dB input bandwidth of 8 GHz but a usable frequency range of better than 10 GHz. For processing the faintest of signals, it features a full-scale (FS) noise floor of −151.8 dB/Hz in dual-channel mode, which drops even further to −154.6 dBFS/Hz in single-channel mode. The ADC incorporates a high-speed JESD204B output interface with as many as 16 serialized lanes which support data transfer rates as high as 12 Gb/s. The ADC (*Fig. 1,* shown on an evaluation board) has a full-power 3-dB input bandwidth of 8 GHz but a usable frequency range of better than 10 GHz. For processing the faintest of signals, it features a full-scale (FS) noise floor of −151.8 dB/Hz in dual-channel mode, which drops even further to −154.6 dBFS/Hz in single-channel mode.

The ADC incorporates a high-speed JESD204B output interface with as many as 16 serialized lanes which support data transfer rates as high as 12 Gb/s. The number of lanes can be configured in different ways for tradeoffs in bit rate. The

1. The evaluation board contains a high-speed ADC12DJ3200 analog-to-digital converter (ADC) with 12-b resolution, sampling rates to 6.4 GSamples/s, and usable bandwidth of 10 GHz.

converter includes synchronization capabilities (e.g., noiseless aperture delay and SYSREF windowing) to simplify system design with multiple elements, such as in phase-array and multiple-input, multiple-output (MIMO) antennas.

This next generation of data converters represented by the ADC12DJ3200 ADC—with a direct-sampling architecture that can be applied at S- or C-band frequencies—brings many attractive benefits to military electronic systems, including smaller system size, larger instantaneous bandwidth (IBW), and reduced signal-chain complexity. Of course, the capability to almost immediately process received signals from a radar or EW system in the digital realm will bring many additional benefits, once system designers apply advanced signal-processing techniques earlier in the system signal chain. Let's take a closer look at these benefits.

SMALLER COMPONENT SIZE

In military electronic systems, the use of higher frequencies involves signals with smaller wavelengths and smaller physical and electrical component sizes, thus affecting most components in the signal chain. These range from the antenna and filters to passive devices like matching elements or bypass capacitors. Radar systems rely on highly directed energy beams and can achieve precisely controlled beams through the use of beamforming techniques with a distributed, phased-array antenna. Such an antenna consists of many separate radiating elements, each with a phase shifter. Beams are formed by shifting the phase of the signal emitted from each radiating element so that the combined contributions of the antenna elements result in a high-power energy beam steered in a desired direction.

COMPARING FREQUENCIES AND WAVELENGTHS FOR DIFFERENT BANDS			
Frequency band	Frequency range	Wavelength (λ)	Antenna size (λ/4)
L-band	1 to 2 GHz	60 to 30 cm	15.0 to 7.5 cm
S-band	2 to 4 GHz	15.0 to 7.5 cm	3.75 to 1.90 cm
C-band	4 to 8 GHz	7.5 to 3.75 cm	1.9 to 0.9 cm

Since modern phased-array radars can have literally thousands of antenna elements to enable simultaneous tracking of multiple targets, individual elements must be very small and operating at very low power levels. Thus, developing a radar system at S- or C-band frequencies with a much smaller electrical wavelength is a major motivation *(see table)*. Operating at a higher frequency also comes with higher transmission path loss; however, techniques such as dual polarization exist to mitigate the increased signal attenuation. C-band weather radars, for example, can achieve ranges as great as 500 km and more.

LARGER IBW

Perhaps the biggest motivation to moving to higher frequency bands is the larger available frequency spectrum, owing to the congestion of so many commercial and industrial applications at lower frequencies. S-band frequencies provide as much as 2 GHz IBW, while C-band frequencies offer as much as 4 GHz IBW—which is more than enough spectrum for frequency hopping, even for systems with larger bandwidth requirements. Direct RF sampling converters that provide frequency coverage to C-band naturally also enable frequency hopping across L-, S-, and C-band frequencies for even greater system design flexibility.

One of the key requirements for processing a higher IBW is sufficient converter sampling rate. Modern RF Gb/s sampling-rate data converters designed with advanced silicon complementary metal-oxide-semiconductor (CMOS) processes are capable of digitizing wide bandwidths with high power efficiency and minimal processing delays. High speed data converters, such as the members of the ADC12DJ3200 product family, support sampling rates to 6.4 GSamples/s for single-channel operation, along with an input bandwidth of greater than 8 GHz. This enables digitization of an IBW of better than 2 GHz at C-band frequencies *(Fig. 2)* and better than 1 GHz at S-band frequencies, while leaving adequate frequency range for the anti-aliasing filter transition band.

Numerous wideband defense electronic systems (such as ECM, ELINT, and SIGINT systems) are designed to operate over broad contiguous frequency ranges (e.g., DC to 18 GHz), although they traditional have covered that frequency range a bit at a time (such as in 1-GHz segments) due to the limitations of the digitizers. With a digitizer capable of wider IBWs, much faster spectrum scanning and response times are possible with those systems.

REDUCED COMPLEXITY

As noted earlier, phased-array systems consist of thousands of separate elements which must each be small and thermally efficient to create an antenna array in a practical size with good long-term reliability. This is especially true when moving to the shorter wavelengths of S- or C-band frequencies. Direct RF sampling offers a very desirable architecture because it removes an entire frequency-downconversion stage within the receiver *(Fig. 3)*. It is the elimination of a number of different high-frequency components, including a frequency mixer, amplifier, filter, and matching networks and power supplies for those components.

In addition to the savings in size, weight, and power (SWaP), elimination of those components also statistically removes potential sources of failure for improved overall system reliability. Maintaining the signal chain at a high frequency simplifies filtering requirements; the values of passive component elements required for filter construction such as resistors, capaci-

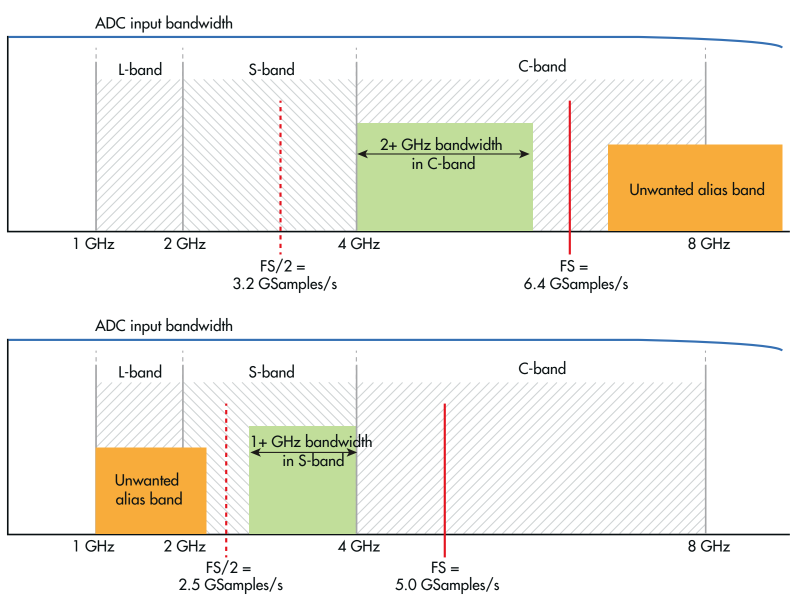

2. This frequency plan shows the strategy for using a high-speed data converter to sample an instantaneous bandwidth of greater than 2 GHz at C-band frequencies and greater than 1 GHz at S-band frequencies.

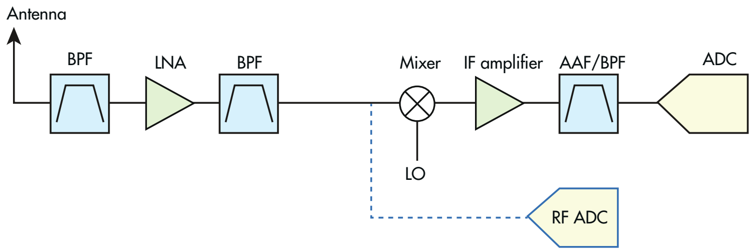

3. The signal chains for two different receiver architectures—standard superheterodyne and direct RF sampling—are shown here.

tors, and inductors are much smaller, and those circuit elements are much smaller in size at the higher wavelengths.

Of course, direct RF sampling does present some differences to a system design compared to traditional superheterodyne receiver architectures where a frequency mixer translates a smaller portion of prefiltered frequency spectrum that will then be digitized by an ADC. In the direct RF sampling approach, the entire input bandwidth is digitized, including any unwanted signals and noise within that bandwidth. Thus, any receiver design with direct RF sampling requires effective RF filter analysis to ensure that undesired out-of-band interferers are sufficiently attenuated and don't reduce the receiver sensitivity.

To minimize signal losses within the RF signal chain, impedance matching circuits are used to provide smooth impedance transitions from one component to the next. Therefore, when digitizing a large amount of frequency spectrum (as with an RF sampling converter), effective matching circuitry is essential. High-speed data converters such as the ADC12DJ3200 ADC with its well-behaved input return loss (S_{11}) across the frequency range simplify the requirements for matching circuitry.

The ADC12DJ3200 family of ADCs provides the performance levels needed for direct conversion across a 3-dB bandwidth of 8 GHz and a usable bandwidth of 10 GHz. By adopting a direct RF sampling architecture, military (and other) receivers can now be designed with one or two fewer frequency-conversion stages, resulting in less components and a simpler receiver architecture. Benefits in system-level performance are yet to be seen, but will surely be realized by creative system-level designers. mw

JACK BROWNE | Technical Contributor

Smart Radios Are Portable Computers

These tactical radios provide secure audio, video, and data communications with a wide range of network options, and even operating-frequency options.

1. The MPU5 is a combination of a radio and computer server in a compact package. It uses plug-in modules to operate at three different frequency bands.

TACTICAL RADIOS require tremendous capabilities and flexibility to remain effective on the battlefield. Most tactical environments consist of mobile ad hoc networks (MANETs) which must be interoperable with many different radio systems and organizations. The MPU5 from Persistent Systems *(www.PersistentSystems.com)* is a smart radio designed to adapt to the changing conditions of the battlefield. Based on software-defined-radio (SDR) technology and the company's own Wave Relay transmission algorithms, this is a tactical radio that also contains a full-featured computer for extensive functionality and advanced mobile networking.

The smart radio *(Fig. 1)* is equivalent to portable computer server that fits in the palm of the hand, with enormous computing and networking capabilities. The processing power that drives the MPU5 is Android-based, with 1-GHz quad-core ARM, 2 GB RAM, and 128 GB of flash memory storage. Users can run Android Tactical Assault Kit (ATAK) software and other programs and to record and review video footage, enhancing situational awareness and increasing operational effectiveness *(Fig. 2)*. The MPU5 was a recent first choice for in-the-field networking by the FBI *(http://www.mwrf.com/systems/fbi-connects-persistent-wireless-network-solution)*.

The MPU5 operates with interchangeable RF front-end modules, providing an operator with a choice of three different frequency bands, depending on module: L-band, S-band, and C-band frequencies. The miniature modules *(Fig. 3)*, which provide as much as 6 W transmit power across each of its three frequency bands, can be swapped in the field for ease of changing operating frequency bands.

With its Cloud Relay networking capability, this compact smart radio can establish a peer-to-peer mobile network anywhere and is designed for mass scalability. Thanks to a flexible radio architecture that supports 3 × 3 multiple-input,

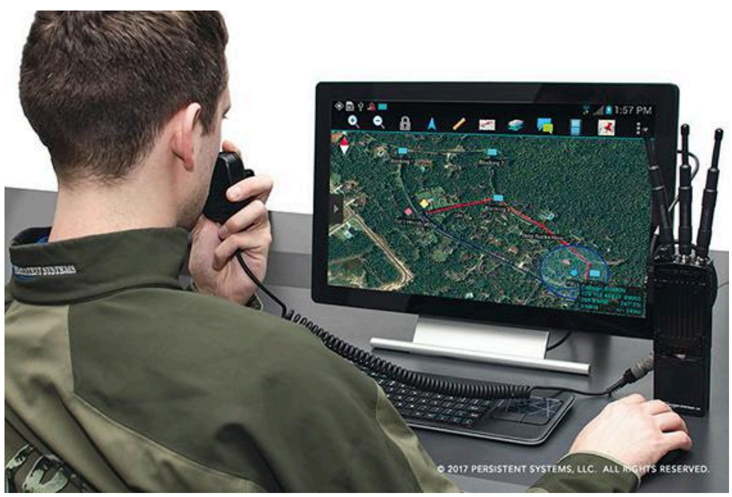

2. The portable MPU5 radio provides flexibility connectivity among troops and different organizations, with the processing power of an Android-based computer.

ULTRA·REL™
CERAMIC MMIC AMPLIFIERS

10 MHz to 7 GHz

Low NF from 0.5 dB   High IP3 up to +42 dBm   Low DC current 65 mA   from $7.45 ea. (qty 20)

When failure is not an option! Our CMA family of ceramic MMIC amplifiers is expanding to meet your needs for more critical applications. Designed into a nitrogen-filled, hermetic LTCC package just 0.045" high, these rugged models have been qualified and are capable of meeting MIL standards for a whole battery of harsh environmental conditions:

Qualified for: *(see website for complete list and details)*

Gross and Fine Leak	*HTOL (1700 hours @ +105°C)*
Mechanical Shock	*Steam Aging*
Vibration	*Solder Heat Resistance*
Acceleration	*Autoclave*
PIND	*And More!*

**Gross leak only*

Robust performance across wide bandwidths makes them ideal for military and defense applications, hi-rel instrumentation, and anywhere long-term reliability adds bottom-line value. Go to minicircuits.com for all the details today, and have them in your hands as soon as tomorrow!

Electrical Specifications *(-55 to +105°C)*

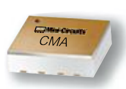

3 x 3 x 1.14 mm

Model	Freq. (GHz)	Gain (dB)	P_{OUT} (dBm)	IP3 (dBm)	NF (dB)	DC (V)	Price $ ea. (qty 20)
CMA-81+	DC-6	10	19.5	38	7.5	5	8.95
CMA-82+	DC-7	15	20	42	6.8	5	8.95
CMA-84+	DC-7	24	21	38	5.5	5	8.95
CMA-62+	0.01-6	15	19	33	5	5	7.45
CMA-63+	0.01-6	20	18	32	4	5	7.45
CMA-545+	0.05-6	15	20	37	1	3	7.45
CMA-5043+	0.05-4	18	20	33	0.8	5	7.45
CMA-545G1+	0.4-2.2	32	23	36	0.9	5	7.95
CMA-162LN+	0.7-1.6	23	19	30	0.5	4	7.45
CMA-252LN+	1.5-2.5	17	18	30	1	4	7.45

RoHS compliant

Mini-Circuits®

www.minicircuits.com P.O. Box 350166, Brooklyn, NY 11235-0003 (718) 934-4500 sales@minicircuits.com

3. The MPU5 radio can operate over three different frequency bands using plug-in radio modules.

multiple-output (MIMO) communications, it is capable of better than 100 Mb/s data throughput. It has a built-in high-definition (HD) video encoder/decoder for distributing real-time HD video feeds, along with an integrated GPS receiver with 1-s updates to provide full geographic situational awareness.

As noted above, the MPU5 operates with one of three interchangeable frequency modules, including the RF-1100 with L-band frequency range of 1,350 to 1,390 MHz; the RF-2100 with S-band frequency range of 2,200 to 2,500 MHz; and the RF-4100 with lower C-band frequency range of 4,435 to 4,980 MHz. All modules provide 6 W transmit power and software configurable bandwidths of 5, 10, and 20 MHz. All support transmit/receive operating modes from single-input, single-output (SISO) to 3 × 3 MIMO.

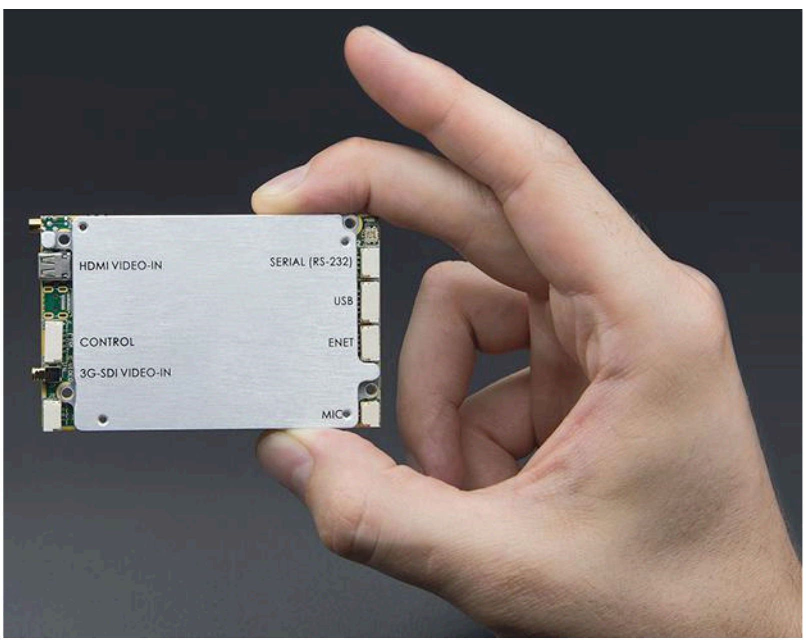

4. For applications that require an embedded radio with the performance of the MPU5, the Embedded Module offers the same basic connectivity and computing power, but without the user controls.

The MPU5 has an advanced audio architecture with 16 channels of PTT audio and radio over IP (RoIP) capability so that legacy narrowband radios can be tethered to the MPU5 and included in a MANET. To ensure networking security, the radio is equipped with CTR-AES-256 encryption, HMAC-SHA-256 authentication and integrity, and cryptographically authenticated over-the-air rekey and key-zero security.

The radio includes USB host and RS-232 serial ports, Ethernet, and USB-on-the-Go connections. It is also well equipped with power pack charging options, including an end-user-device (EUD) data/charging port, a charging downstream port (CDP) port rated for 1500 mA, and a standard charging port (SDP) rated for 500 mA. The power ports feature low-battery alert warning light.

The MPU5 Smart Radio is powered by 8 to 28 V dc, using a three-pin Fly Wheel Twist Lock connector (as used on AN/PRC-148 and AN/PRC-152 equipment). The radio is MIL-STD certified and built in an ISO 9001:2008 certified manufacturing facility. It has an operating temperature range of −40 to +85°C.

When it is necessary to incorporate this kind of networking functionality and capability within another system, the company also offers its Embedded Module *(Fig. 4)* which includes much of the performance provided in the MPU5 but in a more compact modular package and without the operating controls. Optimized for size, weight, and power (SWaP), the Embedded Module is well suited for interconnecting unmanned aerial vehicles (UAVs) and unmanned ground vehicles (UGVs) in the field.

The Embedded Module shares many of the traits of the MPU5, with an HD video encoder and Android-based computer onboard. The module measures just 2.00 × 3.29 × 0.59 in. and weighs just 3.2 oz. The computer has a 1-GHz quad-core ARM, 2 GB RAM, and 128 GB of flash storage. The embedded module operates from voltages of 8 to 30 V dc and draws 0.3 A at 12 V dc. The embedded module also uses interchangeable frequency modules to switch operating frequency bands, and is screened to MIL-STD-810G for vibration, altitude, and temperature, with an operating temperature range of −40 to +85°C. de

PERSISTENT SYSTEMS, LLC, 303 Fifth Ave., Ste. 306, New York, NY 10016; (212) 561-5895; (www.persistentsystems.com)

LOW LOSS

MIXERS

HIGH ISOLATION

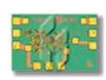

CMD252C4	CMD180	CMD181
4-8 GHz FREQUENCY RANGE	20-32 GHz FREQUENCY RANGE	26-45 GHz FREQUENCY RANGE
52 dB LO TO IF ISOLATION	36 dB LO TO IF ISOLATION	37 dB LO TO IF ISOLATION
6.5 dB CONVERSION LOSS	7 dB CONVERSION LOSS	6.5 dB CONVERSION LOSS

Try our Image Rejection Calculator

Plug in your phase and amplitude errors and see a contoured display of your image rejection using our free calculator.

custommmic.com/calculators/image-rejection

Get more resolution with less effort.

Delivering best in class broadband performance, these mixers increase dynamic range while reducing your design time by easing filter requirements. Download complete data at **CustomMMIC.com/mixers**.

Where can we take you next?

Custom MMIC

JACK BROWNE | Technical Contributor

Polaris Alpha Teams Large Talent in Small Company

Polaris Alpha is prototypical of smaller, more agile modern defense contractors, with a generous amount of design capabilities to tackle problems quickly and creatively.

DEFENSE CONTRACTS usually are awarded to the largest companies—naturally, those with the broadest engineering design and problem-solving capabilities. But every so often, a smaller company wins the prize, and usually for a unique set of skills unmatched by others. In the case of Polaris Alpha *(www.polarisalpha.com)*—which recently won a $48 million IDIQ contract to provide research, development, and technical services to the Naval Research Laboratory (NRL) Electronics Science and Technology Division (ESTD)—the capabilities extend across a wide range of technology areas, from RF to software to optoelectronics.

Small in size compared to major defense contractors, Polaris Alpha and its EOIR Technologies arm will work with NRL on the development of semiconductor materials and devices for next-generation defense sensing and imaging systems. The goal is to produce solutions that are effective on land; at sea; and in the air, space, and cyberspace for comprehensive spectrum management.

Polaris Alpha was created with the idea that a company can never have enough creative designers or problem solvers. The company was formed from a number of smaller, separate companies—EOIR Technologies, Intelligent Software Solutions (ISS), Proteus Technologies, and Intelesys Corp.—which were combined to leverage the creative interaction between and among groups. Now an organization with the agility of a focused mid-sized company strong in handling issues of national security, it still has individual groups. However, they build on their specialties, such as software development, to quickly create solutions—most recently in cyberspace.

"We have a lot of initiatives to affect cyberattacks," said Marcus Featherston, executive vice president of Mission Solutions for Polaris Alpha. "If there is a kinetic attack, such as a missile strike, we have systems, such as radar, that provide early detection and warning of the missile. But for a cyberattack, there is no warning." Featherston shared that artificial intelligence (AI) may provide the key to defending against a cyberattack: "We have seen that AI can identify these threats, and we have been working with DARPA to protect against these threats."

To handle the latest requirements in the cyber and signals intelligence (SIGINT) areas, the company produces cyber and SIGINT software solutions for the DoD and the intelligence community. These solutions make it possible to monitor and visualize an adversary's capabilities and enable actionable decision-making on behalf of the national security. As the software illustrates *(see figure)*, military actions no longer involve one part of the armed forces, but must keep battle groups across the multiple domains in constant contact.

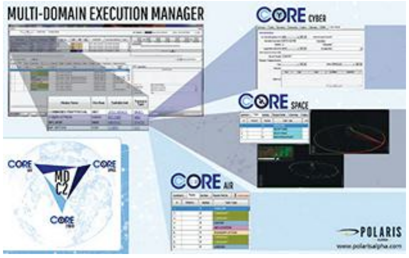

Software developed for multidomain command, communications, and control (C3) applications helps to maintain communications among different branches of the armed forces.

"We can't afford to lose communications during a conflict," said Featherston. He uses the scenario of ground troops relying on a satellite as an example of multidomain command, communications, and control (C3): armed forces are no longer engaged on simply land, or at sea, or in the air. When satellite communications is being jammed, forces within all domains—including in the cyber realm—must contribute to locating and neutralizing the jammer to maintain communications.

Featherston mentioned the company's work with the U.S. Air Force at Vandenberg AFB in California and the Air Force Research Labs (AFRL) in Rome, N.Y. on key areas of interest—notably on space situational awareness and ways to apply machine intelligence within defense electronics systems. "We use simulations in many ways, to model all the connections or PCBS in production," he said. "We also use simulation at the system level, to model and build a system and then model and build an enemy's system to see how well the original system does against it."

Given the growing complexity of defense electronic systems, there will be a place for larger defense contractors to develop them. But with the agility of new threats, the creativity and responsiveness embodied by mid-sized contractors such as Polaris Alpha provide the means to create rapid responses to those threats.

Mid-sized contractors such as Polar Alpha can take fresh looks at traditional as well as new tactical problems. These firms develop innovative solutions that help to synchronize and protect the branches of the armed forces across the multiple domains of modern warfare, all the while providing large scale software and system integration for complete solutions.

JACK BROWNE | Technical Contributor

Durable Frequency Synthesizer Tunes 450 MHz to 18.25 GHz

This compact frequency synthesizer provides fast tuning speed with output power that remains stable with temperature across a wide frequency tuning range.

SIGNAL GENERATION is the start and finish for many electronic defense-oriented systems. High-frequency signals with low noise and high stability are needed for transmit and receive functions, with performance that remains consistent even after the abuse that takes place in rugged military environments. Fortunately, the 435-36105 frequency synthesizer from Cobham Microelectronic Solutions *(www.cobham.com/cscs)*, a member of the company's 1018 series of signal sources, is built for the field rather than the laboratory.

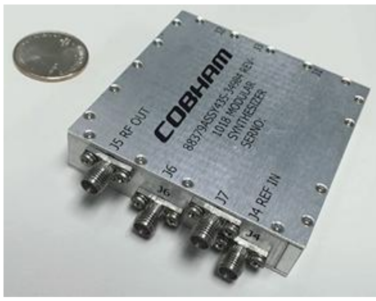

The 435-36105 frequency synthesizer covers a frequency range from 0.45 to 18.25 GHz in 10-MHz steps with at least +3 dBm output power.

The signal source covers a frequency range from 0.45 to 18.25 GHz in 10-MHz steps with at least +3 dBm output power across the frequency range. It is built to operate under the conditions of shock, vibration, and temperature typically found in severe military environments. The design is modular, incorporates custom-designed filters, and can be customized if needed. Cobham has a long history of providing optimized solutions for challenging applications.

The compact signal source *(see photo)* meets the size, weight, and power (SWaP) requirements of most military systems, supplied in a machined housing measuring just 2.6 × 2.6 × 0.6 in. and weighing just 0.25 lb. As with many of the frequency synthesizers designed and developed by Cobham—the former Aeroflex/Comstron—this latest addition to the 1018 series is built for speed, featuring a parallel control interface to facilitate pipelined hopping. This provides better than 250 µs typical switching speed from any start frequency to any stop frequency in the full range. It typically achieves faster switching speed for smaller frequency steps.

While lacking the ultimately low noise levels of laboratory benchtop frequency synthesizers, the 435-36105 synthesizer maintains reasonably low noise with high levels of shock, vibration, and a wide operating temperature range of −40 to +70°C. The spurious content is −55 dBc from 450 MHz to 12 GHz and −50 dBc from 12 to 18.25 GHz. Subharmonics are −20 dBc throughout the frequency range, while second harmonics are −12 dBc from 450 MHz to 12 GHz and −15 dBc or better from 12 to 18.25 GHz.

The compact synthesizer has an SMA port for connection to an external 10-MHz reference oscillator while maintaining the frequency stability of the external reference. The output power remains within a ±2-dB window when the frequency synthesizer is operated within ±5°C of the calibration temperature.

As expected for a PLL frequency synthesizer, the absolute phase noise—including the noise of the external reference source—is higher when measured closer to the carrier and for higher carrier frequencies. For example, the phase noise (measured in a 1-Hz bandwidth) is −73 dBc/Hz offset 1 kHz from a 500-MHz carrier, decreasing to −96 dBc/Hz offset 100 kHz from a 500-MHz carrier, and dropping to −142 dBc/Hz offset 10 MHz from the same carrier.

The phase noise degrades with carrier frequency, with phase noise of −60 dBc/Hz offset 1 kHz from a carrier frequency of 2.25 GHz, −83 dBc/Hz offset 100 kHz from the same carrier, and −138 dBc/Hz offset 10 MHz from the same carrier. At a carrier frequency of 18 GHz, the phase noise is −42 dBc/Hz offset 1 kHz from the carrier, −65 dBc/Hz offset 100 kHz from the carrier, and −120 dBc/Hz offset 10 MHz from the carrier.

The frequency synthesizer is designed for use with a +5 V dc supply (±10%), typically drawing 1.25 A current. It is one example of a diversified product line that includes many of the components required for modern radar and electronic warfare (EW) systems, including integrated frequency converters, switch matrices, and active electronically scanned array antennas (AESAs). One such AESA operates from 8 to 10 GHz with azimuth and elevation scan volumes of ±60 deg. A field-programmable-gate-array (FPGA) controller supports real-time beam forming.

COBHAM MICROELECTRONIC Solutions, 35 South Service Rd., Plainview, NY 11803; (800) 843-1553, (516) 694-6700, MES.Plainview@cobham.com, www.cobham.com/cscs

SDLVA Has Wide Range from 100 MHz to 2 GHz

THE SDLVA-0120-70-100M2G-10DBM is a successive-detection log video amplifier (SDLVA) that operates between 0.1 and 2.0 GHz. It has a minimum dynamic range of 70 dB minimum and a tangential signal sensitivity (TSS) of -65 dBm. The amplifier achieves a rise time of 25 ns and fall time of 30 ns. The amplifier provides a limited intermediate-frequency (IF) output of typically +10 dBm. It measures 3.75 × 1.50 × 0.40 in. in a gold-plated housing with SMA female connectors.

PLANAR MONOLITHICS INDUSTRIES, INC.

7311 Grove Rd., Ste. F, Frederick, MD 21704; (301) 662-5019; www.pmi-rf.com

Threshold Detector Handles 2 to 18 GHz

THE GMTA-1002 threshold detector operates from 2 to 18 GHz. It has a threshold level of –23 dBm with threshold stability of ±3.0 dBm over frequency and temperature. Other specifications include an operating input range of –18 to –23 dBm, with a maximum input power level of +10 dBm without damage. The maximum input VSWR is 2.50:1. The response time for any input greater than 3 dB is 100 µs. The threshold detector draws 50 mA maximum current from a +12 V dc supply. It measures 1.0 × 0.65 × 0.3 in. with female SMA connectors.

PLANAR MONOLITHICS INDUSTRIES, INC.

7311 Grove Rd., Ste. F, Frederick, MD 21704; (301) 662-5019; www.pmi-rf.com

Four-Way Divider/Combiner Channels 30 W to 40 GHz

RFMW LTD. has announced design and sales support for MECA power divider/combiners. As an example, the 804-3-23.000 is a four-way power divider/combiner with female 2.92-mm coaxial connectors that can handle 30 W power from 6 to 40 GHz as a power divider. It is designed to meet the applicable portions of MIL-DTL-23971 and MIL-STD-202 standards. Adding an ML prefix to any MECA 80X series power divider/combiner enhances the screening levels for qualification and verification applications as required.

RFMW, LTD. (MECA STOCKING DISTRIBUTOR)

188 Martinvale Ln., San Jose, CA 95119; (408) 414-1450, www.rfmw.com

High-Power Amplifier Boosts 225 to 450 MHz

THE TR 0.225-0.450-100 is a transmit-only solid-state amplifier optimized for military radio applications. It provides 100 W output power from 225 to 450 MHz, with output power that can be controlled in 1-dB increments. The amplifier, which is based on GaN technology, achieves power-added efficiency (PAE) of typically 30 to 40%. The power gain is 48 to 51 dB. The rugged amplifier is supplied in a housing measuring 6.0 × 10.5 × 3.0 in. The maximum input VSWR is 2.0:1. It features fast on/off switching time of 20 µs. The amplifier is equipped with over/under-voltage protection, reverse polarity protection, output short- and open-circuit protection. It has an operating temperature range of –40 to +85ºC.

AETHERCOMM, INC.

3205 Lionshead Ave., Carlsbad, CA 92010; (760) 208-6002, www.aethercomm.com

Directional Coupler Connects 2.0 to 4.2 GHz

THE N4164-20 is a rugged directional coupler with female Type N connectors. It provides 20-dB coupling from 2.0 to 4.2 GHz with ±1 dB coupling flatness and only 0.2 dB insertion loss (above the coupling loss). The coaxial directional coupler handles 50 W average input power and 3 kW peak input power with VSWR of 1.25:1 or less at both the primary and secondary (coupled) ports.

ARRA, INC.

15 Harold Ct., Bay Shore, NY 11706-2296; (631) 231-8400, www.arra.com

SMT Terminations Stop 150 W to 4 GHz

THE S2525N termination handles as much 150 W of average power from DC to 4 GHz in a tiny surface-mount-technology (SMT) housing measuring only 6.35 × 6.35 mm. The termination is constructed of an aluminum nitride (AlN) base with thick-film resistive element and gold-plated finish. It exhibits low VSWR of 1.11:1 with nominal impedance of 50 Ω and is designed for operating temperatures from –55 to +125ºC. It is manufactured by RN2 Technologies and available with design and sales support from stocking distributor RFMW, Ltd.

RFMW, LTD. (STOCKING DISTRIBUTOR FOR RN2 TECHNOLOGIES)

188 Martinvale Ln., San Jose, CA 95119; (408) 414-1450, www.rfmw.com

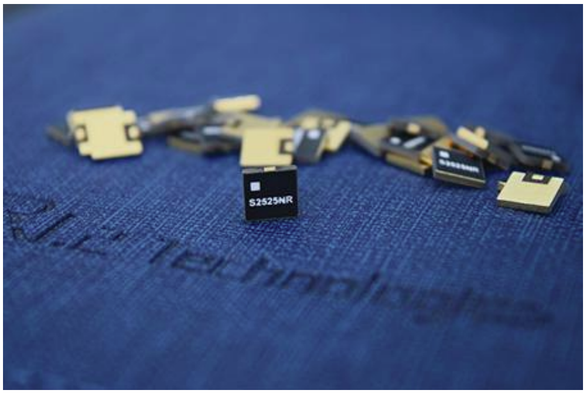

Broadband Amplifier Spans 55 to 95 GHz

THE SBP-5539531012-1212-E1 is a broadband power amplifier that provides +12 dBm output power from 55 to 95 GHz with small-signal gain of 10 dB across the frequency range. The saturated output power is +16 dBm. The amplifier, which is configured with WR-12 waveguide and UG387/U-M flanges, draws 150 mA typically current from a +8-V dc supply. Additional configurations, such as with 1-mm coaxial connectors, are also available (with different model numbers).

SAGE MILLIMETER, INC.

3043 Kashiwa St., Torrance, CA 90505; (424) 757-0168, www.sagemillimeter.com

Low-Noise Amplifier Handles 18 to 40 GHz

THE SBL-1834034030-KFKF-S1 is a low-noise amplifier (LNA) with a typical small signal gain of 40 dB and a nominal noise figure of 3 dB from 18 to 40 GHz. The LNA draws typical current of 200 mA from a +8-V dc supply. It is available in a number of different input/output connector configurations, including with WR-28 and make K connectors for either the input or output ports.

SAGE MILLIMETER, INC.

3043 Kashiwa St., Torrance, CA 90505; (424) 757-0168, www.sagemillimeter.com

Double-Balanced Mixer Spans 5 to 2,000 MHz

THE CLK-7B5S is broadband double-balanced frequency mixer covering an LO and RF range of 5 to 2000 MHz. The intermediate-frequency (IF) range is DC to 1,000 MHz, making the mixer ideal for use in high-performance frequency converters, phase detectors, and biphase and amplitude modulators. It requires LO power of +7 dBm to achieve a typical third-order input intercept point (IIP3) of +13 dBm. The typical 1-dB compression point is +1 dBm. The RF interconnects are SMA type and the package size measures 1.25 × 1.25 × 0.75 in. The 50-Ω mixer is designed for operating temperatures from –40 to +85ºC.

SYNERGY MICROWAVE CORP.

201 McLean Blvd., Paterson, NJ 07504; (973) 881-8800, www.synergymwave.com.

Two-Way Power Divider Channels 2 to 350 MHz

THE DSK-7M2S is a two-way coaxial power divider/combiner with frequency range of 2 to 350 MHz, suitable for many HF and VHF applications. It can handle input power levels to 1 W when used as a power divider and provides at least 26-dB isolation between ports with 0.8 dB maximum insertion loss (beyond dividing losses). The typical amplitude unbalance is 0.2 dB or less and the phase unbalance is 2 deg. or less. The 50-Ω power divider/combiner exhibits typical VSWR of 1.18:1 at all ports. It is supplied in a metal housing measuring 1.25 × 1.25 × 0.75 in. with SMA connectors. The power divider/combiner is designed for operating temperatures from –55 to +100ºC.

SYNERGY MICROWAVE CORP.

201 McLean Blvd., Paterson, NJ 07504; (973) 881-8800, www.synergymwave.com

Broadband I/Q Mixers Extend to 40 GHz

A FAMILY OF in-phase-quadrature (I/Q) MMIC mixers has grown with the addition of three models for applications reaching 40 GHz. Model MMIQ-0520L has an RF and local oscillator (LO) frequency range of 5 to 20 GHz and an intermediate-frequency range of DC to 6 GHz. Model MMIQ-0626L has an RF and LO frequency range of 6 to 26 GHz and an IF range of DC to 6 GHz. Model MMIQ-1040L has an RF and LO frequency range of 10 to 40 GHz and an IF range of DC to 12 GHz. All three work with LO power levels from +3 to +13 dBm and have conversion loss of 9 dB while achieving at least –25 dBc image rejection. The mixers, which are available as bare die or as modules with connectors, can also be used as vector modulators.

MARKI MICROWAVE, INC.

215 Vineyard Ct., Morgan Hill, CA 95037; (408) 778-4200, www.markimicrowave.com

Modules Support Missile Applications

A LINE OF electro-optical (EO) modules has been developed for a variety of defense-related applications, including for missile systems and unmanned-aerial-vehicle (UAV) guidance systems. The optical modules can be customized to mechanical requirements and designed for airborne, naval, and land-based use. Modules include infrared (IR) objective lenses for thermal weapons sights as well as target-acquisition and weapons-aiming EO modules.

QIOPTIQ LTD.

Glascoed Rd., St Asaph, Denbighshire, LL17 0LL, UK; (+44) (0)1745 588000, www.qioptiq.com

Straight Waveguide Sections Connect 5.85 to 110 GHz

A SERIES OF straight rectangular waveguide sections is being offered in sizes from WR-10 through WR-137 for use from 5.85 to 110 GHz. The waveguide sections, for C- through W-band frequencies, are suitable for a variety of systems, including telecommunications and radar. With VSWR as low as 1.03:1, lengths range from 3 to 12 in. The straight waveguide sections are made of either painted copper alloy or gold-plated, oxygen-free hard copper (OFHC) and feature UG-, CPR-, and UBR-style flanges.

FAIRVIEW MICROWAVE, INC.

1130 Junction Dr., Ste. 100, Allen, TX 75013; (972) 649-6678, www.fairview-microwave.com

EXPANDING
PCB Capabilities
Advanced Embedded Component Technology
from Teledyne Labtech
Complex RF Multi-layer PCBs
• Mixed Dielectric Multilayer PCB
• Embedded resistors, connector pins and capacitors
• Complex machined and laser cut structures
• Metal-cored PCB
• Embedded copper coin technology
Applications
• Airborne AESA
• Integrated Electronic Warfare Systems
• High Power Jamming Systems
• IFF Equipment
Advantages
• Improved thermal management
• Increased performance
• Reduced size and costs
TELEDYNE
LABTECH
Everywhereyoulook™
+44 (0) 1544 260093
TeledyneLabtech.com
labtechsales@teledyne.com
The Power of Consolidation
Defence & Space • Labtech • Paradise Datacom
RF & Microwave • TWT Products

GET ANSWERS to Your MIMO Questions

MULTIPLE-INPUT, MULTIPLE-OUTPUT (MIMO) technology is currently receiving a great deal of attention. Specifically, massive MIMO is something that is often discussed with regard to 5G communications, and is the subject of Keysight Technologies' new white paper, "Massive MIMO: Answering Some Common Questions."

The white paper provides a brief history of MIMO technology, explaining how its roots can be traced back many years. Several people involved with the technology's early work are mentioned. Moreover, MIMO technology has been associated with the IEEE 802.11 wireless-local-area-networking (WLAN) standard since IEEE 802.11n, as well as cellular mobile radio since 2007.

After explaining what MIMO technology is, the author describes three different use cases. For one, MIMO technology allows for the use of more than one path to decrease the error rate of a single set of data. It can also allow for the use of more than one path for different sets of data. Lastly, MIMO technology can manipulate the inherent nature of multipath interference to either cancel or augment the signal at any physical location in the radio channel.

Keysight Technologies, 1400 Fountaingrove Pkwy., Santa Rosa, CA, 95403; (800) 829-4444; www.keysight.com

Several MIMO terms are then defined. The first one is single-user MIMO (SU-MIMO), which involves using multiple radio paths to improve communications with a single user. The other terms defined are multi-user MIMO (MU-MIMO), full-dimension MIMO (FD-MIMO), and the aforementioned massive MIMO.

The white paper then answers some oft-asked questions concerning MIMO technology. The first question is simply whether or not MIMO is the same as beamforming. The author states they are not the same, proven in part by the fact that beamforming is utilized in many non-MIMO applications. Another question is with regard to just how many antennas are associated with massive MIMO. The white paper also discusses the feasibility of massive MIMO based on frequency-division-duplex (FDD) communications. The last question concerns whether or not massive MIMO is only usable at millimeter-wave frequencies.

E-PHEMT TECHNOLOGY JETTISONS BIAS SEQUENCERS

BIAS SEQUENCING IS something that is very familiar to many RF/microwave engineers. Essentially, sequencing circuits are needed to ensure that bias voltages are applied in the correct order. However, a tech brief from Custom MMIC titled "Throw out complex bias sequencers along with the negative voltage supply" explains how sequencing circuits can for all intents and purposes be eliminated from the design process.

Custom MMIC, 300 Apollo Dr., Chelmsford, MA 01824; 978-467-4290; www.custommmic.com

Amplifiers based on depletion-mode pseudomorphic-high-electron-mobility-transistor (D-pHEMT) technology have traditionally required bias sequencing circuits. As stated, sequencing circuits are utilized to properly bias transistors. Incorrect biasing often results in damage to a transistor. Furthermore, a depletion-mode device must also be powered down with the same sequence in reverse.

The situation is even more complicated for complex systems that contain multiple amplifiers based on depletion-mode technology. One specific example mentioned is a phased-array radar system in which sequencing must be applied to hundreds (or even thousands) of amplifiers. Any delays or offsets in the biasing scheme could have a major impact on the radar system's overall sensitivity.

The tech brief explains that the solution to the problem lies in physics. Unlike D-pHEMT devices, enhancement-mode pseudomorphic-high-electron-mobility-transistor (E-pHEMT) devices are normally non-conductive and only sink current when both the drain and gate are biased—regardless of the sequence. Thus, sequencing circuitry is not needed for E-pHEMT devices. Furthermore, E-pHEMT transistors achieve performance levels that are comparable with (or even better than) D-pHEMT transistors, according to the tech brief. Specifically, in some instances, E-pHEMT devices can outperform D-pHEMT devices in terms of maximum gain, noise figure, and linearity.

Eliminating the need for bias sequencing can result in a number of benefits, such as a reduced bill of materials (BOM), more simplified circuitry, and a reduced number of extraneous noise sources. Designers can therefore focus on other important aspects of the system design. The tech brief concludes by stating that a number of manufacturers are utilizing E-pHEMT technology, with Custom MMIC currently offering a range of power amplifiers (PAs) and low-noise amplifiers (LNAs) based on E-pHEMT technology.

UP TO 100 Watt AMPLIFIERS

NOW! 100 kHz to 26.5 GHz

from $995 ea. qty. (1-9)

High-powered performance across wide frequency ranges. Mini-Circuits' class A/AB linear amplifiers have set a standard for wideband high-power performance throughout the RF and microwave industry. Rugged and reliable, they feature over-voltage and over-temperature protections and can withstand opens and shorts at the output! Available with or without heat sinks, they're perfect for demanding test lab environments and for integrating directly into customer assemblies. With standard models covering frequencies from 100 kHz up to 26.5 GHz, chances are we have a solution for your needs in stock. Place your order on minicircuits.com today for delivery as soon as tomorrow! Need a custom model? Give us a call and talk to our engineers about your special requirements!

Model	Frequency (MHz)	Gain (dB)	Pout@ Comp. 1 dB (W)	3 dB (W)	$ Price* (Qty. 1-9)
ZVM-273HP+	13000-26500	14.5	0.5	0.5	2195
ZVE-3W-83+	2000-8000	35	2	3	1424.95
ZVE-3W-183+	5900-18000	35	2	3	1424.95
ZHL-4W-422+	500-4200	25	3	4	1160
ZHL-5W-422+	500-4200	25	3	5	1670
ZHL-5W-2G+	800-2000	45	5	5	995
ZHL-10W-2G+	800-2000	43	10	12	1395
• ZHL-16W-43+	1800-4000	45	12	16	1595
• ZHL-20W-13+	20-1000	50	13	20	1470
• ZHL-20W-13SW+	20-1000	50	13	20	1595
LZY-22+	0.1-200	43	16	30	1595
ZHL-30W-262+	2300-2550	50	20	32	1995
NEW! ZHL-25W-63+	700-6000	53	25	-	8595
NEW! ZHL-25W-272+	20-2700	50	10	25	3795.95
ZHL-30W-252+	700-2500	50	25	40	2995
LZY-2+	500-1000	47	32	38	2195
LZY-1+	20-512	42	50	50	1995
• ZHL-50W-52+	50-500	50	63	63	1395
• ZHL-100W-52+	50-500	50	63	79	1995
• ZHL-100W-GAN+	20-500	42	79	100	2845
ZHL-100W-272+	700-2700	48	79	100	7995
ZHL-100W-13+	800-1000	50	79	100	2395
ZHL-100W-352+	3000-3500	50	100	100	3595
ZHL-100W-43+	3500-4000	50	100	100	3595

Listed performance data typical, see minicircuits.com for more details.
• Protected under U.S. Patent 7,348,854
**Price Includes Heatsink*

Mini-Circuits®

www.minicircuits.com P.O. Box 350166, Brooklyn, NY 11235-0003 (718) 934-4500 sales@minicircuits.com

416 rev AM

JEFFREY PHILLIPS | Principal Software Product Marketing Manager, National Instruments (NI)
www.ni.com

Software Centricity Seeks to Make the Impossible Possible

This software-centric platform helps solve today's difficult challenges by allowing for productivity through abstraction, software interoperability, comprehensive data analytics, and the efficient management of distributed systems.

The rapid pace of technological advancement should be celebrated and embraced. It fuels amazing new technologies and scientific achievements that make us more connected and safer. It also pushes the limits of what we previously thought possible. The impact of these achievements is no longer isolated to a narrow market vertical. It permeates every industry and exposes the established market incumbents to an unusual combination of disruption and growth potential.

But the pressure and the challenge to drive business are daunting in this climate. How do you stimulate growth while making large investments in future technologies without dramatically changing your business model? Companies are watching their operational costs balloon as they dip their toes into numerous areas of investment that require significant and often disparate expertise. Meanwhile, small startups with incredible focus and no prior obligations can leverage new technologies in ways that established competitors struggle to answer.

So how do you protect yourself from disruption? How do you innovate without radically increasing the cost of doing business? It all boils down to one simple question: Do you feel secure in the tools you're using? That's the magic question, whether it's your personal finances, career, or the engineering systems of the future. For instance, the Industrial Internet of Things (IIoT) ushers in a new era of both networked potential and significant risk. To best understand which software prepares you to most securely engineer future systems, you should turn to the recent past.

In 2005, the previous three technological decades were defined by one simple observation made by the co-founder of Intel, Gordon Moore. Moore's law was the prediction, based on the recent past, that the number of transistors per square inch on an integrated circuit would continue to double every 18 months. Seemingly linear growth was just the start of exponential growth.

Before we knew it, CEOs from every semiconductor manufacturer talked about the number of parallel-processing cores over the next few years. Intel CEO Paul Otellini promised 80-core chips in the following five years. The demand for more processing power with lower latency marched on. Alternative processing fabric emerged. First, the FPGA stormed into popularity with its software-defined timing and massively complex low-level programming languages. Next, heterogeneous processing was born when the traditional processor and FPGA were combined onto a single chip.

Along with this explosion of processor architectures came a flood of new programming environments, programming languages, and open-source fads biding their time until the inevitable decline into oblivion. And, of course, the whole burden of figuring out how to efficiently program the processors fell on you.

But now, we look to the future. The explosion of processing capabilities is leading us forward into a world of hyperconnectivity. And this world becomes more connected as engineering systems become more distributed. Trends like 5G and the IIoT promise to connect infrastructure, transportation, and the consumer network to enrich the lives of people the world over. It's inarguable that software will be the defining aspect of any engineering system, if it's not already. And it won't be long before hardware becomes completely commoditized and the only distinguishing component of a system will be the IP that defines the logic.

Most test-and-measurement vendors have been slow to respond to the inevitable rise of software; they're just now hitting the market with software environments that help the engineering community. But even those can only get you so far. As the industry continues to evolve, the tools engineers use to design these connected systems must meet four key challenges: productivity through abstraction, software interoperability, comprehensive data analytics, and the efficient management of distributed systems.

PRODUCTIVITY THROUGH ABSTRACTION

Abstraction is one of those words that's so overused it's in danger of losing its meaning. Simply put, it is making the complex common. In the world of designing engineering systems, complexity often comes from programming. The custom logic that adds the *smart* to smart systems typically requires a level of coding that's often so complex, it's what separates the pros from the amateurs.

The complex must become common, though. To solve this challenge, engineers need a "programming optional" workflow that enables them to discover and configure measurement hardware, acquire real-world data, and then perform data analytics to turn that raw data into real insight. NI is introducing a new configuration-based workflow in the form of LabVIEW NXG *(Fig. 1)*.

The NXG workflow is complemented by the graphical dataflow programming paradigm native to LabVIEW, which is known for accelerating developer productivity in complex system design for nearly 30 years. With this configuration-based interaction style, you can progress from sensor connections all the way to the resulting action without the need for programming—and still construct the code modules behind the scenes. That last step is a critical feature that streamlines the transition from one-off insights into repeatable and automated measurements.

SOFTWARE INTEROPERABILITY

With the growing complexity of today's solutions, the need to combine multiple software languages, environments, and approaches is quickly becoming ubiquitous. However, the cost

1. New workflows in LabVIEW NXG enable users to acquire, analyze, and export measurement data without programming.

of integrating these software components is considerable and continues to rise.

Languages for specialized hardware platforms must be integrated with other languages as these compute platforms are being combined into single devices. Typically, the solution to this is that the design team assumes the burden of integration. However, this is essentially just treating the symptoms and not addressing the root cause. The software vendors must fix the root cause.

By design, NI's software-centric platform places this software interoperability at the forefront of the development process *(Fig. 2)*. Though LabVIEW has been at the center of this software-centric approach, many complementary software products from other companies are individually laser-focused on specific tasks, such as test sequencing, hardware-in-the-loop prototyping, server-based data analytics, circuit simulation for teaching engineers, and online asset monitoring.

These products are purposefully limited to the common workflows of the engineers and technicians performing those tasks. This characteristic is shared with other software in the industry tailored to the same purpose. However, for NI software, LabVIEW provides ultimate extensibility capabilities through an engineering-focused programming language that defies the limitations of tailored software.

For example, consider DAQExpress. It is new companion software for USB and low-cost plug-in NI data-acquisition hardware that significantly simplifies the discovery and configuration of hardware, as well as provides access to live data in two clicks. All configuration "tasks" within this product are fully transferrable to LabVIEW NXG, which simplifies the transition from hardware configuration to measurement automation.

In addition to interoperating within the NI platform, products like LabVIEW 2017 feature enhanced interoperability with IP and standard communications protocols. For embedded systems that need to interoperate with industrial automation devices, LabVIEW 2017 includes native support for IEC 61131-3, OPC-UA, and the secure DDS messaging standard. It also offers new interactive machine-learning algorithms and native integration with Amazon Web Services.

COMPREHENSIVE DATA ANALYTICS

Perhaps the most prolific benefit of the mass connectedness between the world's systems is the ability to instantaneously access data and analyze every data point you collect. This process is critical to automating decision-making and eliminating preventable delays in the necessary corrective action when data anomalies happen. To create the future network that can support this need, billions of dollars are being poured into research as algorithm experts from around the globe race to meet the demands of 1-ms latency coupled with 10-Gb/s throughput.

This direction introduces new demands on software. The first is to ensure that the processing elements can be easily deployed across a wide variety of processing architectures and then redeployed on a different processor with minimal (hopefully zero) rework. The second is to be open enough to now interface with data from an infinite number of nodes and via an infinite number of data formats.

NI has invested in server products that allow you to intelligently and easily standardize, analyze, and report on large amounts of data across your entire test organization. A key component is providing algorithms to preprocess files and automatically standardize items such as metadata, units, and file types in addition to performing basic analysis and data quality checks. Based on that data's contents, the software can then intelligently choose which script gets run. This type of interface is critical to eliminating the complexity of real-time data analytics, so that you can focus on what matters: the data.

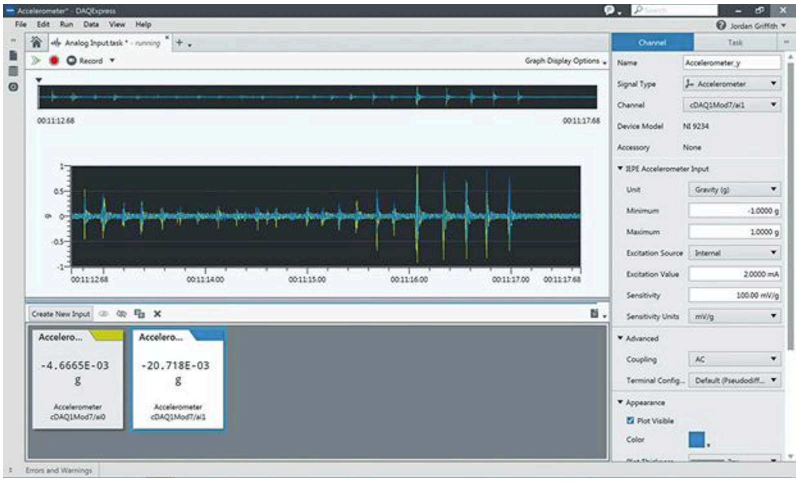

2. The interoperability between products in NI's software portfolio simplifies the sharing of IP and transfer of code for more complex development.

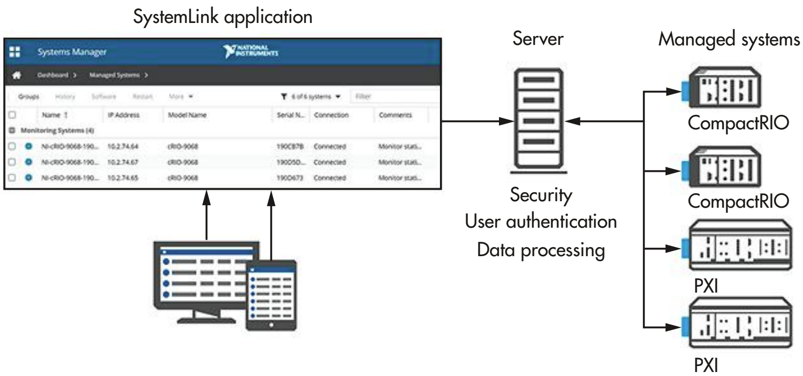

3. SystemLink introduces a web-based interface to manage distributed hardware systems.

DISTRIBUTED SYSTEMS MANAGEMENT

The mass deployment and connectedness of these systems have renewed the need to efficiently manage all of the distributed hardware from a centralized—and often remote—location. Today, this typically requires replicating single-point deployments across hundreds, and even thousands, of systems. Centralizing the management then leads to the ability to see a real-time dashboard of the hardware from the remote depot instead of physically accessing the system.

SystemLink is new software from NI that helps you centralize the coordination of a system's device configuration, software deployment, and data management *(Fig. 3)*. This reduces the administrative burden and logistical costs associated with systems-management functions. The software also improves test- and embedded-system uptime by promoting awareness of operational state and health criteria. It simplifies managing distributed systems and provides APIs from LabVIEW and other software languages such as C++.

ASK YOURSELF AGAIN

Beyond the individual innovation within each of these product releases, the collection represents the culmination of ongoing investment in software that NI has committed to year after year. Again, the unique combination of software products and their inherent interoperability distinguishes NI's platform. From discovering the Higgs boson particle to decreasing test times by 100X for Qualcomm, to being Nokia's and Samsung's solution of choice for their 5G research, NI's software-centric platform is the building block that engineers often use to solve the most complex challenges in the world.

Ask yourself again: How secure do you feel in the tools you're using?

JACK BROWNE | Technical Contributor

Cables and Connectors Head for Higher Frequencies

While they can't match the low loss and power handling of waveguide, coaxial cables and connectors are climbing the frequency ladder to cope with anticipated 5G applications.

THEY ARE OFTEN the forgotten part of a system, the means of moving a signal from one point to another. With the fascination toward wireless applications taking center stage over the past three decades, RF/microwave engineers will tend to forget about the still-important needs for wires (cables) and connectors. They come in handy when interconnecting coaxial modules within a system or making a hookup between a device under test (DUT) and a test instrument, such as a spectrum analyzer or vector network analyzer (VNA).

Coaxial cables and connectors have come a long way from the basic assemblies that spanned dc to 18 GHz for military electronic-warfare (EW) systems and test applications. With the growing interest in millimeter-wave frequencies, a greater number of connector and cable suppliers are offering these parts and assemblies through 40 GHz. In fact, a surprising number offer cable assemblies that exceed 100 GHz. That's in response to the availability of millimeter-wave test instruments and the need for testing higher-frequency DUTs for the anticipated greater use of millimeter-wave frequencies in emerging 5G wireless networks.

FREQUENCY AND BANDWIDTH

The dimensions of connectors and cables necessarily shrink with increasing frequencies to accommodate the smaller wavelengths at those higher frequencies. Government organizations such as the Small Business Innovative Research (SBIR, *www.sbir.gov*) program are well aware of how bandwidth is being rapidly consumed at microwave frequencies, in both commercial and military systems, and all available bandwidth lies at higher frequencies. The SBIR is currently looking for microfabricated broadband connector designs through 400 GHz for millimeter-wave and submillimeter-wave applications (working in particular with Nuvotronics) in support of test and research work.

In the real world, however, available connectors and cables are typically much lower in frequency, although typical cut-off frequencies for the cables now reach into the millimeter-wave region. Many of the cable assemblies to 100 GHz and higher are marketed as VNA cables because they are mostly used for high-frequency coaxial measurements with a VNA.

1. These phase-stable cables employ a proprietary dielectric material to achieve phase stability with temperature. *(Courtesy of Times Microwave Systems)*

As test and system engineers working with such high-frequency cables have learned, the flexible versions of such cables can be susceptible to phase variations with flexure. As is known by anyone who has watched the phase response on a VNA screen while inadvertently (or intentionally) moving the position of a test cable, the phase can change with such cable movement. A cable assembly's amplitude characteristics can also change with time and temperature, which has led a growing number of cable manufacturers to develop "phase-stable" cables and cable assemblies.

COAXIAL CONNECTORS AND THEIR FREQUENCY RANGES

Connector type	Frequency range (GHz)
BNC	DC to 4
TNC	DC to 4
7-16 DIN	DC to 7.5
Type N	DC to 11
C	DC to 12
SMA	DC to 18
Precision SMA	DC to 26.5
3.5 mm	DC to 26.5
2.4 mm	DC to 50
2.92 mm/K	DC to 40
1.85 mm	DC to 65
1.00 mm	DC to 110

GOING THROUGH A PHASE

For example, Times Microwave Systems (*www.timesmicrowave.com*) refers to its PhaseTrack cables (*Fig. 1*) as being "phase critical," and has developed a proprietary dielectric material called TF4 to maintain excellent phase stability with frequency and temperature. The dielectric material was formulated as an enhancement over the polytetrafluoroethylene (PTFE) dielectric material commonly used in microwave cables, but characterized by a "phase knee" or phase transition at room temperature, indicating rapid changes in phase behavior of a PTFE-based cable.

2. These VNA test cables are rated for as many as 100,000 flexures without significant degradation in performance. *(Courtesy of Pasternack Enterprises)*

These 50-Ω phase-critical cables are available with different diameters; the smallest-diameter cables provide the highest frequency of operation, a cutoff frequency (F_{co}) of 80 GHz for the raw cable. When supplied as a cable assembly, the frequency cutoff will depend on the choice of connectors (*see table on page 94*), with 1.0-mm connectors required for the highest frequency of operation.

Many of these VNA-type cables are characterized in terms of their phase variations with flexure, since flexible cables can commonly be moved and repositioned when connecting and unconnecting a DUT to a test setup. Flexible VNA test cables from Pasternack Enterprises (*www.pasternack.com*) are available with cutoff frequencies of 50 and 67 GHz (*Fig. 2*). They have maximum phase variation with flexure of ±6 deg. to 50 GHz and ±8 deg. to 67 GHz. The cables are rated for as many as 100,000 flexing cycles without significant degradation in performance, while the connectors can handle as many as 5000 mating cycles.

When higher-frequency operation is needed, Phase3 coaxial cables from MegaPhase with minimum diameter and 1.0-mm connectors (model CO5) are capable of low-loss operation to 110 GHz (*Fig. 3*). The cables are constructed with solid-gold-plated, copper-clad steel inner conductor; gold-plated, copper braid outer conductor; laminated PTFE dielectric; and blue polyolefin over FEP jacket. While the loss is 4.947 dB/ft. at

110 GHz, it is only 2.068 dB/ft. at 26.5 GHz, and just 0.347 dB/ft. at 1 GHz. The cable assemblies feature outstanding shielding effectiveness (SE) of –110 dB.

Phase stability was one of the design goals of the Stability line of RF/microwave cable assemblies from Maury Microwave. These phase- and amplitude-stable cable assemblies, designed for measurement applications, provide excellent repeatability even after multiple flexures. The cables use the ColorConnect color-coding scheme to identify cable and connector types to avoid improper mating and damage to connectors. The cable assemblies are available with a wide range of connectors, including 2.4-mm and 1.85-mm connectors for use to top frequencies of 50 and 67 GHz, respectively.

3. With 1.0-mm connectors, these high-performance cables can operate to 110 GHz with low loss. *(Courtesy of MegaPhase)*

AT LOWER FREQUENCIES

Of course, not all interconnect applications are in the millimeter-wave frequency range. For many applications, a standard microwave cable assembly will do the job. Mini-Circuits recently added a line of 4-in.-long flexible coaxial cable assemblies for interconnections in tight places. The 141-SMSM+ series Hand-Flex flexible coaxial cables have an SMA female bulkhead connector at one end and an SMA male connector at the other end. The configuration eliminates the need for bulkhead adapters, and the minimum bend radius of 8 mm simplifies interconnection of closely spaced components. The insertion loss is typically 0.05 dB to 2 GHz and 0.21 dB from 2 to 18 GHz.

One of the latest connector developments intended to simplify assembly of printed-circuit boards (PCBs) is a solderless end-launch connector from SV Microwave (*www.svmicrowave.com*). It mounts by means of compression fit and provides the transition from the coaxial signal realm to a PCB using the most popular transmission-line technologies, including microstrip, stripline, and coplanar waveguide (CPW).

The connector, which is fabricated with stainless steel, adjusts to multiple thicknesses of PCBs. It comes in a number of connector configurations, including SMA, 2.92-mm, 2.4-mm, and 1.85-mm types for high-speed digital applications as well as analog frequencies from dc to 50 GHz. mw

DR. GENT PAPARISTO, JOEL KIRSHMAN, DAVID VYE | AWR Group, NI
www.awrcorp.com

Capitalize on EDA When Developing MIMO, Phased-Array Antenna Systems, Part 2

How can advanced software be utilized to develop individual antenna elements that comprise array simulations?

Part 1 of this two-part series discussed the development costs and complexity of new radar and communications systems utilizing phased-array antennas, and how these challenges are being addressed through new functionalities in electronic-design-automation (EDA) software. Part 2 delves into individual antenna-element development and its incorporation into an array simulation that accounts for mutual coupling between radiating elements, as well as positioning (edge, center, corner) within the array and impairments due to element failure.

INDIVIDUAL ANTENNA DESIGN

From the example in Part 1, a 15-×-5 array presented the radiation patterns for an ideal isotropic antenna (gain = 0 dBi) and a simple patch antenna. In addition to the array configuration itself, the design team will likely want to specify the radiation pattern and size constraints for the individual antenna elements. This operation can be performed using the synthesis capabilities in the AntSyn antenna synthesis and optimization module within NI AWR Design Environment.

AntSyn uses an electromagnetic (EM) solver driven by proprietary evolutionary algorithms to explore multiple design options based on antenna specifications defined by the engineer. These specifications include typical antenna metrics, physical size constraints, and optional candidate antenna types (the user may select from a database of antenna types or let the software automatically select likely antenna types to optimize; *Fig. 1)*.

AntSyn creates antenna geometries from its database of design types. It then applies EM simulation and its unique evolutionary optimization to modify those designs to achieve the required electrical performance and size constraints. A run-time update of the design types under investigation is listed, along with a star rating system to indicate which designs are close to achieving the desired performance.

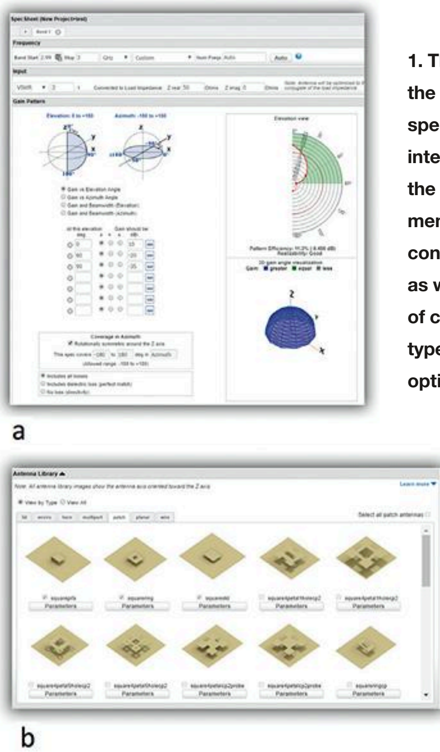

1. This figure depicts the antenna design spec-sheet user interface. Shown are the electrical requirements and physical constraints inputs, as well as a database of candidate antenna types for use in EM optimization.

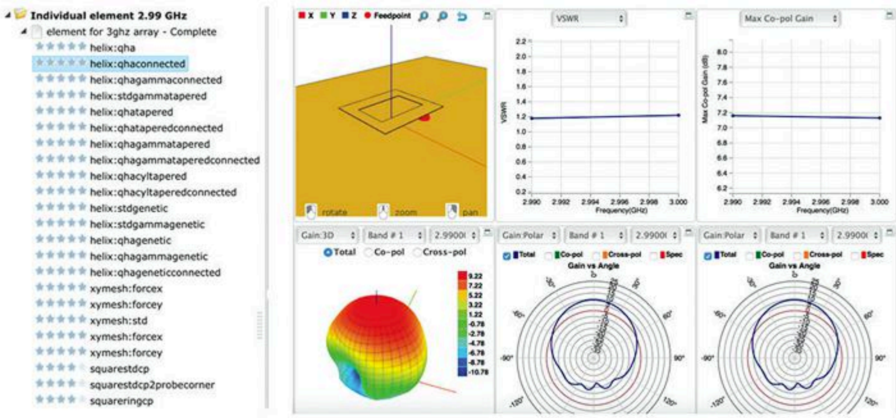

2. The AntSyn project tree (left) lists the original spec sheet, as well as all attempted antenna designs with their star rating, showing how well the antenna came to desired results. Individual antenna results can be viewed with the interface (right) and exported to supported EM tools.

Users are able to review the results and design styles as the simulation progresses. Promising designs can then be exported into an AWR Design Environment EM tool (AXIEM 3D planar simulator or Analyst 3D finite-element method simulator) or through AWR Connected third-party EM simulators *(Fig. 2)*.

Figure 3 shows the design flow between AntSyn and NI AWR Design Environment. AntSyn takes antenna requirements and generates an antenna for use in EM tools, which will create the antenna pattern for the Visual System Simulator (VSS) phased-array model.

Due to its relatively small size and easy fabrication, a square-ring patch antenna was chosen from the potential antennas created by AntSyn. The antenna was exported using the AXIEM options and then imported into a new AXIEM EM structure in the initial phased-array project. *Figure 4* shows the re-simulated antenna.

This simulation provided the antenna pattern used to replace the original patch antenna employed in the 15-×-5 phased array *(Fig. 5a)*. The new antenna pattern is depicted in *Figure 5b*. The new phased-array results for both the original antenna (red trace) and the square-ring patch (green trace) can be seen in *Figures 5c and 5d*.

MODELING COMPLEX INTERACTIONS

The mutual coupling between antenna elements affects antenna parameters like terminal impedances and reflection coefficients, and hence the antenna-array performance in terms of radiation characteristics, output signal-to-interference noise ratio (SINR), and radar cross section (RCS). The most recent V13 release of VSS includes new capabilities for more accurate simulation of these parameters, including enhanced modeling of element patterns and mutual coupling. What we'll examine next are these recent advances in advanced phased-array modeling, including accurate representation of the feed structure.

As mentioned, VSS lets designers define gains or full radiation patterns for each antenna element in the phased array. Thus, they can use different radiation patterns for internal, edge, and corner elements of the phased array *(Fig. 6)*.

The radiation pattern of each antenna element will likely be affected by its position in the phased array. These patterns may be measured in the lab or calculated in AXIEM or Analyst. A simple approach to characterize the appropriate radiation pattern for a given element is to use a 3-×-3 phased array. One element is then excited, while all others are terminated.

AntSyn		
User design input	**Synthesis**	**Export data**
Electrical Properties	EM optimization based on evolutionary algorithm provides design candidates that achieved user specifications	Analyst (3D) AXIEM (planar) ANSYS HFSS (3D) CST (3D) WIPL (3D) DXF (layout) STEP (3D geometry)
Frequency, VSWR, gain pattern, polarization		
Physical Properties		
Geometric constraints, ground-plane details, dielectric properties		
Antenna Type		
Planar, horn, dipole, helix, etc.		

NI AWR Design Environment	
Operation	**Product**
Import AntSyn model (XML) as an EM structure in AXIEM or Analyst (planar or 3D) using EM socket. Perform EM simulation to generate radiation pattern	AXIEM or Analyst AXIEM or Analyst
Assign radiation pattern to phased-array model Simulate new array pattern RF-link budget design	VSS VSS VSS
Array/feed-network interactions	VSS/Microwave Office
Feed-network design	Microwave Office

3. Shown are operations and products used to create a new antenna design for EM analysis and incorporation into the VSS phased-array model.

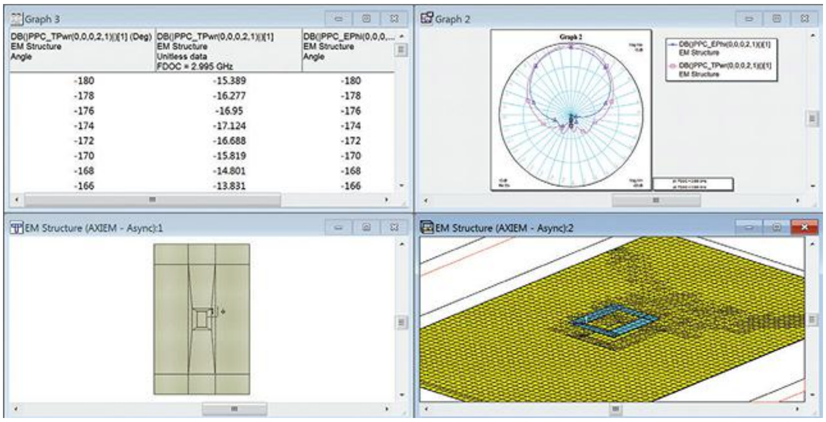

4. Here, an AntSyn-generated square-ring antenna is imported into AXIEM and simulated to generate antenna patterns used by the VSS phased-array model.

This one excited element could either be the internal element, one of the edge elements, or one of the corner elements.

The method described will provide the internal, edge, and corner element radiation patterns, which can then be automatically stored in data files using the NI AWR software output data file measurements (the same technique used in the example above). This approach includes the effect of mutual coupling from first-order neighbors. An array with a larger number of elements may be used to extend mutual coupling to first- and second-order neighbors.

It is also important to capture the mutual coupling between neighboring elements. The VSS phased-array model does this through a coupling table defined in the configuration file. Different coupling levels can be defined based on distance from each other. In *Figure 7*, the coupling, which is specified in magnitude (dB) and phase (degrees), is defined for two different distances (adjacent side elements: radius c_1 and adjacent corner elements: radius c_2).

MODELING IMPAIRMENTS AND YIELD ANALYSIS

RF hardware impairments of the array will affect the resulting side-lobe levels and beam patterns and ultimately reduce system-level performance. For transmitter arrays, side-lobe levels from imperfectly formed beams may interfere with external devices or make the transmitter visible to countermeasures. In radar systems, side lobes may also cause a form of self-induced multipath, where multiple copies of the same radar signal arrive from different side-lobe directions, which can exaggerate ground clutter and require expensive signal processing to remove. Therefore, it is critical to identify the source of such impairments, observe their impact on the array performance, and take steps to reduce or eliminate them.

The VSS phased-array configuration file allows engineers to simulate array imperfections due to manufacturing flaws or element failure. All gain/phase calculations are performed internally and yield analysis can be applied to the block to evaluate sensitivity to variances of any defining phased-array parameters. As an example, VSS was used to perform an element failure analysis on a 64-element (16-×-4) array, producing the plots in *Figure 8*, which illustrates the side-lobe response degradation.

RF impairments can also be caused by any number of items relating to the feed network design and related components. Systematic errors that may be compensated include inter-chain variations caused by asymmetrical routing (layout); frequency dependencies; noise; temperature; and varied mismatching due to changing antenna impedance with steer angle, which also impacts amplifier compression. Therefore, it is imperative to be able to simulate the interactions between the antenna array and the individual RF links in the feed network.

RF LINK MODELING

NI AWR software products include the simulation and modeling technology to capture these impairments accurately and incorporate results into the VSS phased-array assembly model. This is an important functionality, since RF links are not ideal and can cause the array behavior to deviate significantly. The phased-array assembly can operate in either the RX or TX mode, supporting the configuration of the array-element geometry, each element's antenna characteristics, the RF link characteristics, and the common linear characteristics of the combiner/splitter used to join the elements together.

The configuration is performed primarily through a text data file. Commonly swept settings are specified either directly via block parameters (such as steering angles), or specified in the data file but capable of being overridden via block parameters (such as individual element gain and phase adjustments).

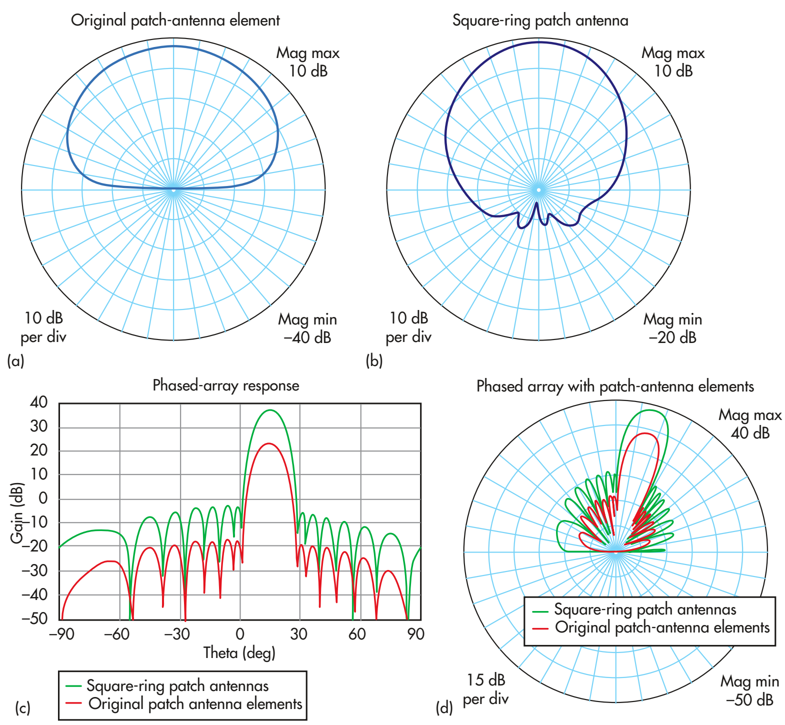

5. Shown are the original antenna pattern of the single-patch antenna used in the original phased-array analysis (a), the antenna pattern for the square-ring antenna generated by AntSyn (b), and radiation patterns from phased arrays based on simple patch antennas and square-ring patches (c; d).

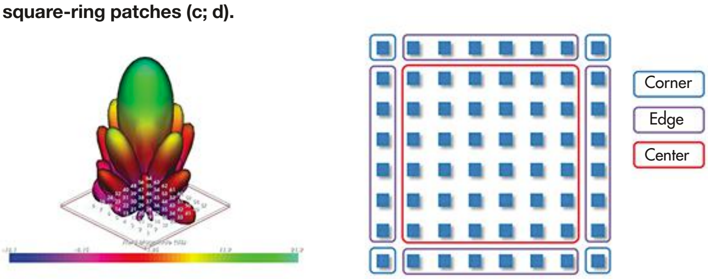

6. The VSS phased-array model supports the ability to assign different antenna patterns to individual elements, enabling designers to more accurately represent corner, edge, and center elements.

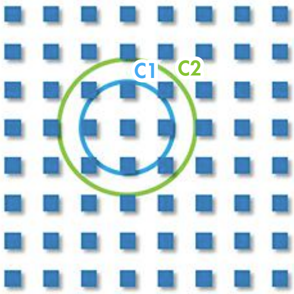

C_1_MAX_DIST = 1.25
C_2_MAX_DIST = 1.75

Freq (,GHz)	C_1 (Mag, dB)	C_1 (Phs, Deg)	C_2 (Mag, dB)	C_2 (Phs, Deg)
1	−5	20	−10	−20

7. This figure shows the 64-element array, as well as the mutual coupling table used in the configuration file to specify the amount of coupling between elements to enable more accurate simulation of terminal impedances, reflection coefficients, etc.

The configuration of the phased-array assembly may be divided into several sections:

- Array geometry: Defines the number of elements, their placement, and any geometry-related gain and phase tapers.
- Antenna characteristics: Defines antenna gain, internal loss, polarization loss, mismatch loss, and radiation patterns for both receive and transmit configurations.
- RF-link characteristics: Defines links for individual elements, including gain, noise, and 1-dB compression point (P1dB). Supports two-port RF nonlinear amplifiers using large-signal nonlinear characterization data typically consisting of rows of input power or voltage levels and corresponding output fundamental, harmonic, and/or intermodulation product levels. Frequency-dependent data is also supported.
- Assignment of antenna and RF-link characteristics to individual elements.
- Power splitter characteristics: Splits the incoming signal into n-connected output ports.
- Mutual coupling characteristics (previously discussed).

One common challenge is that not all RF links should be equal. For example, gain tapers are commonly employed in phased arrays. However, when identical RF links are used for all antenna elements, elements with higher gains may operate well into compression while others operate in a purely linear region, causing undesired array performance. To avoid this problem, designers often use different RF-link designs for different elements. While this is a more complicated task, the designs can be achieved with VSS phased-array modeling, resulting in more efficient phased arrays.

To assist the design team creating the feed network and providing the RF link to the systems team, VSS includes the capability to automatically generate the characteristics of the phased-array element link defined by the data tables. The designer starts by creating a schematic-based link design per the system

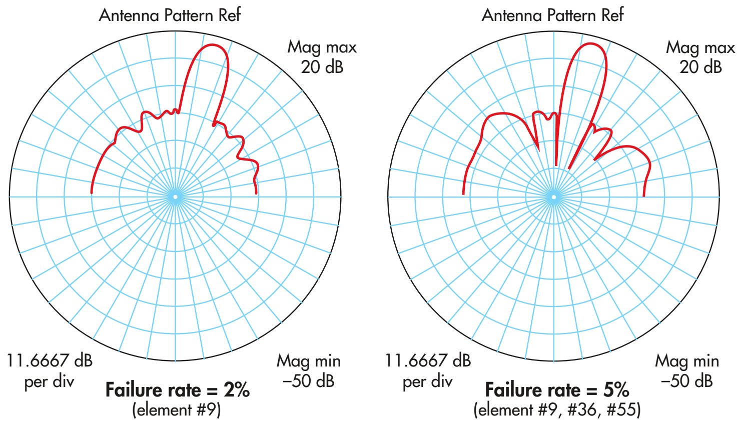

8. Shown are the side-lobe degradations that correspond to element failures of 2% and 5%.

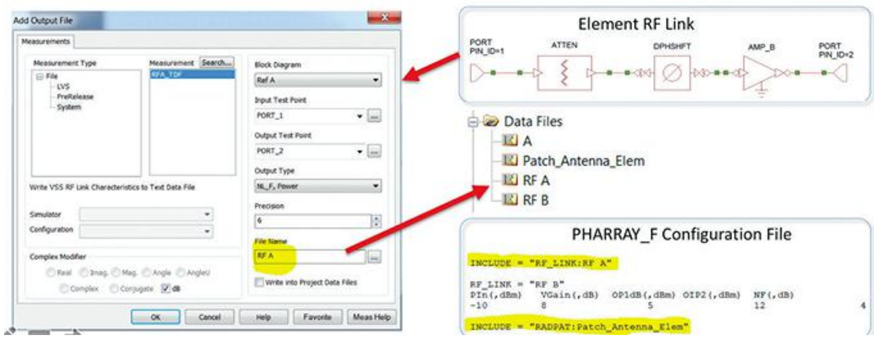

9. VSS has the capability to extract characterization of RF-link designs and allow assignment of individual elements in the phased array.

requirements. A "measurement" extracts the design characteristics (including circuit-level design details like nonlinearities) through NI AWR Design Environment Microwave Office co-simulation, and saves a properly formatted data file for use with the phased-array assembly model *(Fig. 9)*.

IN-SITU NONLINEAR SIMULATIONS

An accurate simulation must also account for the interactions that occur between the antenna elements and the driving feed network. The problem for simulation software is that the antenna and the driving feed network influence each other. The antenna's pattern is changed by setting the input power and relative phasing at its various ports. At the same time, the input impedances at the ports change with the antenna pattern. Since input impedance affects the performance of the nonlinear driving circuit, the changing antenna pattern impacts overall system performance.

In this case, the input impedance of each element in the array must be characterized for all beamsteering positions. The array is only simulated once in the EM simulator. The resulting S-parameters are then used by the circuit simulator, which also includes the feed network and amplifiers. As the phase shifters are tuned over their values, the antenna's beam is steered. At the same time, each amplifier sees the changing impedance at the antenna input to which it is attached. Thus, the amplifier's performance is affected.

In this final example, the power amplifiers (PAs) are nonlinear, designed to operate at their P1dB for maximum efficiency. They are, therefore, sensitive to the changing

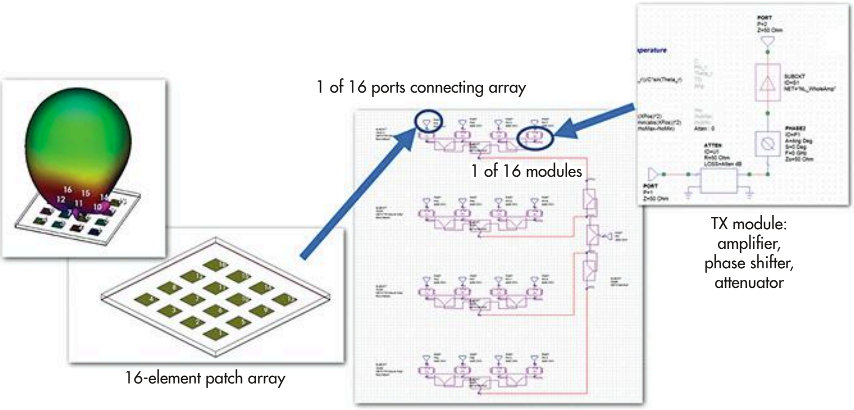

10. The software allows for the characterization of changing antenna feed impedance as a function of beamsteering using the variable phase and attenuator settings defined in the feed network design.

load impedances presented by the array. The beam of a 16-element array is steered by controlling the relative phasing and attenuation to the various transmit modules *(Fig. 10)*. In practice, the harmonic balance simulation in Microwave Office used to characterize the PAs takes substantial time to run with 16 PAs. Therefore, the beam is steered with the amplifiers turned off. The designer then turns on the individual PA for specific points of interest after obtaining the load impedance from the directed antenna.

At this point, the designer can directly investigate the PA's nonlinear behavior as a function of the load (antenna) impedance. With the load-pull capability in Microwave Office, PA designers can investigate output power, compression, and any other number of nonlinear metrics defining the amplifier's behavior *(Fig. 11)*.

With a detailed characterization of the RF links for each individual element, the overall system simulation is able to indicate trouble areas *(Fig. 12)*. These issues would have previously gone undetected until expensive prototypes were made and tested in the lab.

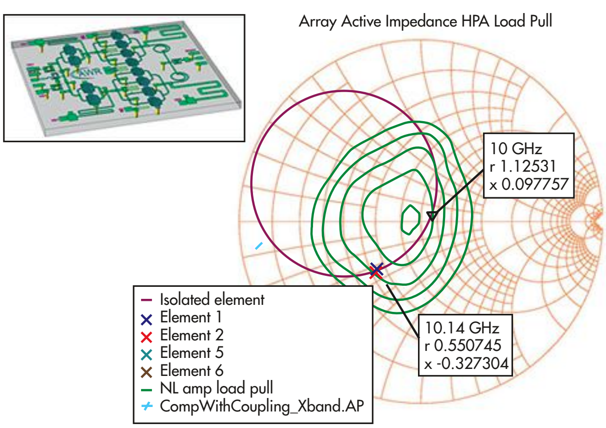

11. Shown is the simulated antenna feed impedance versus frequency superimposed over power load-pull contours for a broadband MMIC PA.

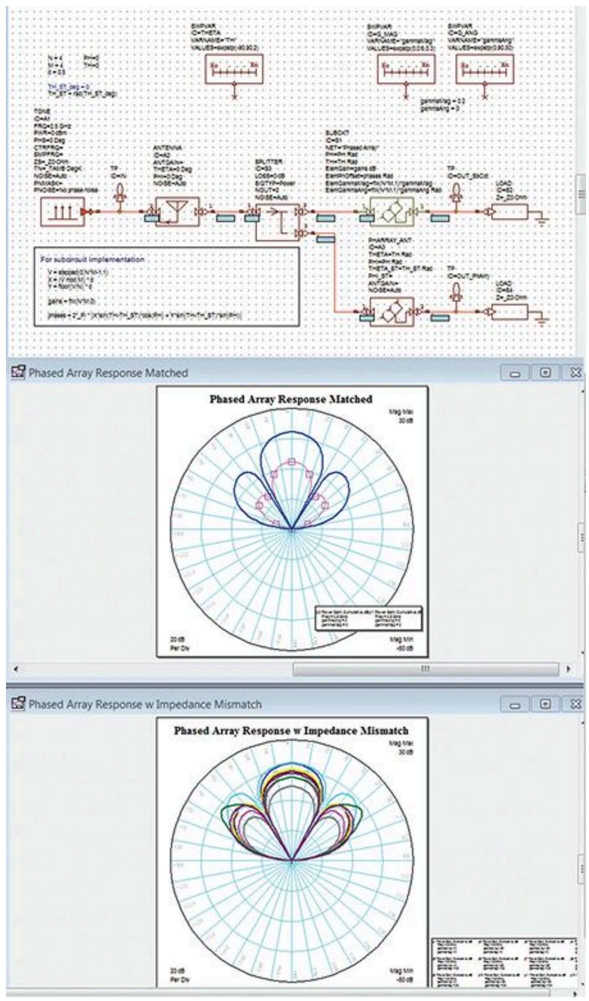

12. This figure illustrates the phased-array simulations with RF-link effects, including the impact of impedance mismatch between a PA and steered antenna array.

CONCLUSION

The capability to design and verify the performance of the individual components, along with the entire signal channel that defines the AESA radar, is a necessity due to increasing element counts and advances in antenna/electronics integration. Through a sophisticated design flow that encompasses circuit simulation, system-level behavioral modeling, and EM analysis operating within a single design platform, development teams can investigate system performance and component-to-component interaction prior to costly prototyping. mw

CHRIS DeMARTINO | Technical Editor

Q&A: Bror Peterson

At Qorvo, Big Expectations for GaN in 5G

Qorvo systems engineer Bror Peterson discusses several topics in regard to 5G communications, such as gallium-nitride technology and more.

When talking about 5G, what role do you expect gallium-nitride (GaN) technology to have?

Peterson: The primary role for GaN, or more specifically, GaN-on-silicon-carbide (GaN-on-SiC), is high-efficiency final stage power amplifiers (PAs) for both traditional high-power macro, as well as emerging massive MIMO base station platforms. Widespread market adoption for GaN-on-SiC power amplifiers has been driven by the demand for wider-bandwidth multi-carrier and multi-band systems. Systems that once covered a single 20-MHz bandwidth now need 10x the power and 20x bandwidth to handle various intraband and interband carrier aggregation combinations.

It is generally accepted that GaN-on-SiC Doherty PAs achieve higher power-added efficiency (PAE) at higher frequencies and over larger bandwidth compared to incumbent LDMOS technology. At a unit-cell level, GaN devices are fundamentally more efficient and inherently have higher output impedance, along with lower parasitic capacitance. This allows easier wideband matching and scaling to very large output powers. In addition, GaN-on-SiC is more reliable at high channel temperatures. The bottom line is that GaN is a fundamentally better semiconductor (high breakdown voltage and saturation velocity) that allows new system level trades to improve size, weight, power, and cost.

As we move toward 5G, significantly wider component carrier bandwidths (up to 200 MHz) and new frequency bands covering 3.3 to 4.9 GHz and beyond are being standardized, requiring the use of GaN. In addition to the sub-6-GHz enhancements, 5G will also introduce new millimeter-wave bands between 24-30 and 37-43 GHz. These millimeter-wave hybrid beamformed base stations will need very compact, fully-integrated front-end-modules. GaN's high power density and low noise figure is particularly well suited for this application and will be key to achieving the effective isotropic radiated power (EIRP) and antenna gain to noise temperature (G/T) needed to close the link to mobile user equipment.

What do you expect to see in terms of module integration?

Peterson: The level of integration really depends on the platform. For traditional macro base stations, the final PA stage will integrate the main and peaker amplifier with pre-matching and harmonic traps into a single compact dual-path package. For massive MIMO platforms with up to 128 transmit and receive paths, a much higher level of integration is needed. Initially, the driver plus fully matched Doherty PA will be integrated into a single package.

On the receive side, dual-channel switch low-noise amplifiers (LNAs) with multiple stages of variable gain are already mainstream. Over time, a single fully-integrated 2T2R or 4T4R module will directly interface to the antenna and transceiver, and may include the isolators and filters. This module would also provide a separate feedback path for closed loop pre-distortion and a digital interface for control and biasing.

At millimeter-wave frequencies, the antenna array element spacing is extremely small (3.75 mm at 39 GHz). It will be necessary to integrate at least the PA, TR Switch, and LNA into a single module. Further integration with a core-beamformer RFIC is expected, but may be delayed due to export compliance considerations that limit output power when integrated with phase and amplitude controls.

Can you tell us a little about the filter requirements and solutions that you expect to be associated with 5G?

Peterson: There are several significant trends impacting filter requirements for 5G. First, most of the new bands for 5G are unpaired and use time-division duplexing. Unlike paired-spectrum where the uplink and downlink frequencies can be closely spaced and require complex duplexing filters, unpaired spectrum typically allows simpler band filters. Second, the shift to full-dimensional beamforming and massive MIMO base stations gives additional freedom to null potential out-of-band interferers. In addition, massive MIMO base stations require as many as 128 filters, so a compact form factor and lower cost will be critical. mw

CHRIS DeMARTINO | Technical Editor

Software Tool Proves its Merit for Filter Design

To help designers, WaveCon's Parfil and Elliptic programs facilitate the creation of a wide variety of filters.

To accomplish their design goals, RF/microwave filter designers have various options to choose from in terms of software tools. One such tool is currently offered by WaveCon *(www.waveconsoft.com)*, which was founded back in 1989. Today, WaveCon's software can be utilized to design a wide range of filter types, including microstrip, stripline, and round-rod.

WaveCon's original program is known as Parfil, which can be used to design bandpass, lowpass, highpass, and bandstop filters. In addition to Parfil, WaveCon offers the Elliptic and ProCap design tools. Elliptic is intended to be used for the design of elliptic filters, while ProCap is a nodal analysis program.

As stated, the Parfil tool can be used to design bandpass, lowpass, highpass, and bandstop filters. *Figure 1* shows the software's filter selection menu, with filter types that include *Parallel Coupled Half Wave, Interdigital Tapped Input, Combline Tapped Input, Hairpin Coupled Line Input*, and many others.

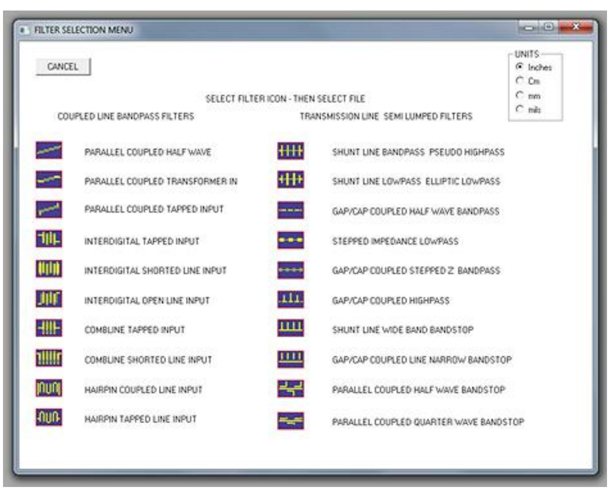

1. The Parfil program allows for the construction of a large number of filter types.

MICROSTRIP BANDPASS FILTER EXAMPLE

As an example, when selecting the *Parallel Coupled Half Wave* filter type, users are presented with a list of input parameters that includes *Transmission Media, Filter Center Frequency, Filter Bandwidth, Ripple, Number of Filter Sections (Poles)*, and many more *(Fig. 2)*. One simply has to enter the parameters that are needed to satisfy the specific design requirements. Figure 2 shows the input parameters for a microstrip filter with a center frequency of 10 GHz.

Figure 3 shows the computed results for the specified filter.

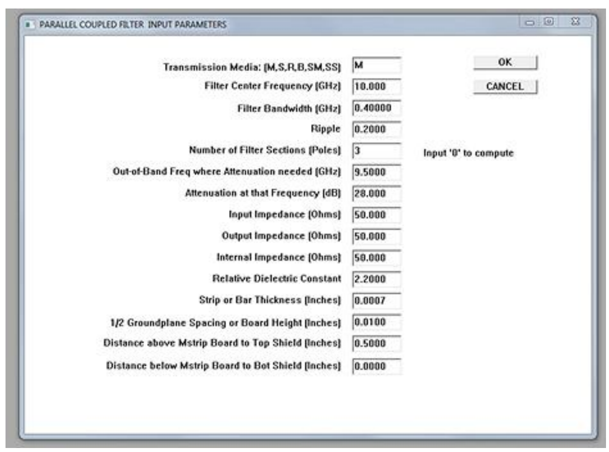

2. Shown is the software's interface in which users must enter the filter parameters.

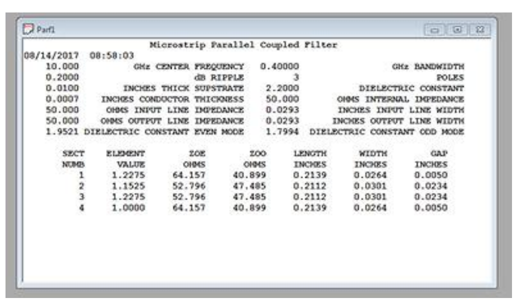

Parfl

Microstrip Parallel Coupled Filter

08/14/2017 08:58:03

10.000	GHz CENTER FREQUENCY	0.40000	GHz BANDWIDTH
0.2000	dB RIPPLE	3	POLES
0.0100	INCHES THICK SUPSTRATE	2.2000	DIELECTRIC CONSTANT
0.0007	INCHES CONDUCTOR THICKNESS	50.000	OHMS INTERNAL IMPEDANCE
50.000	OHMS INPUT LINE IMPEDANCE	0.0293	INCHES INPUT LINE WIDTH
50.000	OHMS OUTPUT LINE IMPEDANCE	0.0293	INCHES OUTPUT LINE WIDTH
1.9521	DIELECTRIC CONSTANT EVEN MODE	1.7994	DIELECTRIC CONSTANT ODD MODE

SECT NUMB	ELEMENT VALUE	ZOE OHMS	ZOO OHMS	LENGTH INCHES	WIDTH INCHES	GAP INCHES
1	1.2275	64.157	40.899	0.2139	0.0264	0.0050
2	1.1525	52.796	47.485	0.2112	0.0301	0.0234
3	1.2275	52.796	47.485	0.2112	0.0301	0.0234
4	1.0000	64.157	40.899	0.2139	0.0264	0.0050

3. The numerical results are displayed in a tabular form.

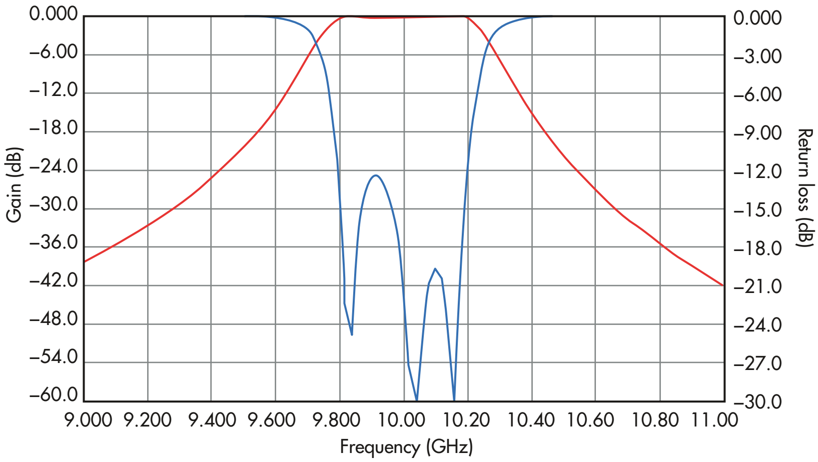

4. Shown is a plot of a filter's insertion loss and return loss.

While this article focused on the Parfil and Elliptic software programs, the ProCap program also offers its own analysis capabilities.

The lengths and widths of the sections are shown along with the gap separation values. In addition, the even- and odd-mode impedance values are shown in Fig. 3.

At this stage, users have a number of options at their disposal. For example, the *Plot Window* menu item includes a number of display options, such as *Gain/Return Loss and Gain/Group Delay (Fig. 4)*. Furthermore, the *Tune* option allows users to adjust the filter's response.

FURTHER ANALYSIS

Of course, a designer may also want to use an electromagnetic (EM) simulator to verify the filter's performance at this stage in the design process. The results obtained from Parfil could then be incorporated into an EM simulator for performance verification and optimization. In essence, Parfil is effective in terms of obtaining numerical filter values and then viewing results.

The process described is similar for other filter types. For example, *Fig. 5* shows the input parameter list when selecting the *Interdigital Tapped Input* filter type. Users essentially follow the same approach of entering the required parameters for this type of filter.

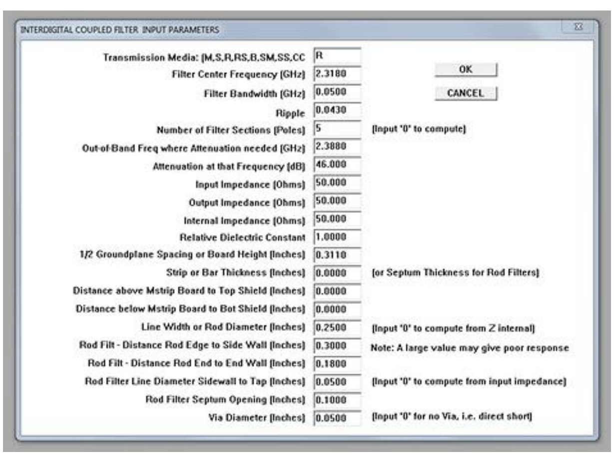

5. This figure shows the input parameters for an interdigital filter.

In addition to Parfil, WaveCon offers the Elliptic program. This software tool is intended for the design of elliptic filters. *Figure 6* shows the program's filter selection menu, which includes *Parallel Coupled Half Wave Elliptic, Interdigital Shorted Line Input Elliptic, Combline Shorted Line Input Elliptic*, and several others. A similar list of input parameters is displayed after a filter type is selected.

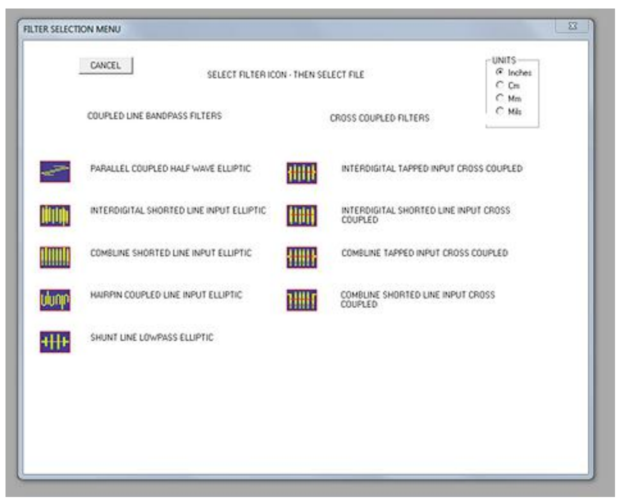

6. The Elliptic program allows users to select from a range of elliptic filters.

In summary, WaveCon's software is certainly a helpful tool for filter design. While this article focused on the Parfil and Elliptic software programs, the ProCap program also offers its own analysis capabilities. For additional information about any of the company's offerings, visit its website. mw

REFERENCE

Pramanick, Protap and Bhartia, Prakash, *Modern RF and Microwave Filter Design*, 2016.

CHRIS DeMARTINO | Technical Editor

Will Today's Microwave Oven Soon be a Thing of the Past, Part 2?

How can solid-state RF energy impact the microwave oven? This article attempts to answer that question.

Recently I wrote an editorial titled, "Will Today's Microwave Oven Soon Be a Thing of the Past?" That piece discussed the possibility of microwave ovens based on solid-state RF energy, which would essentially replace traditional magnetron-based microwave ovens. The potential benefit of healthier cooked food was specifically mentioned.

A few readers have since commented in regard to that editorial. One specific question concerns exactly how solid-state RF energy can cook healthier food. Since not much detail was offered in that editorial piece, I thought it would be beneficial to write another article in an attempt to provide a better explanation. This article will hopefully shed some light on the topic of solid-state RF energy.

MEET THE SKEPTIC

Of course, it is common that any new technology will lead to skepticism. Solid-state RF cooking can certainly fit that description, as some may seriously doubt the legitimacy of microwave ovens based on solid-state RF energy. One question could simply be this: How can solid-state cooking help to enable healthier eating? Let's try to answer that question.

As mentioned in the previous editorial, MACOM (*www.macom.com*) is one company that is at the forefront of solid-state RF energy (*see figure*). Mark Murphy is currently the company's senior director, RF power. He says, "Anytime food is heated, its nutrients and state can be degraded if the cooking process is not controlled properly. That is why precise temperature control is so important for healthier cooking. Microwave ovens that leverage solid-state power amplifiers are superior to conventional magnetron-based microwave ovens in that they enable far greater precision and control of the directed energy, which helps to preserve the nutritional integrity of the food."

Although magnetron-based microwave ovens have been used for many years, Murphy can plainly state their shortcomings. He explains, "Magnetron-based microwave ovens aren't equipped to measure and adapt to energy that's absorbed by or reflected from the food into the cavity as it cooks. They instead deliver open-loop, crudely-averaged heating that's assisted by a rotating turntable at the base of the cavity. This imprecise energy delivery often results in overcooking and hot spots that can lower the food's nutritional value."

Murphy continues, "By using multiple solid-state power amplifiers and antennas with closed-loop feedback to adjust for precise energy absorption, the energy can be directed with greater precision to exactly where it's needed and in a controlled way that ensures optimal temperature control. Rather than relying on moisture sensors that measure humidity in the cooking cavity—an indirect mode of measurement that's sometimes implemented in modern magnetron-based microwave ovens—solid-state microwave ovens measure the properties of the food itself while it cooks and adapt accordingly. This promotes the retention of the nutrients, moisture, and flavors of the food."

ECONOMICS OF SOLID-STATE MICROWAVE OVENS

Another possible question concerning solid-state RF cooking is with regard to its economic viability. In other words, will solid-state microwave ovens be economical for the commercial market? According to Murphy, the short answer is yes. He states, "The adoption of solid-state microwave ovens will commence in the industrial and commercial cooking market, where the value that these systems provide will be well worth the modest increase in cost. Customers will gain significant advantages centric to system reliability, food processing speed, and throughput."

Murphy believes that reliability is a major benefit of solid-state RF cooking. He notes, "With regard to system reliability, solid-state RF transistors can provide 10X longer lifespans that magnetrons—this is a major benefit in 24/7 production environments where frequent magnetron failures can slow production and require numerous expensive service calls. By eliminating the rotating platters common to magnetron-based microwave ovens, system reliability is further increased due to the reduction of mechanical moving parts, which are a common point of failure."

Greater reliability is not the only benefit of solid-state RF cooking, according to Murphy. He adds, "Food processing speed and throughput are increased due to solid-state microwave ovens' ability to heat and cook food much faster than magnetron-based systems, owing to the rapid energy transfer enabled by RF power. Solid-state RF technology is particularly valuable for food defrosting processes, enabling food to be defrosted much faster and more evenly than it can today without drying or damaging the food."

To sum it all up, Murphy does indeed believe that microwave ovens based on solid-state RF energy will eventually find their way into homes. He says, "With continued innovation in solid-state GaN based RF technology and cost structure improvements, this technology will eventually migrate to consumer kitchens, and in so doing will change our perceptions of the modern microwave oven. Its value will evolve from that of a simple heating device, to a device that's capable of cost-effectively cooking healthier, multi-course meals with unprecedented efficiency. In a way, this evolution will do for cooking what the smartphone did for the way we use our cell phones."

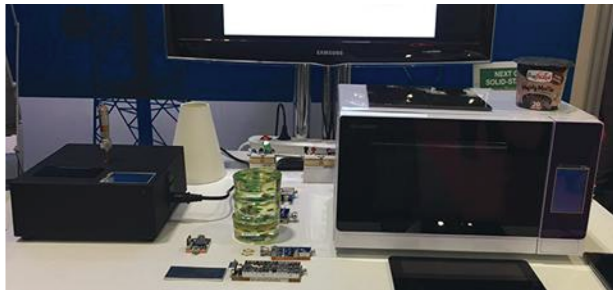

This microwave oven based on solid-state RF technology was demonstrated at IMS 2017.

In summary, this article hopefully answered some questions that one may have concerning the possibility of cooking based on solid-state RF energy. Some interesting points were made in an attempt to validate this technology. While everyone still may not be convinced, one thing can be said: it will be interesting to see how solid-state RF cooking unfolds in the future. mw

CHRIS DeMARTINO | Technical Editor

New Magnetic Sheets Silence the Noise

These new magnetic sheets can be incorporated into the design of today's products, such as smartphones, tablets, and notebooks, to defeat noise problems.

Today's products, such as smartphones, have become smaller and thinner while still offering multi-functional performance. One example of multi-functional capability is a product that contains both near-field communications (NFC) and wireless charging technology. Thus, it is even more essential that noise is adequately suppressed in today's electronic products. One method of suppressing noise is by using magnetic sheets.

TDK Corp. is one company that offers magnetic sheets for noise suppression. The company recently expanded its Flexield series by introducing the new IFM10M noise suppression sheets, which can be used in a number of products *(see figure)*. According to Harvey Espinoza, director of product marketing, communications devices business group at TDK Corporation of America, "The magnetic sheets are used in various types of electronic devices, such as smartphones, tablets, notebooks, stylus pens, point-of-sale (POS) systems, and industrial terminals."

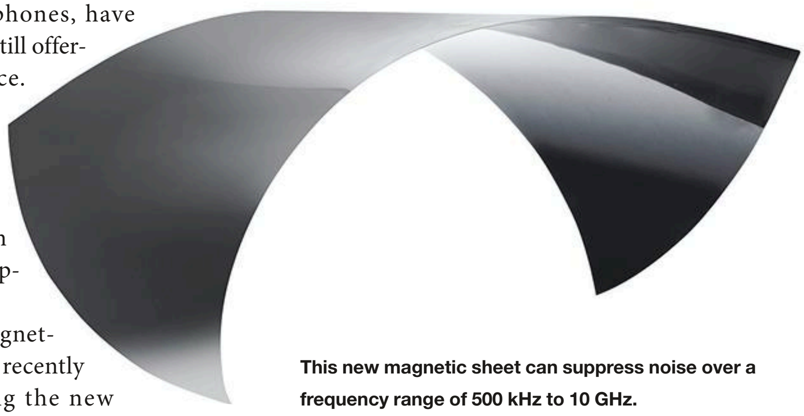

This new magnetic sheet can suppress noise over a frequency range of 500 kHz to 10 GHz.

The IFM10M magnetic sheets feature a laminated design, consisting of a magnetic layer and a copper-plated layer. With a total thickness of 0.04 mm, the new IFM10M sheets are 60% thinner than existing magnetic sheets with a similar magnetic layer thickness, according to the company. Furthermore, the new sheets cover a frequency range of 500 kHz to 10 GHz. The dimensions are 300 × 200 mm. In addition, the IFM10M magnetic sheets operate over a temperature range of -40 to +85°C.

The thin size of the IFM10M noise suppression sheets allows them to be well suited for slim products, such as smartphones, tablets, notebooks, and stylus pens. Essentially, the sheets are well equipped to be installed in dense environments. According to Espinoza, "As electronic devices become more compact, thinner, and multi-functional (NFC, wireless charging), electronic components are increasingly being mounted in higher densities. This increased density can lead to noise emissions from the integrated circuits (ICs), components, and cables interfering with other systems within the electronic device.

"In smartphones, the magnetic sheets have been used on power coils, systems-on-a-chip (SoCs), and have been attached at the surface of flexible cables," Espinoza continues. "They can be used between printed circuit boards (PCBs) to reduce the effect of noise emissions from one PCB to another."

The new magnetic sheets offer several benefits, says Espinoza, noting that "the noise-absorbing properties of magnetic sheets can reduce the impact of radiated noise when applied to the radiating sources. The sheets can also be applied to components/circuits that are vulnerable to noise emissions to reduce the potential impact."

In addition, the IFM10M sheets are flexible, meaning they can be cut to the desired size and shape and installed in very small gaps. Lastly, the company asserts that the magnetic sheets improve receiver sensitivity for stylus input devices that utilize inductive coupling and also improve radio-frequency identification (RFID) performance on metal surfaces. mw

TDK CORP., www.global.tdk.com

Modular Test Systems Built Your Way

and Delivered Within 2 Weeks!

Accelerate the solution for your test setup!

Whether you're working in production test or R&D, Mini-Circuits' modular test systems give you a solution that's flexible, reliable, affordable and fast! Choose from either a rack-mountable chassis or a space-efficient, bench-top module, and configure your system with any combination of extra-long-life SPDT, SP4T, SP6T and transfer switches and programmable attenuators with attenuation ranges from 0 to 30, 60, 90, 110 and 120 dB. We'll build and ship a system tailored to your requirements within just 2 weeks! Define your system with our online configuration tool for a fast quote today!

Features

- *Customizable Front Panel Layout*
- *USB and Ethernet Controllable*
- *User-friendly GUI and DLLs Included*
- *19" Rack-Mountable Chassis or…*
- *8.25" Compact Module*

Choose from hundreds of possible configurations!


SPDT Switches
DC – 18 GHz


SP4T Switches
DC – 18 GHz


SP6T Switches
DC – 12 GHz


Transfer Switches
DC – 18 GHz


0 – 30, 60, 90, 110 or 120 dB
Programmable Attenuators
1 MHz – 6 GHz

Configure your system online now for a fast quote!

Mini-Circuits®

www.minicircuits.com P.O. Box 350166, Brooklyn, NY 11235-0003 (718) 934-4500 sales@minicircuits.com

560 rev org

Power Splitters/Combiners Go 4 and 8 Ways to 40 GHz

MODELS ZN4PD-44+ and ZN8PD-K44+ are power splitters/combiners each rated for 20 W input power as splitters from 10 to 40 GHz. The four-way ZN4PD-44+has typical insertion loss of 1.5 dB (above theoretical 6-dB splitting loss) and typical isolation between ports of 22 dB. The maximum VSWR at all ports is 1.35:1. The four-way splitter/combiner has typical amplitude unbalance of 0.3 dB and typical phase unbalance of 6 deg., both across the full bandwidth. It is supplied in a rugged aluminum-alloy case measuring 2.06 × 1.50 × 0.50 in. with female 2.92-mm coaxial connectors. The eight-way ZN8PD-44+ has typical full-band insertion loss of 2.5 dB (above theoretical 9-dB splitting loss) and typical isolation between ports of 20 dB. It has typical amplitude and phase unbalance of 0.4 dB and 8 deg., respectively, with maximum VSWR of 1.50:1 at all ports. It is supplied in an aluminum-alloy enclosure measuring 4.09 × 1.93 × 0.5 in. with 2.92-mm connectors. The RoHS-compliant power splitters/combiners serve applications in wideband communications links, satellite communications, 5G wireless networks, and test systems.
MINI-CIRCUITS, P.O. Box 350166, Brooklyn, NY 11235-003; (718) 934-4500, *www.minicircuits.com*

Stable VCO Tunes from 500 to 1,200 MHz

THE DCMO50120-5 is an octave-band voltage-controlled oscillator (VCO) with tunable frequency range of 500 to 1200 MHz. It changes frequency by means of a 24-V tuning range with typical tuning sensitivity of 25 to 50 MHz/V. The oscillator delivers at least +7 dBm output power across the full frequency range with typical phase noise of −102 dBc/Hz offset 10 kHz from the carrier and −121 dBc/Hz offset 100 kHz from the carrier. Harmonic suppression is typically −15 dBc. The VCO draws 40 mA current from a +5-V dc supply. It is housed in a RoHS-compliant surface-mount package measuring 0.5 × 0.5 × 0.180 in. and is designed for operating frequencies from −40 to +85°C.
SYNERGY MICROWAVE CORP., 201 McLean Blvd., Paterson, NJ 07504; (973) 881-8800, *www.synergymwave.com*

VCOs Generate 10 to 4350 MHz

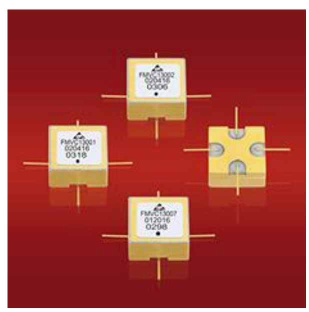

A SERIES OF 16 voltage-controlled oscillators (VCOs) provides total frequency coverage of 10 to 4350 MHz. Suitable for military and commercial communications and test applications, the oscillatorsoperate on tuning voltages from +0.5 to +20 V dc and supply voltages from +5 to +15 V dc and provide output levels from +4 to +12 dBm. Second harmonics are suppressed to −25 dBc and phase noise is as low as −120 dBc/Hz offset 10 kHz from the carrier. The RoHS-compliant VCOs are supplied in 0.5 × 0.5 in. hermetic housings that meet MIL-STD-883 and MIL-STD-202 environmental test conditions for shock, vibration, and temperature cycling.
FAIRVIEW MICROWAVE, 1130 Junction Dr., Ste. 100, Allen, TX 75013; (972) 649-6678, *www.fairviewmicrowave.com*

Long-Range Sensors Link with LoRaWAN and BLE

THE RS1XX series of battery-powered, long-range integrated sensors combine the benefits of LoRaWAN and Bluetooth Low Energy (BLE). Members of the LORA family of sensors, the RS1xx series sensors offer LoRaWAN options at 868 and 915 MHz along with BLE for local data display, configuration, and troubleshooting. The integrated sensors are based on proven silicon devices from Semtech and Nordic Semiconductor and provide a LoRa range to 10 miles with 2.4-GHz connectivity. The RS1xx series sensors work with the company's RG1xx series of LoRa/multi-wireless gateways for simple integration with electronic devices in need of wireless connectivity.
LAIRD, 3481 Rider Trail S., Earth City, MO 63045; (636) 898-6000, *www.lairdtech.com*

Compact Panel Antenna Fits 2.4-GHz Wi-Fi Designs

THE 1011-005 small-form-factor panel antenna from Southwest Antenna is now available from stocking distributor RFMW Ltd. The antenna operates from 2.4 to 2.5 GHz and is only 0.5 in. thick. It is designed for IEEE 802.11g/n Wi-Fi and unlicensed ISM-band applications and can be integrated into electronic designs or used as a standalone solution. It features a UV-resistant and weather-sealed Kydex radome for indoor or outdoor use. The antenna provides 6.5-dBi gain and can handle 10 W power. It is supplied with 12 in. of RG-58 RF cable terminated with a female SMA female connector.

RFMW, LTD. (SOUTHWEST ANTENNA STOCKING DISTRIBUTOR), 188 Martinvale Ave., San Jose, CA 95119; (408) 414-1450, e-mail: info@rfmw.com, *www.rfmw.com*

Cavity Bandpass Filter Passes 2016.5-MHz Wi-Fi

THE AB2016B617 Wi-Fi cavity bandpass filter offers a 12-MHz bandwidth centered at 2016.5 MHz. The 50-Ω filter has a maximum 50-dB bandwidth of 30 MHz. The passband insertion loss is 2.5 dB, with maximum passband amplitude ripple of 0.5 dB. The passband return loss is greater than 14 dB. The bandpass filter, which exhibits 1.50:1 input and output VSWR, handles input power levels to 25 W. It measures 10.07 × 1.5 × 0.76 in. and is supplied with female SMA connectors. It has an operating temperature range of –45 to +85°C.

ANATECH ELECTRONICS, INC., 70 Outwater Ln., Garfield, NJ 07026; (973) 772-4242, *www.anatechelectronics.com*

Coupler Directs 0.38 to 2.7 GHz

MODEL 1CN3827-05 is a single directional coupler for use from 380 MHz to 2.7 GHz. It provides 5-dB nominal coupling and 20-dB typical directivity. It is part of the 1CN3827-DB series of couplers with coupling values of 5 to 30 dB. The low-PIM, 5-dB coupler measures 5.8 × 2.0 × 1.0 in. and can be supplied with Type N or SMA female connectors.

WERBEL MICROWAVE LLC, 622 Rte. 10 W., Unit 9, Whippany, NJ 07981; (973) 515-3001, *www.werbelmicrowave.com*

Quadrature Mixer Converts 33 to 50 GHz

THE SFQ-33350313-2F2FSF-F2 Q-band quadrature mixer provides frequency translation of RF and LO signals from 33 to 50 GHz, using a DC-coupled IF range. The typical LO-to-RF isolation is 25 dB. The conversion loss for in-phase (I) and quadrature (Q) IF signals is typically 13 dB when operating with LO source power of +17 dBm. The mixer can be configured as an image-rejection mixer or single-sideband (SSB) modulator by adding an IF quadrature coupler.

SAGE MILLIMETER, INC., 3043 Kashiwa St., Torrance, CA 90505; (424) 757-0168, *www.sagemillimeter.com*

Stub Antenna Connects UAVs in ISM Band

THE SA-900-930 stub antenna is optimized for unmanned aerial vehicle (UAV) applications in the 900-MHz ISM band. It measures just 2.65 × 0.52 × 0.43 in. and weighs just 0.35 oz. and provides 2 dBi gain at 915 MHz. The antenna operates with vertical polarization and exhibits less than 2.50:1 VSWR. Usable over the frequency range of 902 to 928 MHz, the stub antenna is supplied with a make SMA coaxial connector.

PHARAD LLC, Octane Div., 1340 Charwood Rd., Ste. L, Hanover, MD 21076; (410) 590-3333, *www.pharad.com*

TCXOs Offer CMOS, Sine-Wave Outputs to 125 MHz

THE T1265 and T1266 Series temperature-compensated crystal oscillators (TCXOs) are available with square-wave CMOS (T1265) or sine-wave (T1266) outputs from 50 to 125 MHz. The oscillators feature low noise floors of –165 dBc/Hz and outstanding stability with temperature of ±0.5 ppm. The oscillators are supplied in low-profile 17.3-mm2 housings and can operate on +3.3 or +5.0 V dc supplies. They are suitable for use as frequency reference sources in test equipment, mobile communications systems, and wireless base stations.

GREENRAY INDUSTRIES, INC., 840 W. Church Rd., Mechanicsburg, PA 17055; (717) 766-0223, *www.greenrayindustries.com*

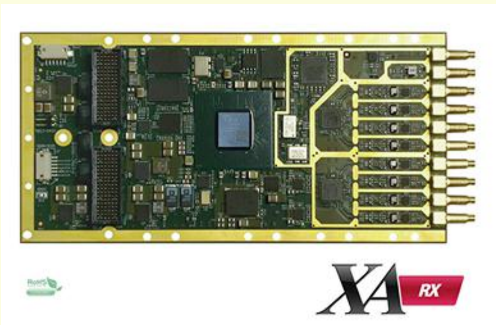

Digitizing Module Serves Wide-Channel-Count Systems

THE XA-RX is an XMC input/output (I/O) module featuring eight 16-b, 125-MSamples/s analog-to-digital-converter (ADC) channels and an Artix-7 field-programmable gate array (FPGA) designed for wide-channel-count communications and instrumentation applications. It is capable of independent real-time signal processing on each analog input channel. The digital-signal-processing (DSP) functionality can be customized using VHDLor Simulink via an optional FrameWork toolset. The four-lane, PCI Express 2.0 interface supports continuous data streaming at 1600 MB/s, and multiple modules can be synchronized for large meshes.

INNOVATIVE INTEGRATION, A MOLEX CO., 741 Flynn Rd., Camarillo, CA 93012; (805) 383-8994, *www.innovative-dsp.com*

Amplifier Helps Broadcast COFDM Digital Video

THE TA1029 power amplifier is designed for broadcast applications from 6.4 to 7.1 GHz with coded-orthogonal-frequency-division-multiplex (COFDM) digital video signals. Based on GaN semiconductor technology, the amplifier achieves saturated output power of +44 dBm with typical gain of 58 dB. It boosts COFDM video signals while maintaining adjacent-channel power ratio of –30 dBc. The amplifier operates from a supply of +9 to +36 V dc and is supplied in a compact housing measuring 6.0 × 2.5 × 1.06 in.

TRIAD RF SYSTEMS, 11 Harts Lane, Ste. 1, E. Brunswick, NJ 08816; (855) 558-1001, *www.triadrf.com*

Miniature Limiter Handles 100-W Power

FULL DESIGN support for the UltraCMOS PE45361 limiter from Peregrine Semiconductor is now available from Richardson RFPD. The limiter, which can be used from 10 MHz to 6 GHz, handles as much as 100-W (+50-dBm) pulsed input power with better than 1-ns response time. Insertion loss is 0.95 dB. The low-power limiting threshold can be set from +7 to +13 dBm using positive threshold control voltage from 0 to +0.3 V dc. The compact limiter is supplied in a 12-lead 3 × 3 × 0.5 mm QFN package.

RICHARDSON RFPD, 1950 S. Batavia Ave., Ste. 100, Geneva, IL 60134; (630) 262-6800, *www.richardsonrfpd.com*

Variable Attenuator Provides 0.1-dB Step Size to 3 GHz

Mini-Circuits' model ZVVA-3000 is a 50-Ω variable attenuator with adjustable 0.1-dB-resolution attenuation via USB or RS-232 control (with 9-pin D-Sub connector). It covers 20 MHz to 3 GHz with 50-dB maximum attenuation to 500 MHz, 33-dB maximum attenuation to 1500 MHz, and 25-dB maximum attenuation to 3000 MHz. Attenuation flatness is typically ±1.6 dB or better and attenuation accuracy is typically ±0.7 dB. Insertion loss (above attenuation setting) is typically 2.8 dB to 500 MHz, 3.5 dB to 2500 MHz, and 4.0 dB to 3000 MHz. The RoHS attenuator exhibits 0-dB glitches when changing attenuation settings, ideal for ATE applications. It is provided with a 2.6-ft. USB type A (male) to USB type Mini-B (male) cable, and GUI software is available for free download from the Mini-Circuits' website.

Monolithic 75-Ω Amp Boosts 5 to 300 MHz

Mini-Circuits' model PGA-32-75+ is a wideband, wide-dynamic-range monolithic 75-Ω amplifier based on E-PHEMT technology. With a bandwidth of 5 to 300 MHz, it is well suited for cable-television (CATV) applications including DOCSIS 3.1 upstream path. Typical gain at +9 VDC ranges from 15.8 dB at 5 MHz to 15.4 dB at 300 MHz. Typical output power at 1-dB compression (P1dB) ranges from +20.4 dBm at 5 MHz to +23.6 dBm at 300 MHz. The RoHS-compliant amplifier achieves a wide dynamic range by merit of a low 2.9-dB noise figure at 100 MHz, a typical output IP3 of +43.3 dBm at 100 MHz, and typical IP2 of +58.1 dBm at 100 MHz. The amplifier is supplied in a thermally stable SOT-89 package.

Six-Way Splitter/Combiner Spans 2 to 18 GHz

Mini-Circuits' model ZN6PD-02183+is a DC-pass, six-way power splitter/combiner with wide frequency range of 2 to 18 GHz. It is capable of handling as much as 25 W input power as a splitter. Insertion loss is typically only 1.4 dB (above the theoretical 7.8-dB splitting loss) across the full frequency range with typical VSWR of 1.50:1 at the sum port and 1.35:1 at all other ports. Isolation between channels is typically 22 dB. The six-way power splitter/combiner features typical full-band amplitude unbalance of 0.4 dB and typical phase unbalance of 6 deg. The RoHS-compliant splitter/combiner is supplied in an aluminum-alloy case measuring 4.0 × 6.0 × 0.38 in. with female SMA connectors.

Ultrawideband Class A Linear Amplifier Powers 0.5 to 18.0 GHz

Mini-Circuits' model ZVA-183G+ is a four-stage, Class A linear amplifier that is unconditionally stable from 0.5 to 18.0 GHz. It provides as much as 0.5 W output power (+27 dBm) with 27-dB typical gain and ±2-dB typical gain flatness across the full bandwidth. The RoHS-compliant amplifier typically draws 700 mA from a +15-VDC supply. It features a typical output third-order-intercept point (IP3) of +36 dBm and low noise figure of typically 3 dB. The amplifier is supplied in a rugged housing measuring 4.18 × 3.36 × 3.57 in. with female SMA connectors and is available with an optional heatsink.

MMIC Quadrature Power Splitter/Combiner Covers 7.0 to 12.5 GHz

Mini-Circuits' EPQ-133+ is a two-way, 90-deg., MMIC surface-mount power splitter/combiner with frequency range of 7.0 to 12.5 GHz. It handles as much as +32 dBm input power as a splitter in a tiny MCLP package measuring 0.157 × 0.157 × 0.039 in. (4 × 4 × 1 mm). Insertion loss is typically 0.7 dB from 7 to 11 GHz and typically 0.8 dB from 11.0 to 12.5 GHz. Isolation between ports is typically 19 dB from 7 to 10 GHz and better than 16 dB from 10.0 to 12.5 GHz. The tiny power splitter/combiner exhibits typical input VSWR of 1.70:1 or better and typical output VSWR of 1.40:1 or better. The amplitude and phase unbalance are typically better than 0.8 dB and 3.3 deg., respectively. The power splitter/combiner is designed for operating temperatures from -45 to +85°C.

25-W Class AB Amplifier Powers 20 to 2700 MHz

Mini-Circuits' ZHL-25W-272+ is a Class AB linear high-power amplifier capable of 25 W saturated output power from 20 to 2700 MHz. Suitable for commercial and military communications, radar, and test applications, the RoHS-compliant amplifier provides 50-dB gain with ±1 dB gain flatness across the frequency range. It delivers +40 dBm output power at 1-dB compression (P1dB) with+44 dBm saturated output power; the third-order intercept point (IP3) is typically +49 dBm. It is supplied in an aluminum-alloy case measuring 5.6 × 8.8 × 1.2 in. with female SMA connectors and available with an optional heat sink and fan. It draws 3.5 A from a +28-VDC supply. The rugged amplifier features built-in self-protection against reverse polarity, overdrive, and overheating, and can deliver 15 W output power even while withstanding output short- and open-circuit operating conditions.

This index is provided as an additional service by the publisher, who assumes no responsibility for errors or omissions.

Subscription Assistance and Information:
(ISSN 0745-2993)
Microwaves & RF is published monthly. Microwaves & RF is sent free to individuals actively engaged in high-frequency electronics engineering. In addition, paid subscriptions are available. Subscription rates for U.S. are $95 for 1 year ($120 in Canada, $150 for International). Published by Penton Media, Inc., 9800 Metcalf Ave., Overland Park, KS 66212-2216. Periodicals Postage Paid at Kansas City, MO and additional mailing offices. POSTMASTER: Send change of address to Microwaves & RF PO Box 2100, Skokie, IL 60076-7800. For paid subscription information, please contact Microwaves & RF at PO Box 2100, Skokie IL 60076-7800. Canada Post Publications Mail agreement No. 40612608. Canada return address: IMEX Global Solutions PO Box 25542, London ON N6C 6B2.